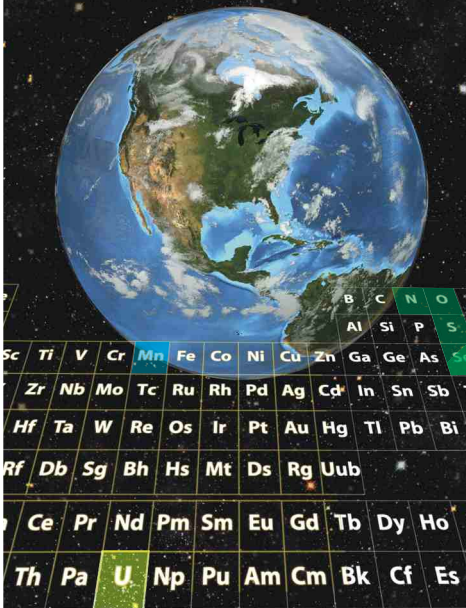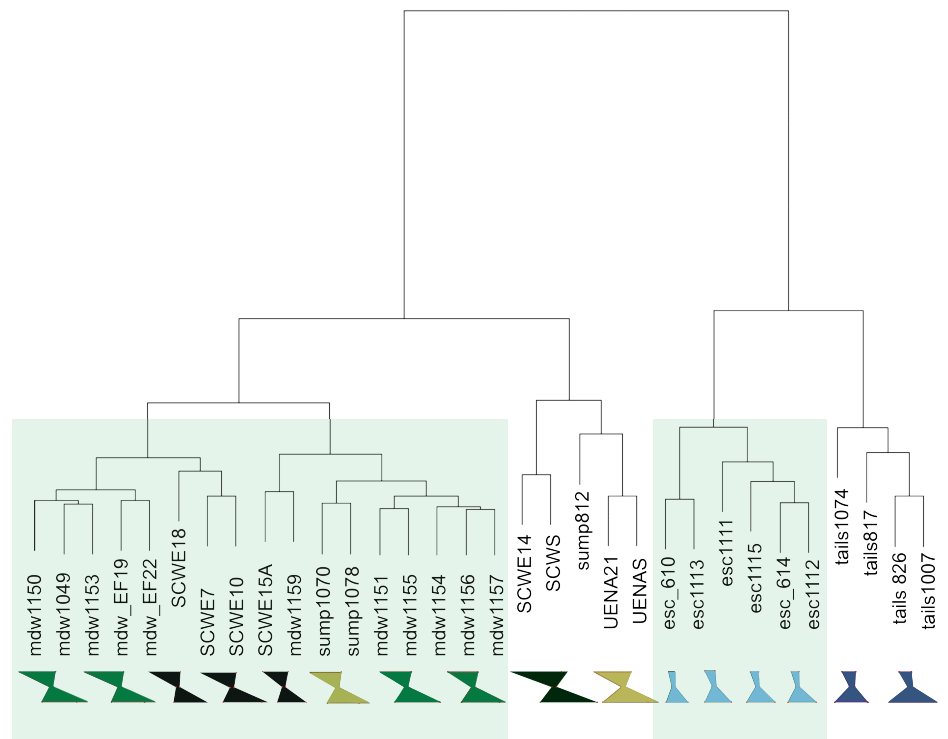# Environmental Sciences Laboratory

Multivariate Statistical Analysis of Water Chemistry in Evaluating the Origin of Contamination in Many Devils Wash, Shiprock, New Mexico

December 2012

Prepared for

U.S. DEPARTMENT OF ENERGY | Legacy Management

This page intentionally left blank

Multivariate Statistical Analysis of Water Chemistry in Evaluating the Origin of Contamination in Many Devils Wash, Shiprock, New Mexico

December 2012

This page intentionally left blank

Contents

Figures

U.S. Department of Energy   Multivariate Statistical Analysis to the Origin of Contamination–Shiprock, NM
December 2012   Doc. No. S09257
Page i

Tables

This page intentionally left blank

Abbreviations

AHC   agglomerative hierarchical clustering

ANOVA   analysis of variance

AR   activity ratio

CBE   charge balance error

CV   coefficient of variation

DOC   dissolved organic carbon

DOE   U.S. Department of Energy

ft   foot

HCA   hierarchical cluster analysis

HSD   honestly significant difference (statistical test)

L   liter

LM   Office of Legacy Management

μg/L   micrograms per liter

μS/cm   microsiemens per centimeter

mg/L   milligrams per liter

mL   milliliters

n number of samples

PAM   partitioning around medoids

PC   principal component

PCA   principal component analysis

PLFA   phospholipid fatty acids

s_i average silhouette width

VSS   Variable Size Symbol (plots)

Populations/Sample Location Prefixes

EF   East Fork (Many Devils Wash)

MDW   Many Devils Wash

SCW   Salt Creek Wash

UENA   (upper) Eagle Nest Arroyo[†]

[†] Eagle Nest Arroyo samples collected in this region were identified as "UENA" to distinguish them from a sample location previously established in the lower portion of the arroyo.

U.S. Department of Energy   Multivariate Statistical Analysis to the Origin of Contamination–Shiprock, NM
December 2012   Doc. No. S09257
Page v

This page intentionally left blank

Executive Summary

This report evaluates the chemistry of seep water occurring in three desert drainages near Shiprock, New Mexico: Many Devils Wash, Salt Creek Wash, and Eagle Nest Arroyo. Through the use of geochemical plotting tools and multivariate statistical analysis techniques, analytical results of samples collected from the three drainages are compared with the groundwater chemistry at a former uranium mill in the Shiprock area (the Shiprock site), managed by the U.S. Department of Energy Office of Legacy Management. The objective of this study was to determine, based on the water chemistry of the samples, if statistically significant patterns or groupings are apparent between the sample populations and, if so, whether there are any reasonable explanations for those groupings.

For years, contamination of seep and surface water in Many Devils Wash was attributed to historical milling activities at the Shiprock site. The assumed hydrologic connection between the two areas was based primarily on the observation that the constituents detected at elevated levels in seep water in the wash—nitrate, selenium, sulfate, and uranium—were also the primary contaminants of concern in groundwater impacted by mill operations. Although early characterization studies at the site indicated that leaching of Mancos Shale, the predominant bedrock formation in the Shiprock region, could also cause moderately high concentrations of these constituents in local groundwater, the interpretation at that time was that the concentrations in Many Devils Wash were so high that mill-related contamination was the likely source.

Examination of water chemistry data collected over the past decade at the Shiprock site has led to the development of two hypotheses regarding the source of the contaminated seep water in Many Devils Wash. The first hypothesis is consistent with the previous assessments of the site, maintaining that the contaminated seep water was caused by leakage from raffinate ponds and tailings seepage in the mill area, with underlying groundwater subsequently transporting the contamination to the wash. The second hypothesis attributes the seep contamination in Many Devils Wash to the natural leaching of Mancos Shale bedrock by groundwater in portions of the wash located upgradient of the seeps.

In 2011, seep contamination similar to that observed in Many Devils Wash was identified in two arroyos located 5 to 10 miles north of Shiprock. Known as Salt Creek Wash and Eagle Nest Arroyo, these two drainages are referred to as analog sites in this study because they are geologically similar to the lowermost portion of Many Devils Wash. Because they are far removed from, and on the opposite side of, the San Juan River, the analog sites could not have been affected by contamination from the mill site. Water samples were collected in Many Devils Wash and at the analog sites and in three locales at the Shiprock site (tailings, escarpment, and swale areas) for a total of six sample populations. Samples were analyzed for nitrate, selenium, uranium, major ions, and other constituents representative of water-rock interactions.

The data set used in the statistical analysis consisted of 32 cases (sampling locations) representing the 6 different sample populations or study areas. Chemical signatures of groundwater were compared using traditional geochemical plotting tools, Piper and Stiff diagrams, and two widely used multivariate statistical methods, principal component analysis (PCA) and cluster analysis. Both the piper and stiff diagrams plot cations (Na, K, Ca, and Mg) and anions (Cl, SO_4, HCO_3 and CO_3) to provide chemical signatures of the groundwater samples.

Piper diagrams showed association of tailings and escarpment samples; these points are distinctly separate from sample results from all other areas. Stiff diagrams, which provide a visual means of displaying total concentrations of certain dissolved solids (major ions) were useful in distinguishing between groups. Two general shapes, depicted by a tilted hourglass ( ) and an Erlenmeyer flask ( ), were revealed in the data collected for this study. Stiff diagrams of sample data from the tailings and escarpment areas have the flask-shaped appearance, whereas diagrams for samples collected from Many Devils Wash, Salt Creek Wash, Eagle Nest Arroyo, and the swale area resemble the tilted hourglass. These results suggest that chemical characteristics (and likely hydrologic histories or origins) of groundwater from Many Devils Wash, the analog sites, and the swale area are different from those of the tailings and escarpment areas.

Based on major ion chemistry, PCA revealed similar distinctions as those observed in the Piper and Stiff plots. The analysis was extended to include the major contaminants common to Many Devils Wash and the Shiprock site (nitrate, selenium, and uranium). In all PCA iterations, for both major ions and the extended data set, tailings and escarpment area samples grouped separately from those from all other study areas. Analysis of variance and subsequent post-hoc tests on the factor scores for the principal components accounting for most of the variation of the data indicated that chemistries of the tailings area samples differ from those of Many Devils Wash and the analog sites, and in most cases the swale area samples as well.

Cluster analysis, a multivariate statistical analysis technique designed to reveal underlying data structures or groups, was also useful in distinguishing between sample populations. Two distinct cluster analysis methods were used (Ward's method and partitioning around medoids); both yielded similar results. For all iterations, tailings and escarpment area samples grouped separately from samples collected from other areas, and the agreement of the cluster partitions with the chemical signatures defined using the Stiff diagrams was striking.

The combined results of these analyses indicate a commonality in chemical signatures of groundwater samples from Many Devils Wash, the swale area, and the analog sites. These signatures are distinct from those of the tailings and escarpment area samples. The most discriminating variables were sodium, sulfate, bicarbonate, and uranium. Selenium, commonly associated with Mancos Shale, was less discriminating due to variable and elevated concentrations in the swale area. The variations in the chemical signatures are interpreted as being derived from two independent sources: (1) interaction with the Mancos Shale, and (2) tailings fluids. A major finding stemming from the combined statistical and geochemical assessments is that contaminated water in Many Devils Wash tends to resemble water sampled at the analog sites and the swale area, and it is unrelated (statistically) to contaminated groundwater in the former mill area.

An unexpected result of this study was that the constituents receiving the greatest focus in previous site investigations (nitrate, selenium, and uranium, the primary contaminants at the Shiprock site) were less useful than the major ions in discriminating between the sample populations investigated in this study. The combination of the Stiff diagrams with the PCA and cluster analysis results for the major ions best illustrated the differences in chemical signatures between the Mancos Shale impacted groundwater and tailings-related groundwater.

1.0   Introduction

This report evaluates the chemistry of seep water occurring in three desert drainages near Shiprock, New Mexico: Many Devils Wash, Salt Creek Wash, and Eagle Nest Arroyo. The chemistries of water in the drainages are compared with the groundwater chemistry at three separate locations in the vicinity of a former uranium-ore processing facility near Shiprock. The mill and associated raffinate ponds and tailings were located on a terrace overlooking a floodplain of the San Juan River. The tailings and other mill-related wastes have been disposed of in a 77-acre disposal cell about 0.5 mile northwest of Many Devils Wash (Figure 1). The mill operated from 1954 to 1968 on property leased from the Navajo Nation. The site, now formally known as the Shiprock, New Mexico, Disposal Site, is managed by the U.S. Department of Energy (DOE) Office of Legacy Management (LM).
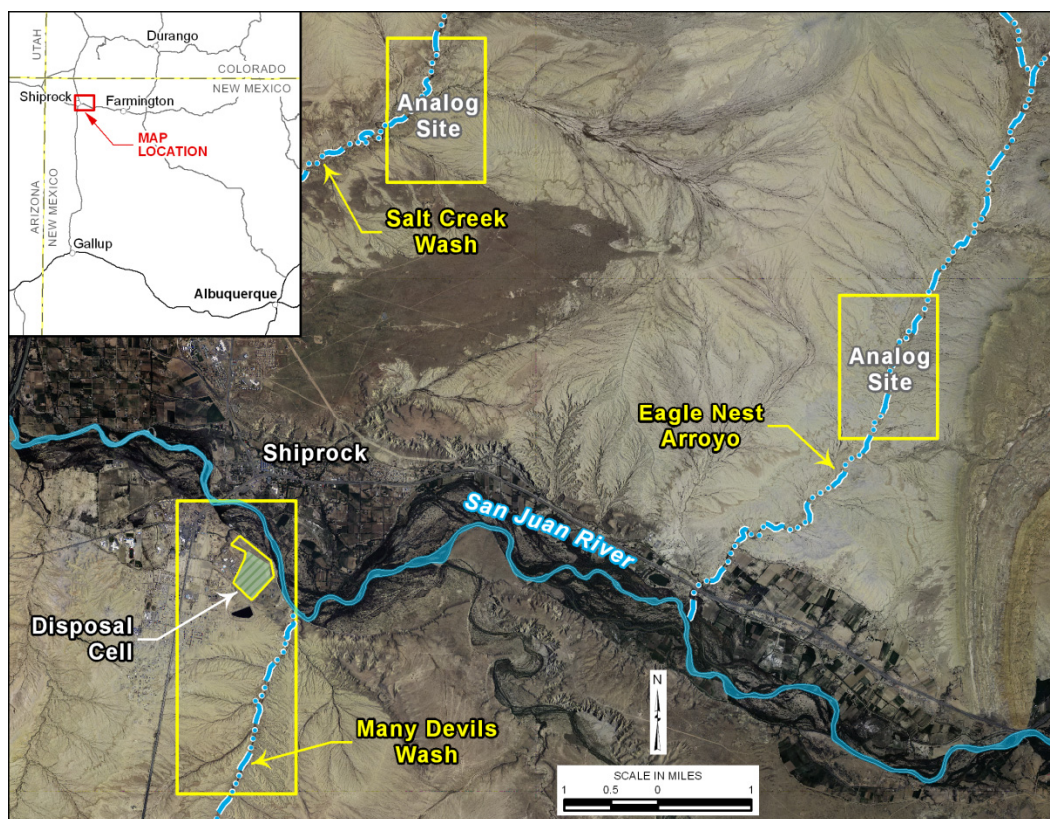
Figure 1. Locations of Many Devils Wash, Shiprock Site, and Salt Creek Wash and Eagle Nest Arroyo Analog Sites
Outlined areas are shown in more detail on Figure 2.

For years, surface water contamination in Many Devils Wash, the primary focus of this evaluation, was attributed to historical milling activities. This attribution was based on the observation that the dissolved constituents detected at elevated levels in the wash water and in the seeps providing the water—nitrate, selenium, sulfate and uranium—were also the primary contaminants of concern in groundwater impacted by the former mill operations. As a result, DOE has regularly sampled surface water and groundwater in downstream parts of the wash and has accepted responsibility for its remediation in the *Groundwater Compliance Action Plan* (DOE 2002, 2005, 2011a).

Examination of water chemistry data collected in the Shiprock area has led to the development of two principal hypotheses regarding the source of the contaminated seep water in Many Devils Wash. The first is consistent with previous assessments of the site, maintaining that the contaminated seep water was caused by leakage from raffinate ponds and tailings seepage in the mill area that feed underlying groundwater on the terrace, and subsequent transport of contamination to the wash. The second hypothesis attributes the seep and surface water contamination in Many Devils Wash to the natural leaching of Mancos Shale bedrock by groundwater in parts of the wash located upgradient of the seeps.

Several observations suggest that the source of contaminated water seeping into Many Devils Wash arroyo is not derived from the mill site. During early Shiprock site characterization investigations, it was noted that the Mancos Shale could provide a source of uranium and other aqueous phase constituents (e.g., nitrate, selenium, and sulfate) in groundwater (DOE 2000). Inconsistency with a mill site origin as the source of contamination was also suggested by observed activity ratios for uranium isotopes ($^{234}U/^{238}U$) detected in local groundwater. The activity ratios (ARs) were found to be near secular equilibrium (AR = 1) in groundwater at the mill site, but greater than 2.0 in Many Devils Wash. Secular equilibrium AR values are also characteristic of tailings samples from other uranium milling sites where isotopic data are available. In contrast, AR values in groundwater (from natural systems not impacted by uranium milling) commonly exceed 1.0 and often exceed 2.0 (Osmond and Cowart 1976).[1]

Finally, it was noted during early site characterization efforts that seeps in the downstream, arroyo portion of Many Devils Wash issue from the east side of the arroyo, which is opposite the side nearest the mill site (DOE 2000). Groundwater flow paths that could cause this paradox were not obvious and seemed unlikely, although not impossible to explain. For example, for the groundwater in Many Devils Wash to be derived from the tailings area, it would have to travel deep within the Mancos Shale through fractures and then resurface along vertical fractures and travel to the seepage areas on the east side of the arroyo.

Despite these inconsistencies, the evidence refuting a mill site origin for the contamination in Many Devils Wash was considered circumstantial (DOE 2000), and DOE accepted responsibility for its maintenance and remediation. Efforts to collect contaminated subsurface and near-surface water in the wash have been extensive (e.g., installation of a concrete dam and collection system) but largely unsuccessful. To better understand the source of the contamination, investigations were undertaken in Many Devils Wash in spring 2010 (DOE 2011b), and shortly afterward DOE undertook a broader investigation (*Natural Contamination from the Mancos Shale*) that identified elevated concentrations of nitrate, selenium, sulfate, and uranium in seeps issuing from the Mancos Shale throughout much of its depositional basin (DOE 2011c; Morrison et al. 2012).

Since 2011, evidence from investigations funded by LM's Applied Science and Technology program—collectively referred to as the Origins Project—prompted a reevaluation of the origin of contamination in Many Devils Wash. As part of this project, in August 2011 eight new wells (1150, 1151, 1153, 1154, 1155, 1156, 1157, and 1159) were installed in unconsolidated sediments along the axis of Many Devils Wash, upgradient from existing wells in the seeps area, or arroyo portion, of the wash (Figure 2). These locations were sampled shortly after the wells were installed, and again as part of a broader field investigation undertaken in March 2012.

---

[1] The enrichment of ^{234}U in groundwater is often explained by the recoil of ^{234}Th following the emission of alpha particles from mineral-bound ^{238}U and the subsequent decay of ^{234}Th to ^{234}U, a process referred to as alpha-recoil (refer to discussion in DOE 2012a).

The March 2012 field effort involved sampling at a large number of locations, including Many Devils Wash and the two analog sites, Salt Creek Wash and Eagle Nest Arroyo (Figure 2). The latter two drainages are referred to as analog sites because they are geologically similar to the lowermost portion of Many Devils Wash. Because they are far removed from, and on the opposite side of the San Juan River, the analog sites could not have been affected by contamination from the mill site.

Previous reconnaissance work at the analog sites had shown that surface waters in both arroyos were fed by seep water emerging from Mancos Shale bedrock, and concentrations of sulfate and uranium in the seeps were elevated (DOE 2011c). Two areas at the Shiprock site, referred to as the tailings area (disposal cell) and the swale (Figure 2), were also sampled in March 2012. Wells in a third area considered representative of the Shiprock site, referred to as the escarpment area, had been previously sampled in September 2011. Tailings area wells 817, 826, 1007, and 1074 were selected because they were the only wells that met the following criteria: (1) they were located close to the disposal cell, (2) all had high uranium concentrations clearly reflective of a tailings signature, and (3) all were screened in the terrace alluvium.

The statistical evaluation in this study describes analytical data from the six sample populations, comparing their respective chemical signatures and identifying correlations between them. In addition to the primary contaminants (nitrate, selenium, sulfate, and uranium), other variables, including major ions, were included in the analysis. The data were initially characterized using standard univariate statistical methods (e.g., box plots) and traditional geochemical plotting tools (Piper and Stiff diagrams). Multivariate statistical methods, primarily principal component analysis and cluster analysis, were then applied to further evaluate differences (or similarities) between the sample populations.

This statistical evaluation was conducted in tandem with a recently issued companion study—*Application of Environmental Isotopes to the Evaluation of the Origin of Contamination in a Desert Arroyo: Many Devils Wash, Shiprock, New Mexico* (DOE 2012a)—that evaluated the distribution of a suite of isotopes measured in seep water and groundwater collected from the same study areas evaluated herein. For that investigation, isotopes of hydrogen (^{2}H/^{1}H, ^{3}H), nitrogen (^{15}N/^{14}N), oxygen (^{18}O/^{16}O), sulfur (^{34}S/^{32}S), and uranium (^{234}U/^{238}U) were used to discriminate between groundwater contaminant sources. The major findings of that study are summarized in Section 6.2 of this report.

2.0   Site Descriptions

2.1   Shiprock Site (Tailings, Escarpment, and Swale)

The Shiprock tailings disposal cell is located on a terrace elevated about 50 to 60 feet (ft) above a floodplain of the San Juan River, where a steep escarpment separates the terrace from the floodplain (Figure 2). The mill operated from 1954 through 1968 and processed about 1.5 million tons of uranium ore. DOE (2000) estimated that the mill used about 1 billion gallons of water. Much of this water was placed in unlined ponds, and a portion infiltrated the subsurface. It was later estimated that between 50 million and 390 million gallons of milling-related fluids percolated into the subsurface during the operational life of the mill (DOE 2012d).
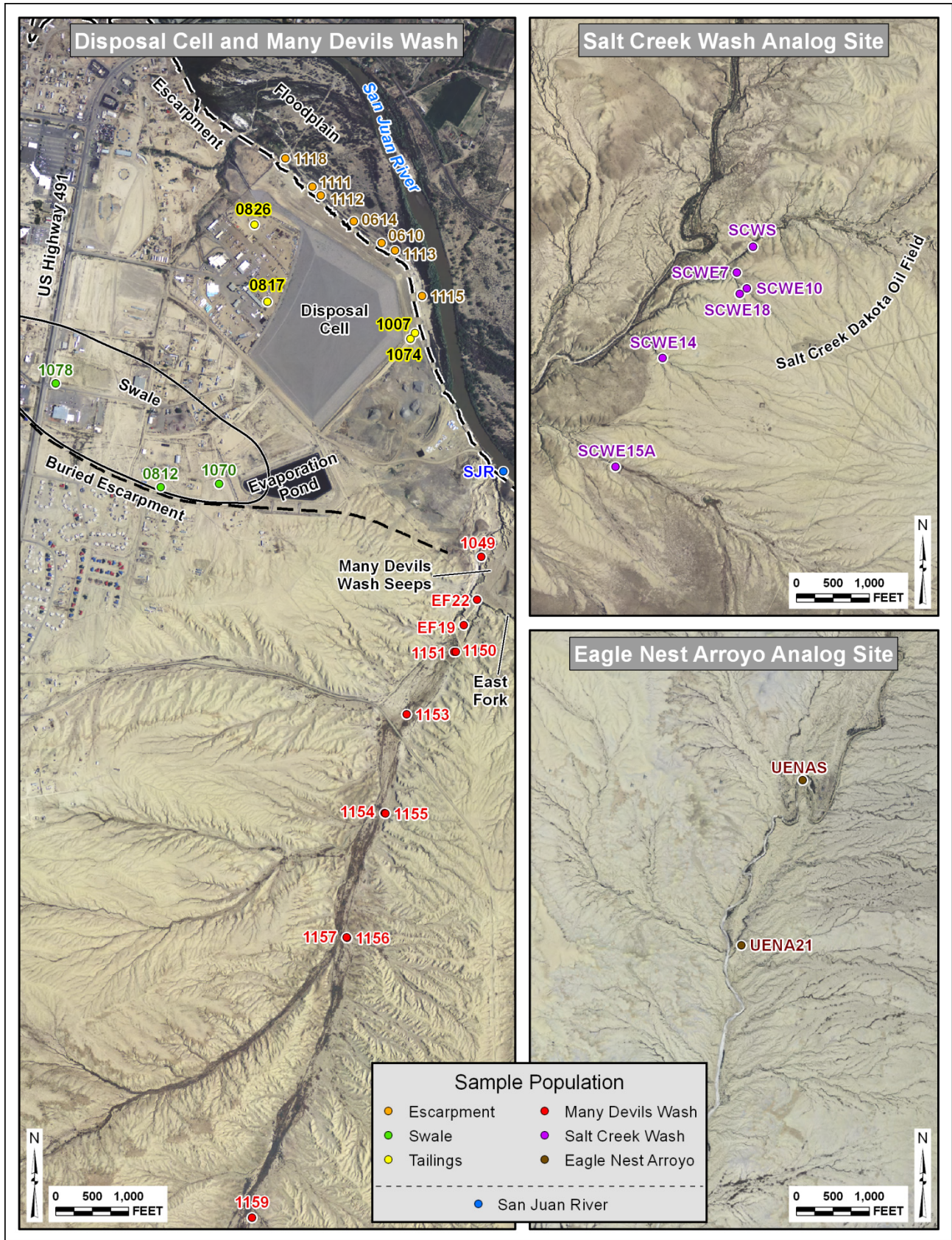
Figure 2. Sample Location Maps for the Data Populations Used in this Study
Study area locations are shown in Figure 1.

DOE decommissioned surface features at the site by stabilizing the mill tailings and other milling waste in an engineered disposal cell at the same location as the former mill; surface remediation was completed in 1986. Characterization of groundwater flow, fate and transport processes at the site was conducted in 1998 and 1999, the results of which are documented in the *Final Site Observational Work Plan for the Shiprock, New Mexico, UMTRA Project Site* (DOE 2000).

About 10 to 35 ft of terrace alluvium, consisting of sand and gravel, underlies the disposal cell; Mancos Shale bedrock of late Cretaceous age underlies the alluvium. The Mancos Shale is composed predominantly of dark gray shale and locally contains minor siltstone, bentonite, and dolomitic beds. The near-surface portion of the Mancos is weathered, as manifested by a color change from the dark gray shale of competent, unweathered shales to light yellowish-gray shades of weathered beds. Chemically, the weathered portion is characterized by a loss of organic carbon, the oxidation of pyrite, and increases in iron oxide minerals and gypsum.

South of the disposal cell, the terrace alluvium is overlain by as much as 60 ft of eolian loess. The alluvium contains gravel and sand layers that filled ancestral channels (paleochannels) of the San Juan River, as defined by a map showing contoured elevations on top of the Mancos Shale (DOE 2005). The terrace alluvium is absent south of a buried Mancos Shale escarpment, the location of which was defined using borehole logs (DOE 2005). A predominant paleochannel, called the "swale," abuts and is subparallel to the buried escarpment (Figure 2).

Groundwater in the swale area has elevated concentrations of the same suite of contaminants as detected in the tailings and escarpment areas (nitrate, selenium, sulfate, and uranium). However, the concentrations of these constituents in the respective areas tend to be noticeably different. For example, whereas some of the highest uranium concentrations are in the groundwater nearest the disposal cell and on the floodplain, uranium concentrations in the swale area are much lower (Figure 3). The opposite spatial trend is apparent for nitrate and selenium: concentrations of these constituents are most elevated in the swale area and typically lower in the tailings and escarpment areas. Although sulfate concentrations are generally more uniform in the vicinity of the Shiprock site, the highest concentrations have been measured in the swale area. Notably, some of the highest sulfate concentrations are present in Many Devils Wash, where concentrations are similar to those in swale area wells (Figure 3).

Because all four contaminants have been detected at relatively high levels in the three areas of the Shiprock site, DOE accepted responsibility for remediation of groundwater in the terrace alluvium (DOE 2002, 2003). In previous years, it was assumed that groundwater in the terrace alluvium and underlying weathered Mancos Shale was derived solely from anthropogenic sources, dominantly the tailings operations, with additional contributions from irrigation west of Highway 491 (Figure 2) and leaky pipe systems used for municipal water supply (DOE 2000).

The alluvial groundwater systems beneath the terrace and in the floodplain are not directly connected. Consequently, contamination of the floodplain is the result of flow from the tailings area through Mancos Shale separating the two systems. Partial evidence of groundwater flow through the Mancos is provided by the presence of localized seeps of contaminated groundwater that daylight on the escarpment wall. Additional evidence is provided by high concentrations of contaminants in alluvial wells at the base of the escarpment. Groundwater seepage through the shale occurs along bedding plane partings and subvertical fractures in the Mancos (DOE 2000).
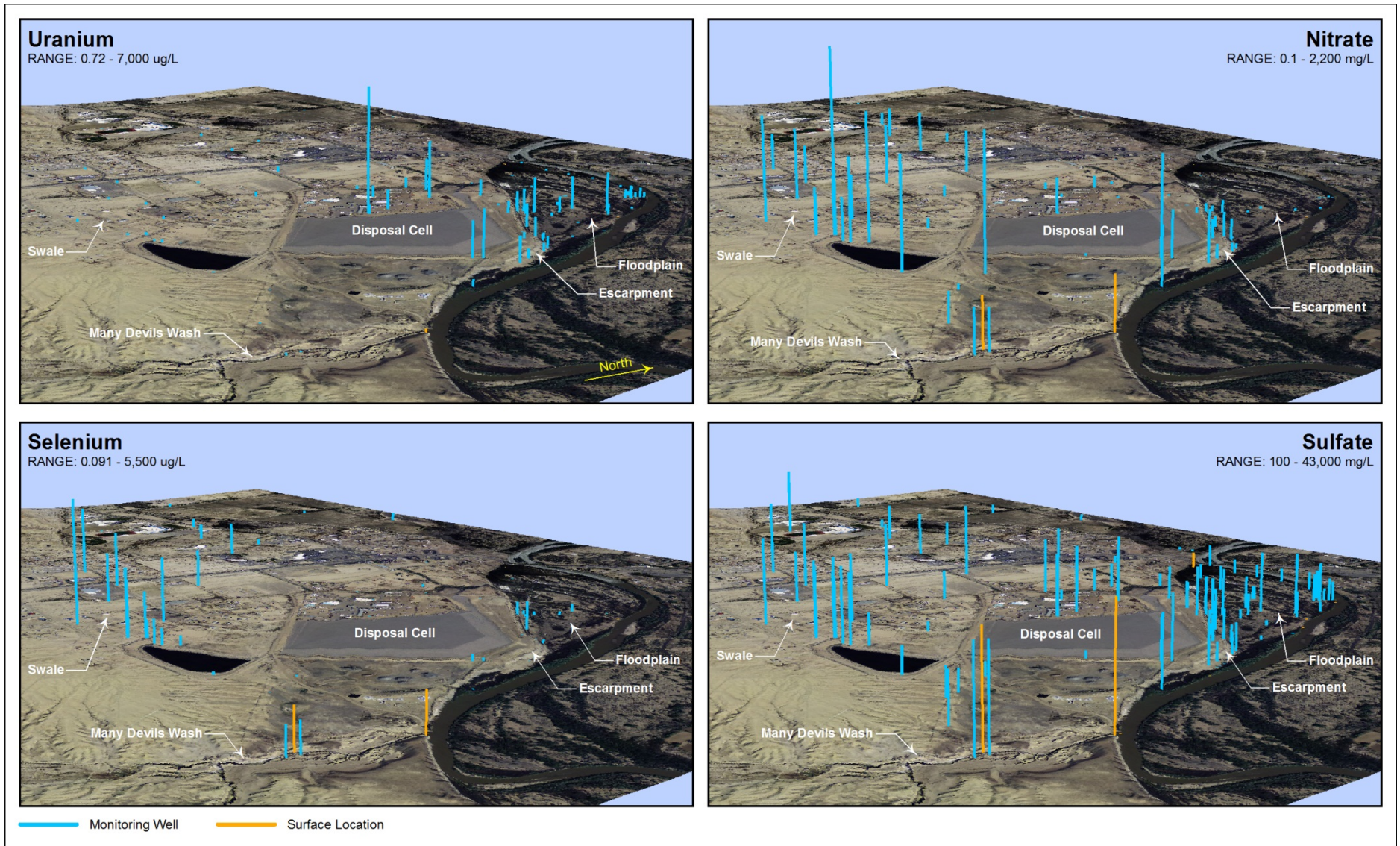
Figure 3. Relative Concentrations of Shiprock Site Contaminants of Concern in Groundwater and Surface Water

Data are from March 2012 semiannual monitoring (DOE 2012c). In each plot, the vertical bars denote the magnitude of contaminant concentrations relative to the maximum. The difference in spatial distributions between uranium, the primary site-related contaminant, and those for the other contaminants of concern are apparent. Although data points for uranium in Many Devils Wash, the swale, and distal areas east/southeast of the disposal cell are barely discernible due to low magnitude (note faint blue dots in these areas), sample locations are the same as those shown in the remaining plots. Elevated sulfate concentrations in Many Devils Wash surface water samples likely reflect some evaporation and should not be directly compared with the groundwater results.

2.2   Many Devils Wash

Many Devils Wash drains an area of about 11.5 square miles and empties into the San Juan River about 1,500 ft upstream of the Shiprock site (Figures 1 and 2). The lowermost 0.5 mile of Many Devils Wash is an arroyo, whereas upstream portions of the wash flow within a broad, flat valley about 400–500 ft wide. The arroyo, located about 0.5 mile southeast of the disposal cell, cuts through 20 to 30 ft of steep-walled loess deposits; up to 3 ft of gravelly alluvium is found in the bed of the arroyo. The alluvium is directly underlain by weathered Mancos Shale (DOE 2011a), and unweathered Mancos Shale comprises low-permeability bedrock throughout the arroyo area and upstream portions of the watershed drained by the wash. Contaminated seepage occurs along a 400-ft section of the southeast wall of the arroyo and at the intersection of Many Devils Wash and East Fork (Figure 2). The seep water tends to collect in pools of surface water in the bed of the wash. The color of the surface water is typically either yellow or red; the origin of the color is unknown, but the color is not due to iron. Results from laboratory tests conducted to determine the cause of the coloration are reported separately (DOE 2012b).

2.3   Salt Creek Wash and Eagle Nest Arroyo Analog Sites

The Salt Creek Wash and Eagle Nest Arroyo analog sites are geologically similar to the lowermost portion of Many Devils Wash. Both sites consist of arroyos incised in loess and Mancos Shale. Seeps issue from bedding plane partings and joints in the Mancos. Surface water flowing in the bed of Salt Creek Wash has a deep red color, while water in Eagle Nest Arroyo has a light yellow color. These colors are similar to the colors of surface water observed in Many Devils Wash.

3.0   Overview of Multivariate Statistical Approaches

Multivariate statistics have been widely applied in the earth and environmental sciences (Schuenemeyer and Drew 2011). Examples include the disciplines of hydrogeology and geochemistry (Güler et al. 2002; Cloutier et al. 2008), hydrology (Ali et al. 2010), biology (for species identification and taxonomy), and microbiology (Schryver et al. 2006). Multivariate methods involve the simultaneous analysis of multiple variables rather than an examination of each variable individually. These methods are particularly suited to the identification of commonalities as well as differences between large data sets, such as the water chemistries observed in the respective areas included in this study.

Although it has been established that nitrate, selenium, sulfate, and uranium are contaminants common to both the Shiprock site and Many Devils Wash, the combined signatures of these constituents have not been fully characterized. Multivariate methods assist in refining descriptions of those signatures by characterizing the extent to which the chemical properties of the two areas are similar, as well as the degree to which they differ. The major objectives of this evaluation are to: (1) discriminate between the study areas based on chemical signatures and (2) identify the variables (chemical parameters) that best explain the underlying differences. Two multivariate statistical methods are applied: principal component analysis and cluster analysis. The general concepts explaining these approaches are discussed below; more detailed information is provided in Section 4.

3.1　Principal Component Analysis

Principal component analysis[2] (PCA) is a widely applied multivariate data analysis method. Graphical output from the method provides insight into the structure of a data set and the relationships between variables comprising the data set. The main objective of PCA is to reduce the dimensionality of data sets consisting of a large number of interrelated variables. This reduction is achieved by transforming the original variables into a new set of variables, the principal components (PCs). The PCs are then ordered such that the first few PCs retain most of the variation present in all of the original variables (Joliffe 1986).

3.2　Cluster Analysis

Cluster analysis comprises several statistical techniques aimed at classifying data by determining underlying data structures or groups (Kauffman and Rousseeuw 1990; Everitt et al. 2011). For a given series of observations, the objective of cluster analysis is to form groups in the data such that the observations are as *similar* as possible *within* groups, but as *dissimilar* as possible *between* groups (Everitt et al. 2011). Unlike typical applications of cluster analysis, the data groups in this study, defined by six spatially distinct areas, are known at the outset—Many Devils Wash, the two analog sites (Salt Creek Wash, Eagle Nest Arroyo), and the three subareas at the Shiprock site (tailings, escarpment, swale). However, if these spatial labels are ignored, and the data set is treated as though the site description information in the previous section was unknown, based on the chemical signatures alone, how would they group? That is one of the questions this analysis attempts to answer.

3.3　Summary

Although the title of this report refers only to multivariate statistical analysis, the approach is really more of a weave—of standard univariate statistical approaches, the subsequent multivariate analysis, and incorporation of the underlying geochemical processes. Incorporating the geochemical processes is imperative because statistical analysis is only meaningful if the underlying science can explain the results. For example, correlations between two or more variables may result from commonality of source or genesis, but they could also be fortuitous and caused by unrelated processes. To the extent possible, all statistical interpretations are augmented by identifying explanatory geochemical factors.

4.0　Methods

4.1　Sampling

Samples from the floodplain wells near the escarpment were collected in September 2011. Sampling for all other locations was conducted on March 21 and 22, 2012 (Table 1).

---

[2] Although sometimes referred to as "principal components analysis" (e.g., Everitt et al. 2011), the singular form of "component" is the original usage based on Joliffe (1986) and is retained here.

Table 1. Groundwater Sampling Location Details

Population	Location	Case ID	Sample Date	Screened Interval (ft bgs)	Sampling Method	Geologic Unit
Escarpment	0610	esc_610	9/13/2011	4 – 9	Low Flow (p)	Qal
Escarpment	0614	esc_614	9/13/2011	10 – 15	Low Flow (p)	Qal
Escarpment	1111	esc1111	9/14/2011	7 – 12	Low Flow (p)	Qal
Escarpment	1112	esc1112	9/13/2011	7 – 12	Low Flow (p)	Qal
Escarpment	1113	esc1113	9/13/2011	7 – 12	Low Flow (p)	Qal
Escarpment	1115	esc1115	9/13/2011	7 – 12	Low Flow (p)	Qal
Escarpment	1118	see Note 2	9/14/2011	Seep	Extraction Pump	Km
Many Devils Wash	EF19	mdw_EF19	3/21/2012	5.2 – 7.6	Low Flow (p)	Qal/Km
Many Devils Wash	EF22	mdw_EF22	3/21/2012	2.8 – 3.8	Low Flow (p)	Qal/Km
Many Devils Wash	1150	mdw1150	3/21/2012	30.6 – 35.6	Bailed	Qal/Km
Many Devils Wash	1151	mdw1151	3/21/2012	27.5 – 32.5	Bailed	Qal/Km
Many Devils Wash	1153	mdw1153	3/22/2012	28.5 – 33.5	Bailed	Qal/Km
Many Devils Wash	1154	mdw1154	3/22/2012	30 – 35	Bailed	Qal/Km
Many Devils Wash	1155	mdw1155	3/22/2012	28 – 33	Bailed	Qal/Km
Many Devils Wash	1156	mdw1156	3/22/2012	26.2 – 31.2	Bailed	Qal/Km
Many Devils Wash	1157	mdw1157	3/22/2012	26.7 – 31.7	Bailed	Qal/Km
Many Devils Wash	1159	mdw1159	3/22/2012	20.2 – 25.2	Bailed	Qal/Km
Many Devils Wash	1049	mdw1049	3/21/2012	4.3 – 9.3	Low Flow (p)	Qal/Km
San Juan River	SJR	see Note 2	3/21/2012	NA	Low Flow (p)	na
Salt Creek Wash	SCWS	SCWS	3/20/2012	Seep	Low Flow (p)	Km
Salt Creek Wash	SCWE7	SCWE7	3/20/2012	Seep	Low Flow (p)	Km
Salt Creek Wash	SCWE10	SCWE10	3/20/2012	Seep	Low Flow (p)	Km
Salt Creek Wash	SCWE14	SCWE14	3/20/2012	Seep	Low Flow (p)	Km
Salt Creek Wash	SCWE15A	SCWE15A	3/20/2012	Seep	Low Flow (p)	Km
Salt Creek Wash	SCWE18	SCWE18	3/20/2012	Seep	Low Flow (p)	Km
Swale	0812	sump812	3/23/2012	51.3 – 61.3	Bailed	Qal/Km
Swale	1070	sump1070	3/21/2012	52.5 - 62	Extraction Pump	Qal/Km
Swale	1078	sump1078	3/21/2012	35.5 – 45	Extraction Pump	Qal/Km
Tailings	0817	tails817	3/22/2012	21.6 – 31.6	Low Flow (b)	Km
Tailings	0826	tails826	3/22/2012	10 – 20	Low Flow (p)	Qal/Km
Tailings	1007	tails1007	3/23/2012	36.8 – 46.3	Bailed	Qal/Km
Tailings	1074	tails1074	3/23/2012	27 – 36.5	Low Flow (b)	Qal
Eagle Nest Arroyo	UENA21	UENA21	3/20/2012	Seep	Low Flow (p)	Km
Eagle Nest Arroyo	UENAS	UENAS	3/20/2012	Seep	Low Flow (p)	Km

(b) = bladder pump, (p) peristaltic pump, bgs = below ground surface, Km = Cretaceous Mancos Shale,
NA = not applicable, Qal = Quaternary alluvium (alluvium)

Notes

1. Case IDs listed above are the abbreviated sample locations used in subsequent PCA and cluster analysis plots. MDW, SCW, and UENA denote samples from Many Devils Wash, Salt Creek Wash, and Eagle Nest Arroyo areas, respectively. The escarpment is simplified to "esc," the swale to "sump" (based on terminology in DOE 2000), and tailings to "tails." Eagle Nest Arroyo samples used in this study have the UENA prefix to distinguish them from a sample location previously established in a lower part of the drainage, just above its confluence with the San Juan River (seep sample 1220; DOE 2012c).

2. As explained in Section 4.3.1, two sample locations listed above were not used in the statistical evaluation: the San Juan River sample (SJR) and escarpment seep sample 1118.

All seeps sampled for this study issued from Mancos Shale bedrock. Seeps flowed at low rates (generally less than 0.5 liter [L] per minute), and samples were collected from small (typically about 2 ft diameter by 2 ft deep) pits dug into the seepage zone. Water was purged from the pits, usually 2 to 3 times, to ensure that groundwater was seeping directly from Mancos Shale. Water was pumped through a flow-through, air-exclusion sampling cell. A YSI sonde immersed in the sampling cell was used to measure dissolved oxygen, oxidation-reduction potential, pH, specific conductivity, and temperature. After these parameters stabilized, usually after about 1 to 3 L of purge, the sample was collected. The sample was passed through an in-line, 0.45 micrometer (μm) filter prior to collection in Nalgene bottles.

Shallow wells were sampled with a peristaltic pump and deeper wells with a bladder pump or bailer (Table 1). The pump intake was positioned in the middle of the well screen, and flow was maintained at a rate of about 250 milliliters per minute until about 1 to 3 L of water was purged. The same method described above was used for seeps; samples were collected through a 0.45 μm filter after field-measured parameters had stabilized. For wells that were bailed (Table 1), several passes were made with the bailer, sufficient to remove about 3 L, prior to sampling. Following purging, a 1 L Nalgene bottle was filled, and parameters were measured by immersing an YSI sonde. Parameters were measured a second time to ensure stability. Samples were then collected through a 0.45 μm filter using a peristaltic pump.

At the locations labeled "extraction pump" in Table 1, samples were collected from spigots installed on the pumping system used to extract the groundwater for remediation. Samples were taken after purging for several minutes. A peristaltic pump was used to pump water through a flow-through cell, and filtered samples were collected using the same methods as described above.

All samples were kept cooled to below 4 $^{\circ}$C until analysis. Samples for analysis of boron (B), calcium (Ca), iron (Fe), magnesium (Mg), manganese (Mn), molybdenum (Mo), potassium (K), sodium (Na), selenium (Se), and uranium (U) were preserved at pH less than 2 with nitric acid. Samples for analysis of ammonia (NH_3), chloride (Cl), color, dissolved organic carbon (DOC), nitrate (NO_3), and sulfate (SO_4) were kept cool but not otherwise preserved. Unpreserved samples were analyzed soon after collection to minimize constituent degradation. Analyses of Cl, NO_3, and SO_4 were completed within 5 days of sample collection, and color, DOC and NH_3 within 8 days.

4.2   Laboratory Analysis

The following analysis methods were used for the samples collected in March 2012. Similar methods were used for the escarpment samples collected during the previous year (DOE 2012c). Alkalinity was measured in the field on filtered (0.45 μm) samples by titration with sulfuric acid. The pH endpoint was determined using a visual color change of a bromocresol green–methyl red indicator solution. Bicarbonate (HCO_3) was determined from alkalinity and pH. Boron (B), Ca, Fe, K, Mg, Mn, Mo, Na, and Se were analyzed by inductively coupled plasma optical emission spectrometry. Chloride, NO_3, and SO_4 concentrations were determined by ion chromatography and U by laser-induced kinetic phosphorescence.

Dissolved organic carbon was determined by digesting a filtered sample in persulfate at 105 °C to liberate carbon dioxide and measuring the resulting pH change, after removing inorganic carbon in acid. Color was determined on filtered samples by absorbance of the 420 nanometer light wavelength and comparison to a platinum-cobalt (Pt-Co) standard.

For all analyses, independent standards were measured regularly to confirm instrument accuracy. Independent standards are standards from a different batch or vendor than were used for instrument calibration. Standard additions and duplicates were analyzed on at least every 10 samples. As a measure of data quality, samples collected in March 2012 had relatively small charge balance errors of ±3 percent. Charge balance errors (CBEs) are a traditional gauge for evaluating the quality of water chemistry analyses (Fritz 1994), where larger CBEs (e.g., >5–10 percent) may indicate laboratory error or that not all ions have been captured in the analysis.

4.3   Statistical Methods

A three-step approach was used to assess the data for the six sample populations: (1) univariate analysis (analysis of individual chemical parameters); (2) characterization of major ion concentrations using traditional geochemical plotting tools; and (3) multivariate analysis (principal component analysis and cluster analysis). The univariate analysis made use of standard exploratory data analysis methods that depict the distributions of measured chemical parameters within each study area (variable size symbol plots and box plots). Summary statistics (means and coefficients of variation) were also calculated. The variable size symbol plots were produced using RockWorks (Rockware 2012); univariate statistical plots and summary statistics were generated using Statistica Version 10 (StatSoft, Inc. 2004–2011) and XLSTAT Version 2012.2.03 (Addinsoft 1995–2012). The concentrations of major ions in the respective study areas were depicted using Piper (trilinear) and Stiff diagrams, as produced by the RockWorks package.

The multivariate analyses, consisting of PCA and cluster analysis, were conducted using XLSTAT Version 2012.2.03 and the R cluster package, respectively. Similar to approaches used by Güler et al. (2002) and Cloutier et al. (2008), the multivariate techniques were initially applied to the major ions (Na, Cl, Ca, Mg, SO_4, K, HCO_3). Use of the major ions enabled comparisons of the statistical analyses with the Piper and Stiff diagrams. The multivariate techniques were then applied to a larger (expanded) data set that included the primary Shiprock site and Many Devils Wash contaminants (NO_3, Se, and U).

There is no single, recommended approach to conducting PCA or cluster analysis (Joliffe 1986; Everitt et al. 2011; Khattree and Naik 2000; Schuenemeyer and Drew 2011). Selection of the appropriate technique to employ requires examination of the raw data and understanding of the computational impacts of applying various approaches. For both PCA and cluster analysis, proper data preparation is required. The remainder of this section discusses the specific multivariate techniques employed and documents the rationales for using them.

For detailed discussions of multivariate statistical methods and underlying mathematical theory, the reader is referred to the books by Joliffe (1986) and Everitt et al. (2011). The overview provided in Khattree and Naik (2000) is recommended as well.

4.3.1 Data Preparation

Factors that need to be considered prior to conducting multivariate statistical analyses include the variables and cases to include in the analysis, the representativeness of the data, and whether or not to weight or transform variables.

Variables Selected for Analysis

Ten variables (chemical parameters) were chosen for multivariate analysis in this study because they met a primary selection criterion of being representative of water-rock interactions. The ten variables consisted of the major ions—Na, K, Ca, Mg, Cl, SO_4, and HCO_3—and the contaminants NO_3, Se, and U.

Rationales for excluding additional parameters are documented below:

- CO_3 was excluded because the carbon inventory in groundwater is dominated by HCO_3. Also, preliminary PCA results indicated that CO_3 was not an influential variable (i.e., it was not well represented on the principal components).

- Fe and Mo were excluded due to a high proportion of nondetects in all six study populations (study areas).

- Although Mn concentrations were elevated in groundwater samples from the Shiprock site tailings area and, to a lesser extent, in the escarpment area, Mn was not detected in about 60 percent of non-Shiprock site samples (Table 3). Although nondetect concentrations could be replaced with numerical surrogates (e.g., the detection limit or one-half the detection limit), Helsel (2010) cautions about the dangers of such simplified substitutions. Therefore, Mn was excluded from the quantitative analysis.

- As with Mn, NH_3 was excluded despite the fact that it is detected at elevated levels in groundwater samples from the Shiprock tailings area. NH_3 is temporally and spatially variable, perhaps because of its high volatility.

- Although potentially representative of water-rock interactions, boron (B) was excluded because, as with DOC and color, it was not analyzed in escarpment area samples. Also, it was not possible to verify whether measured concentrations were representative of the six study areas because little to no historical data are available for this constituent.

- Field parameters alkalinity, pH, and specific conductance were excluded because they are redundant (strongly correlated) with other parameters used in the analysis (e.g., alkalinity is strongly correlated with HCO_3).

Some variables that were excluded from the quantitative multivariate analyses were included in the univariate analysis, or were used as supplementary qualitative variables in the PCA.

Cases Selected for Analysis

With two exceptions, all sample locations listed in Table 1 were used in the multivariate statistical analysis. The San Juan River sample (SJR) was excluded because it represents river (vs. ground-) water and is therefore not germane to this study. Also, it is an outlier due its very low solute concentrations. The groundwater sample from escarpment location 1118 was excluded because it consists of mixed water from two seep locations on the escarpment face and is not representative of floodplain groundwater at the base of the escarpment. Although not

included in the multivariate analyses, the river and escarpment 1118 samples were included in the graphical depictions of major ion chemistry using Piper and Stiff diagrams.

Consideration of Temporal Variability

Temporal (seasonal) variability of chemical parameters was assessed prior to performing statistical analyses. For most locations, the data used in this analysis, from sampling events in September 2011 and March 2012, were found to be consistent with historical results. Although some exceptions to this general finding were observed in samples collected from the tailings and swale areas, analyte concentrations at sample locations on the Shiprock site have tended to remain uniform over time.

Variable Standardization or Transformation

Many investigators use log or *z*-score transformations to standardize the data (Güler et al. 2002; Cloutier et al. 2008). Consistent with the approach used by Schryver et al. (2006) in another investigation of the Shiprock site, for this study, chemical data were rescaled to values between 0 and 1 based on the range. This approach is consistent with recommendations in Everitt et al. (2011), who note that standardization using the range showed good recovery of clusters and "should be considered as an alternative to the more usual standardization using standard deviations." Data were standardized only for cluster analysis, not for PCA. The raw data were used for PCA because the underlying correlation matrix has the effect of standardizing the data.

4.3.2   Principal Component Analysis

PCA is used to reduce the dimensionality of a data set with correlated variables by creating new uncorrelated variables (the PCs) that are linear combinations of the original data (Joliffe 1986). When conducting PCA, the investigator must decide what type of matrix (correlation or covariance) to use, and how many factors (or principal components) to retain. Additionally, the presence of outliers must be accounted for.

Joliffe (1986) states that although the assumed requirement of a normal distribution may not necessarily be problematic, outliers can have a disproportionate effect on the PCs. Outliers are present in this data set, and further examination indicated that those results are legitimate. Therefore, a robust estimation technique based on the Spearman (rank-based) correlation matrix was used because it is less sensitive to extreme values than the more commonly applied (default) Pearson correlation matrix.

There is no clear consensus on the number of PCs to retain. A general rule established by Jolliffe (1986) suggests retaining only those components with eigenvalues (the measure of variability associated with the PCs) greater than 0.7. A more stringent, and also more practical, criterion is the Kaiser criterion, in which only the components with eigenvalues greater than 1 are retained (Kaiser 1960). The Kaiser criterion was used in this study; however, only the first two PCs, those PCs accounting for most of the variability in the data set, were used for graphical purposes. Similar to factor analysis, a related multivariate analysis technique, with PCA the investigator has an option to rotate the axes (e.g., using a Varimax rotation method). Preliminary rotations did not facilitate interpretation of the data so this approach was not used.

Although PCA is a descriptive rather than inferential technique, it is possible to test for the significance of the discrimination of the objects on the principal components. Therefore, factor scores of the objects (cases) saved for the retained PCs were used in an analysis of variance (ANOVA) to assess whether significant differences could be detected between groups. Residuals, the difference between actual and predicted values, were examined to ensure that distributional assumptions were met. Theoretically, residuals should be normally distributed ($< \pm 3$); for this data set, all residuals were within ± 2.

4.3.3 Cluster Analysis

Cluster analysis was performed using two techniques. First, an agglomerative hierarchical clustering (AHC) approach was applied using the R (cluster) script, Ward's method, and Euclidean distance measure. This method was chosen because of its widespread application (Schryver et al. 2006; Güler et al. 2002). As a verification step, and to provide an approach that is more robust with respect to outliers, an alternate method referred to as Partitioning Around Medoids (PAM) was used (again using the R cluster script). Factors that must be considered prior to conducting cluster analysis include deciding which cases and variables to include and what standardization approach, if any, to use; the clustering method and corresponding distance measure; and the number of clusters to use (Everitt et al. 2011). These factors are summarized below along with identification of the specific approaches used in this study.

Objects (Sample Data) to Cluster

Only 32 locations were sampled for this study, a rather small data set for cluster analysis. Therefore, despite the presence of extreme values or outliers in the data set, all cases were retained.

Variables to Include and Standardization Approaches

According to Everitt et al. (2011), irrelevant or "masking" variables, or variables that play no role in defining the clusters, should be excluded if possible. Initial PCA results were useful for this purpose because correlated variables were identified, as were the variables that were not well represented. As discussed above, the raw data were rescaled based on the range prior to performing the cluster analysis.

Clustering Method

There are two basic approaches to clustering techniques: hierarchical and partitioning. Both approaches were applied in this analysis. The more traditional hierarchical methods can be further subdivided into two categories: agglomerative (ascending, forming one cluster from two or more existing clusters) and divisive (descending). For this study, only agglomerative hierarchical clustering methods were used. The primary output of a hierarchical cluster analysis is a dendrogram, a graphic reminiscent of a tree, in which the branches are the clusters and the leaves the data objects.

Agglomerative hierarchical clustering approach options include single linkage, complete linkage, weighted and unweighted pair group average linkage, centroid linkage, and Ward's method. Ward's method was used for this analysis because it is commonly applied in the literature germane to this study (Güler et al. 2002: Cloutier et al. 2008). One of the reasons it is widely applied is that it tends to yield spherical clusters of the same size (i.e., classification variables

over all classes essentially have the same variance). However, Ward's method is also sensitive to outliers (Everitt et al. 2011).

Following the application of Ward's method, the PAM (partitioning) method was also applied because this technique is robust to outliers. PAM is similar to the more widely known k-means algorithm in that the number of clusters must be specified in advance. However, instead of using a centroid (mean-based value) as the cluster center, it computes medoids (similar to medians), the most centrally located object in a cluster (Kaufman and Rousseeuw 1990: Pison et al. 1999). PAM was run iteratively using the R script to yield partitions into two to six groups. Because six sample populations were defined in this study (Figure 2), it was useful to examine how they would extract from the data. Whereas hierarchical methods yield a dendrogram, partitioning methods yield a plot referred to as a clusplot (Kaufman and Rousseeuw 1990: Pison et al. 1999), in which clusters are displayed as spheres and the distance between objects is more apparent.

Distance (Proximity) Measure

The more commonly applied distance measures are Euclidean distance, squared Euclidean distances, and Manhattan (city block) distances (Güler et al. 2002; Cloutier et al. 2008). Euclidean distance was used in this study because it is invariant under translations of the origin and rotations of pattern space (Dubes and Jain 1995). Euclidean distance is the shortest distance (a straight line) between any two objects. Given two objects (or sample locations) a and b, based on two variables x and y, the Euclidean distance (d_E) is calculated as:

$$d_E = \sqrt{(x_a - x_b)^2 + (y_a - y_b)^2}$$

As demonstrated later, some variables (most notably Na, SO_4, and Cl) were found to be strongly correlated. To ensure that this correlation (or collinearity) in variables would not bias the analysis, the Mahalanobis distance, a measure less sensitive to redundancy in variables, was also used as a verification step.

Determining the Number of Clusters

Using the agglomerative clustering (Ward's) method, it is not clear at the outset how many clusters (based on the branching) are meaningful. Although partitioning methods require that the number of clusters is pre-defined, a means for determining the number of clusters that yield the most meaningful solution is necessary. For this analysis, the "optimal" number of clusters was determined using a technique developed by Kauffman and Rousseauw (1990), which uses average silhouette widths.[3] With this approach, each cluster member (each sample) is represented by a silhouette, which graphically represents the cluster's tightness and separation and overall validity. The average silhouette width is used to select an optimal (or appropriate) number of clusters. Because this approach is more easily understood when discussed along with the presentation of results, further discussion is reserved for Section 5.3.2.

Table 2 summarizes the sequence of multivariate analytical techniques employed and identifies the variables that were used at each stage of the analysis.

---

[3] Although the term "optimal" is sometimes used in this report, a certain amount of subjectivity is inherent to cluster analysis. There is no true single cluster solution, even when numerical approaches for optimization or verification are employed.

U.S. Department of Energy   Multivariate Statistical Analysis to the Origin of Contamination–Shiprock, NM
December 2012   Doc. No. S09257
Page 15

Table 2. Sequence of Multivariate Analyses and Samples/Variables Used

Multivariate Method	Variables Used	Comment
Major Ion Data Subset (results in Section 5.3)		
PCA, based on Spearman correlation matrix (XLSTAT)		The supplementary variables were included to facilitate understanding of correlations, but these did not affect the numerical analysis. Object groupings based on factor scores then tested using ANOVA.
Cluster Analysis—Agglomerative Hierarchical Clustering (AHC) using Ward's method (R script)	Ca, Mg, Na, K, Cl, SO_4, HCO_3 (*n*=7 variables; *n* = 32 cases) Supplementary Variables: pH, alkalinity	Ward's AHC method is commonly applied in the literature; this yields the most commonly presented graphical output (the dendrogram). Silhouette plots were used to test cluster structure. Analysis based on Euclidean distance measure (Mahalanobis distance measure used as a verification step)
Cluster Analysis using Partitioning Around Medoids (PAM; R script)		The PAM partitioning technique was applied because it is more sensitive to outliers.
Extended Suite of Analytes (results in Section 5.4)		
PCA (Spearman correlation matrix)	Major ions (Ca, Mg, Na, K, Cl, SO_4, HCO_3) + NO_3, Se, and U (*n*=10 variables; *n* = 32 cases)	Supplementary variables were the $^{234}U/^{238}U$ activity ratios (ARs), Mn, NH_3 (Table 3).
AHC Cluster Analysis using Ward's Method	Major ions (Na, K, Cl, SO_4, HCO_3) + NO_3, Se, and U (*n*=8 variables; *n* = 32 cases)	Ca and Mg were excluded because, based on the 2nd PCA, these variables were not well represented.
Cluster Analysis using PAM		See above.

5.0   Results and Discussion

Analytical results from the March 2012 sampling event and the September 2011 sampling of the floodplain escarpment area are provided in Table 3. These data are used to compare individual and multivariate chemical signatures, focusing on contrasts (or similarities) between Many Devils Wash and other areas. This section begins by presenting the results of the univariate analysis. Major ion data are then evaluated using traditional geochemical plotting tools (Piper and Stiff diagrams). Finally, PCA and cluster analysis are applied to the major ion subset and to the larger data set that includes the primary contaminants at the Shiprock site and Many Devils Wash (NO_3, Se, and U).

Table 3. Analytical Results

| Population | Sample ID | Field Parameters | | | Major Ions | | | | | | | Others | | | Supplementary Variables | | | | | |
		pH (s.u.)	Alkalinity (mg/L as CaCO$_3$)	Spec. Cond. (µS/cm)	Na (mg/L)	K (mg/L)	Ca (mg/L)	Mg (mg/L)	Cl (mg/L)	SO$_4$ (mg/L)	HCO$_3$ (mg/L)	NO$_3$ (mg/L)	Se (µg/L)	U (µg/L)	AR	NH$_3$ (mg/L)	Mn (mg/L)	B (µg/L)	DOC (mg/L)	Color (Pt-Co)
Eagle Nest Arroyo	UENA21	7.0	282	29,230	6,940	50.9	434	1,390	4,390	13,300	343.7	877	249	51	2.02	2.0	<0.05	1,060	32	2
	UENAS	7.3	332	26,930	6,170	44.4	472	1,200	3,870	12,100	404.2	838	336	38.8	2.03	3.0	<0.05	850	23	<25
Salt Creek Wash	SCWE7	7.5	970	32,850	9,070	95.2	427	1,130	1,960	20,200	1,179	1,670	2,390	145	2.64	2.0	<0.05	851	48	398
	SCWE10	7.3	992	29,340	7,790	74.2	406	1,170	1,590	18,300	1,208	1,120	1,400	155	2.11	1.0	<0.05	652	64	424
	SCWE14	7.3	1,190	40,570	10,400	113.0	474	1,730	4,990	21,500	1,449	2,340	2,560	209	2.85	1.0	<0.05	779	80	545
	SCWE15A	7.4	594	21,170	5,020	48.9	416	839	1,450	10,800	723	1,520	1,490	140	2.00	1.0	<0.05	957	46	218
	SCWE18	6.9	964	24,770	7,120	70.3	389	525	932	15,100	1,175	599	1,090	99	2.43	1.0	0.26	824	29	284
	SCWS	7.1	1,026	39,020	11,100	92.6	407	1,010	3,980	20,000	1,250	2,050	2,280	142	3.38	1.0	0.45	482	61	267
Many Devils Wash	mdw_EF19	7.2	680	30,610	8,560	56.8	408	1,080	1,250	17,500	828.3	3,180	1,560	156	2.51	2.0	<0.05	766	34	211
	mdw_EF22	7.2	604	29,490	7,990	43.4	394	1,330	1,440	18,100	735.8	2,590	1,620	188	2.42	3.0	<0.05	765	40	186
	mdw1049	7.3	592	28,480	7,420	54.6	440	1,350	1,470	17,500	720.7	2,270	1,220	154	2.42	3.0	<0.05	1,040	33	149
	mdw1150	7.3	644	29,510	7,840	85.8	432	1,210	1,360	17,800	784.1	2,660	1,440	158	2.52	1.0	<0.05	923	37	186
	mdw1151	7.5	548	25,950	6,460	50.6	428	1,500	1,590	16,500	666.5	1,700	820	149		2.0	0.063	1,220	32	118
	mdw1153	7.7	720	29,200	7,350	66.7	431	1,340	1,550	17,900	873.8	2,410	1,140	172		4.0	0.68	992	50	320
	mdw1154	7.3	580	25,230	6,040	48.0	416	1,520	1,540	15,800	706	1,390	627	139	2.19	2.0	0.066	1,430	31	110
	mdw1155	7.6	580	26,000	6,420	56.2	442	1,510	1,570	16,200	705	1,430	453	153		4.0	0.44	1,350	37	195
	mdw1156	7.1	592	24,150	5,660	38.0	417	1,580	1,460	15,000	721.2	1,250	569	150	2.15	5.0	<0.05	1,480	21	87
	mdw1157	7.2	566	24,110	5,540	42.4	426	1,510	1,440	15,100	689.3	1,210	556	148		1.0	0.16	1,600	31	96
	mdw1159	7.4	565	20,200	4,370	25.9	424	1,340	1,100	11,900	687.3	860	388	106	2.45	2.0	0.10	1,460	23	64
Swale	sump812	6.9	668	33,650	7,220	81.9	486	2,640	2,560	17,000	814.3	6,670	5,660	144		3.0	0.11	590	36	153
	sump1070	7.1	636	27,370	6,720	79.5	431	1,340	1,200	15,700	774.8	2,900	2,730	82.9	2.75	5.0	0.12	510	23	152
	sump1078	7.1	628	25,230	6,100	68.3	429	1,180	1,070	14,600	765.3	2,850	2,730	129	2.18	6.0	0.11	589	34	161
Tailings	tails817	6.4	1,350	21,850	1,780	238	499	1,970	505	11,100	1,647	2,750	52	9,280	0.99	840	2.3	860	32	164
	tails826	6.4	1,575	18,430	2,420	132	448	2,640	563	13,700	1,921	812	68	3,660	1.07	100	2.5	944	31	227
	tails1007	6.4	1,440	21,050	3,280	116	487	2,490	606	13,300	1,756	2,360	167	2,480	1.11	26	2.0	1070	52	251
	tails1074	6.6	1,185	20,360	2,410	52.8	619	2150	1,130	7510	1,445	5,330	523	2,110	1.12	2.0	0.98	3,310	59	263
Escarpment	esc_610	7.0	374	11,109	1,300	150	520	1,000	220	6400	455.8	1,595	140	1,100	1.03	2.3	0.06			
	esc_614	7.1	583	12,787	1,500	150	420	1,200	290	8600	710.4	930	630	1,500	1.05	31.0	2.40			
	esc1111	6.8	1,178	13,307	2,100	73.0	390	1,100	400	8500	1,436	142	300	950		0.5	0.95			
	esc1112	7.0	689	14,147	1,900	130	430	1,300	330	9200	839.8	1,285	1000	1,500		25.0	2.20			
	esc1113	7.0	445	9,669	1,000	130	490	830	190	5500	542.4	1,285	30	760		25.0	1.80			
	esc1115	6.7	934	15,565	1,500	180	380	1,300	310	8500	1,139	2,569	140	1,400		320	3.20			
San Juan River	SJR	8.3	98	512	35	2.4	62.4	35.0	13.0	131	117.2	2.0	<10	1.5		2.0	0.016	45.5	2.9	<25

Alternate shading is used to denote the six different spatial groups evaluated. Chemical parameters in red denote the primary variables used in the analysis.
Bicarbonate (HCO$_3$) was calculated from alkalinity and pH. ^{234}U/^{238}U activity ratios (ARs) for escarpment area locations are from samples collected in 2001.
s.u. = standard units; mg/L = milligrams per liter; µS/cm = microsiemens per centimeter; µg/L = micrograms per liter

5.1   Univariate Statistical Analysis

Univariate analysis was used in this study to examine the distributions in the data and to identify outliers. Distributions of the primary Many Devils Wash contaminants (NO_3, Se, SO_4, and U) are illustrated using variable size symbol (VSS) plots (Figure 4), and box plots (Figure 5) are used to better illustrate the spread in the data. Box plots also facilitate comparisons of central tendency, based on the mean or median concentrations, between groups.

Nitrate concentrations are highly variable. The most elevated concentrations are observed in the swale area (about 3,000 to 7,000 milligrams per liter [mg/L]), and the next highest concentrations are seen in the tailings area. These two areas also exhibit the greatest variability in nitrate concentrations (Figure 5a). Moderate nitrate concentrations (about 2,000–3,000 mg/L) are present in the northernmost arroyo portion of Many Devils Wash, in Salt Creek Wash, and in the easternmost escarpment area location (1115). Eagle Nest Arroyo and the northwestern escarpment area have relatively low nitrate concentrations.

Selenium concentrations are distinctive among the populations, with the highest values (about 3,000 to 6,000 mg/L) occurring in the swale area and low values in Eagle Nest Arroyo, tailings, and escarpment areas (Figure 4b). The Se concentration at location 812 in the swale area is an extreme value relative to other observations (Figure 5b). Moderate Se concentrations were measured in groundwater near the Many Devils Wash seeps and in Salt Creek Wash. Low selenium concentrations were measured in the two samples from Eagle Nest Arroyo and in several samples from southern Many Devils Wash.

Sulfate concentrations are highest in Salt Creek Wash, the swale area, and the arroyo portion of Many Devils Wash (Figure 4c). Mean concentrations in these areas range from about 16,000 to 18,000 mg/L (Figure 5c). Moderate sulfate concentrations are present in Eagle Nest Arroyo, the tailings area, and at the southernmost location (mdw1159) in Many Devils Wash. Sulfate concentrations in the escarpment and tailings areas are distinctly lower than those observed in other sample populations (Figure 5c).

Uranium concentrations are highest in the tailings and escarpment areas, and these high concentrations mask the distributions in other areas (Figures 4d and 5d). U concentrations in the tailings area vary widely (from about 2,000 to 9,000 micrograms per liter [µg/L]), while concentrations in the escarpment area are moderate (about 1,000 µg/L) but still notably higher than in other areas. Excluding tailings and escarpment results, U concentrations are highest in Salt Creek Wash and Many Devils Wash samples. U concentrations are lower and quite variable in the swale area and are the lowest and the least variable in Eagle Nest Arroyo samples. With only one exception (the minimum UENA uranium result), concentrations of NO_3, SO_4, and U measured in the Salt Creek Wash and Eagle Nest Arroyo samples exceed corresponding groundwater protection standards (Title 40 *Code of Federal Regulations* [CFR] Part 192 maximum concentration limits).
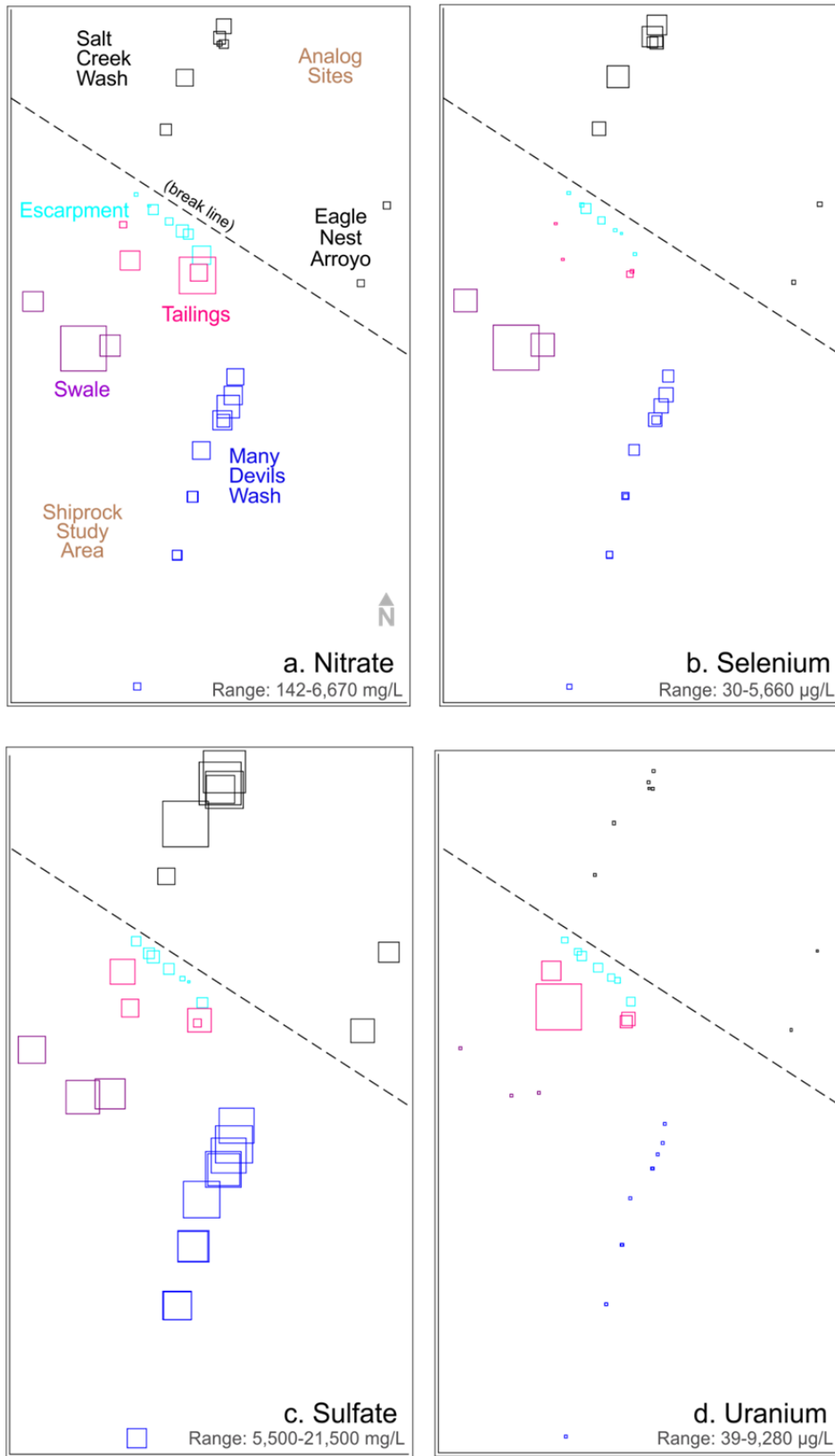
Figure 4. Relative Concentrations of a. Nitrate, b. Selenium, c. Sulfate, and d. Uranium
The size of symbols is proportional to concentration. For clarity of presentation, Salt Creek Wash and Eagle Nest Arroyo analog sites are shown closer to the mill site than their actual locations (see Figures 1 and 2). Escarpment data are from September 2011; all other data are from March 2012.
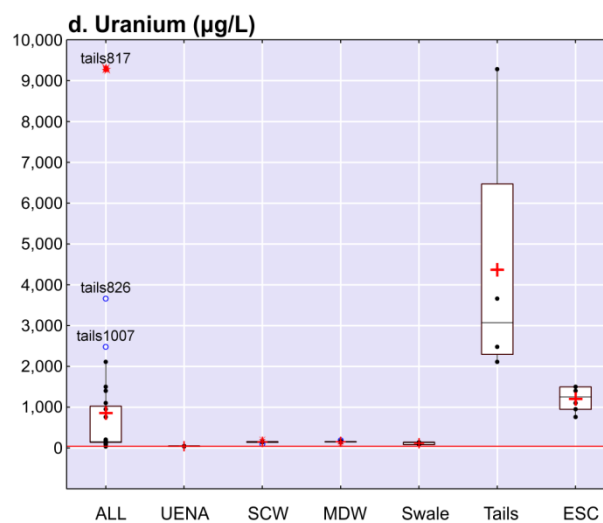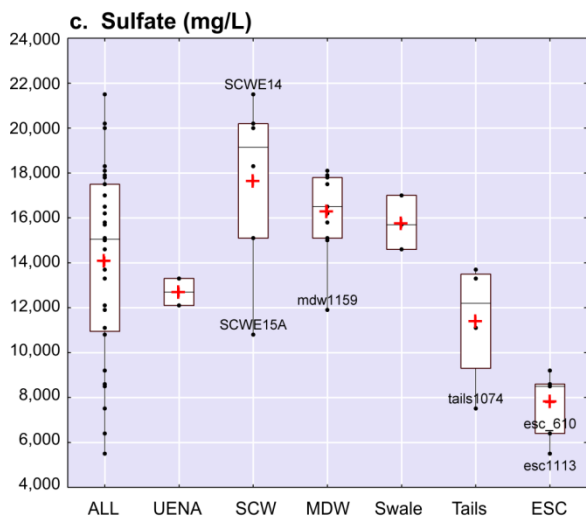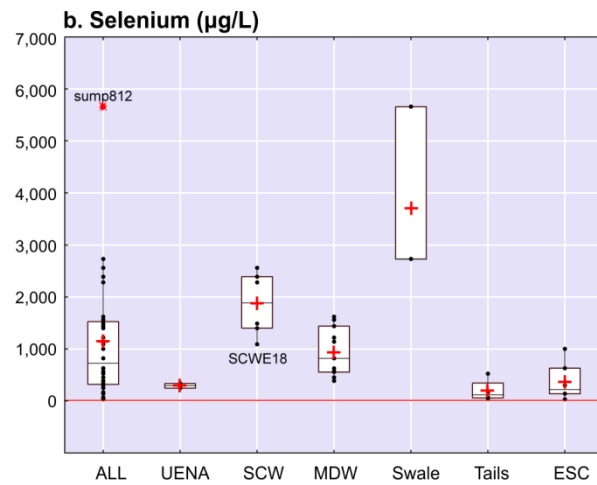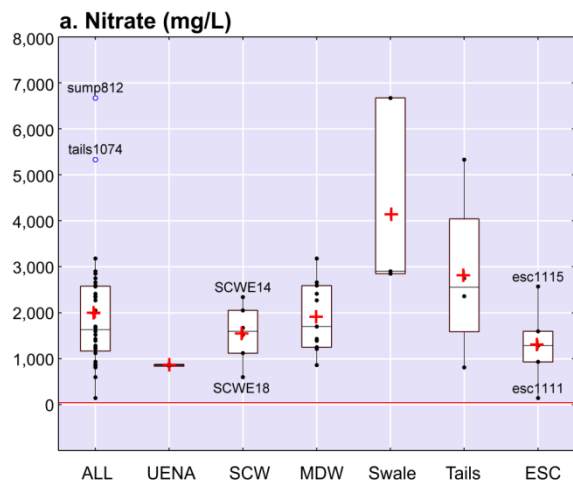
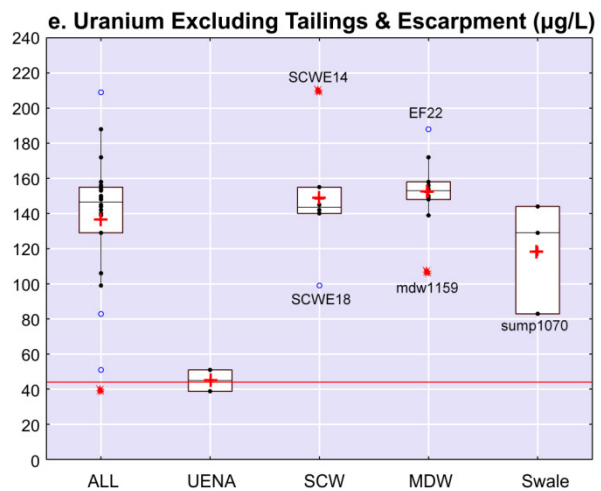Figure 5. Box Plots of Nitrate (a), Selenium (b), Sulfate (c), and Uranium (d & e)

These plots show the distribution of the variables by area. The left-hand column in each plot combines all results to facilitate identification of outliers and the overall spread in the data. Uranium is plotted twice (d & e) because elevated tailings and escarpment results mask the distributions in other areas.

Figure 6 plots distributions for the remaining analytes addressed in the multivariate analysis, the major ions. (The plot for sulfate is duplicated from Figure 5c.) Specific conductance is plotted in Figure 6 because it is a useful indicator of dissolved solids concentrations. Figure 7 presents box plots for the supplementary variables pH, B, alkalinity, Mn, NH$_3$, and ^{234}U/^{238}U activity ratios.

Na and SO$_4$ concentrations in Salt Creek Wash, Many Devils Wash, and the swale area are elevated relative to those in the tailings and escarpment (Figure 6). A similar but less marked pattern is evident for Cl, with the highest concentrations observed in Eagle Nest Arroyo samples. In contrast, the opposite trend is apparent for K, which is generally highest (although some overlap is apparent) in the tailings and escarpment samples. HCO$_3$ concentrations vary widely but are clearly elevated in the tailings area samples. A similar trend is apparent for Mg; concentrations are less variable but are still most elevated in the tailings area. Ca is less discriminating—concentrations are fairly uniform in most study areas (the analog site samples, Many Devils Wash, and the swale) and more variable, although not notably different, in the tailings and escarpment areas. Distributions of specific conductance parallel the variation and between-group differences shown for Na and SO$_4$.

In Figure 7, discrimination between the tailings area and other sample populations is apparent for all variables except boron. Mn, NH$_3$, and pH are clearly discriminating, as are the ^{234}U/^{238}U activity ratios. Boron (which was not analyzed in escarpment samples) shows no apparent overall pattern, but distributions within Many Devils Wash are interesting in that concentrations in southern (upgradient) Many Devils Wash wells are elevated relative to those in the northern area of the wash. This finding is consistent with results for several isotopic signatures documented in the companion isotope study (DOE 2012a), possibly suggesting separate water sources of upgradient and downgradient groundwater.

Figures 4 through 7 illustrate the complex nature of the data and demonstrate the need for an alternative data visualization approach. Differences in constituent concentrations between the sample populations are apparent for several constituents, especially when comparing tailings area samples with those from other areas. However, no clear, consistent pattern or correlations between variables are evident. This is one of the main reasons this multivariate analysis was undertaken.

Table 4 presents descriptive statistics—means and coefficients of variation (CVs)—for the variables used in this study. CVs, equivalent to the arithmetic mean divided by the standard deviation, are useful measures of variability that allow comparison between parameters measured on a different scale or with different magnitudes. Eagle Nest Arroyo results are the least variable, with most CVs less than 0.1 (but this group has only two samples). Many Devils Wash results are also uniform for most constituents. For most analytes, the greatest variability is found in the tailings area samples.
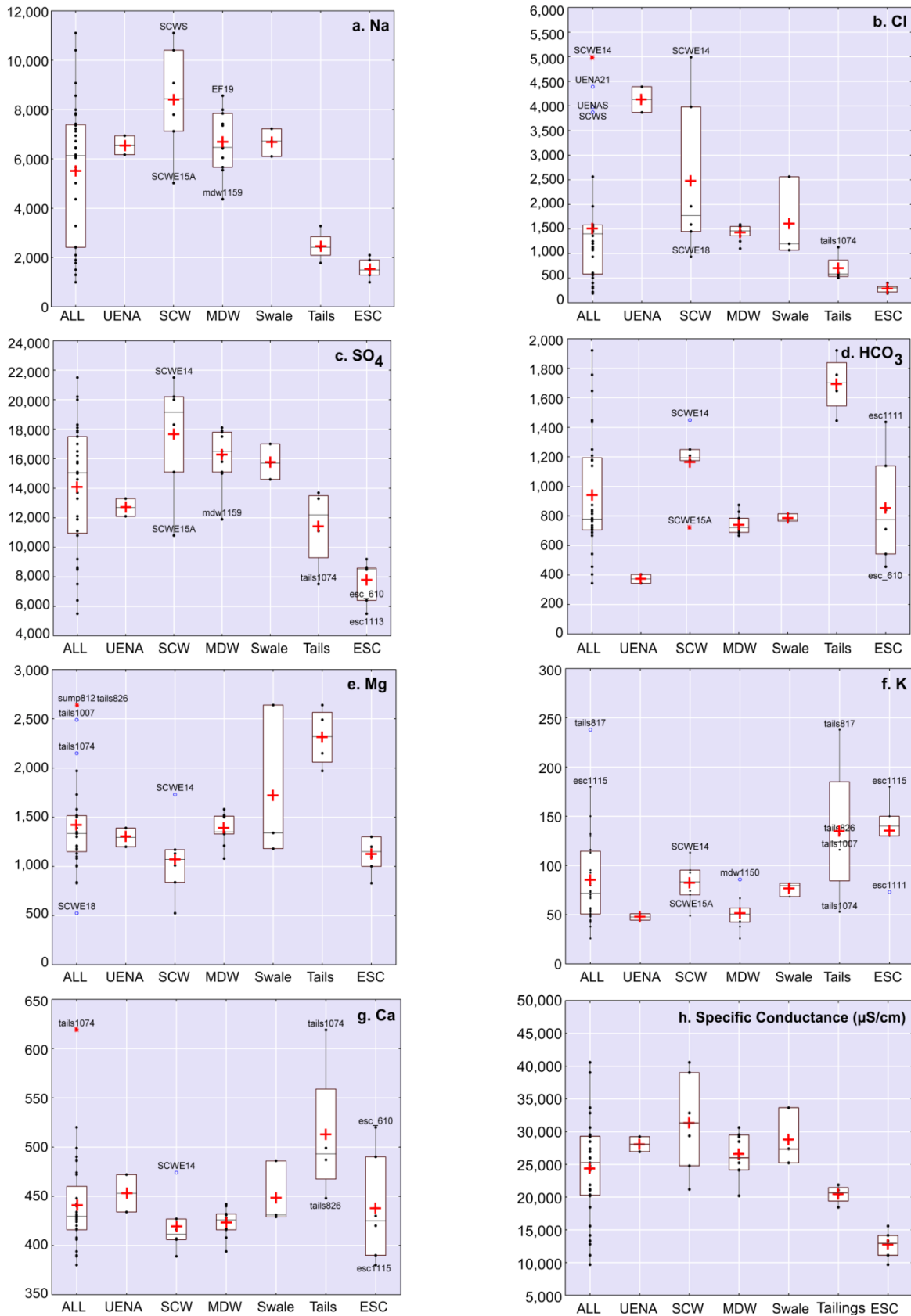
Figure 6. Distributions of Major Ions and Specific Conductance by Study Area

See legend from Figure 5; note the differing distributions between study areas apparent for each variable.

Figure 7. Box Plots of Supplementary Variables

See legend from Figure 5. These variables were not used in the multivariate analysis but were addressed as supplementary variables. The greatest discrimination is evident for pH, Mn, NH$_3$, and $^{234}U/^{238}U$ activity ratios.

Table 4. Descriptive Statistics by Study Area

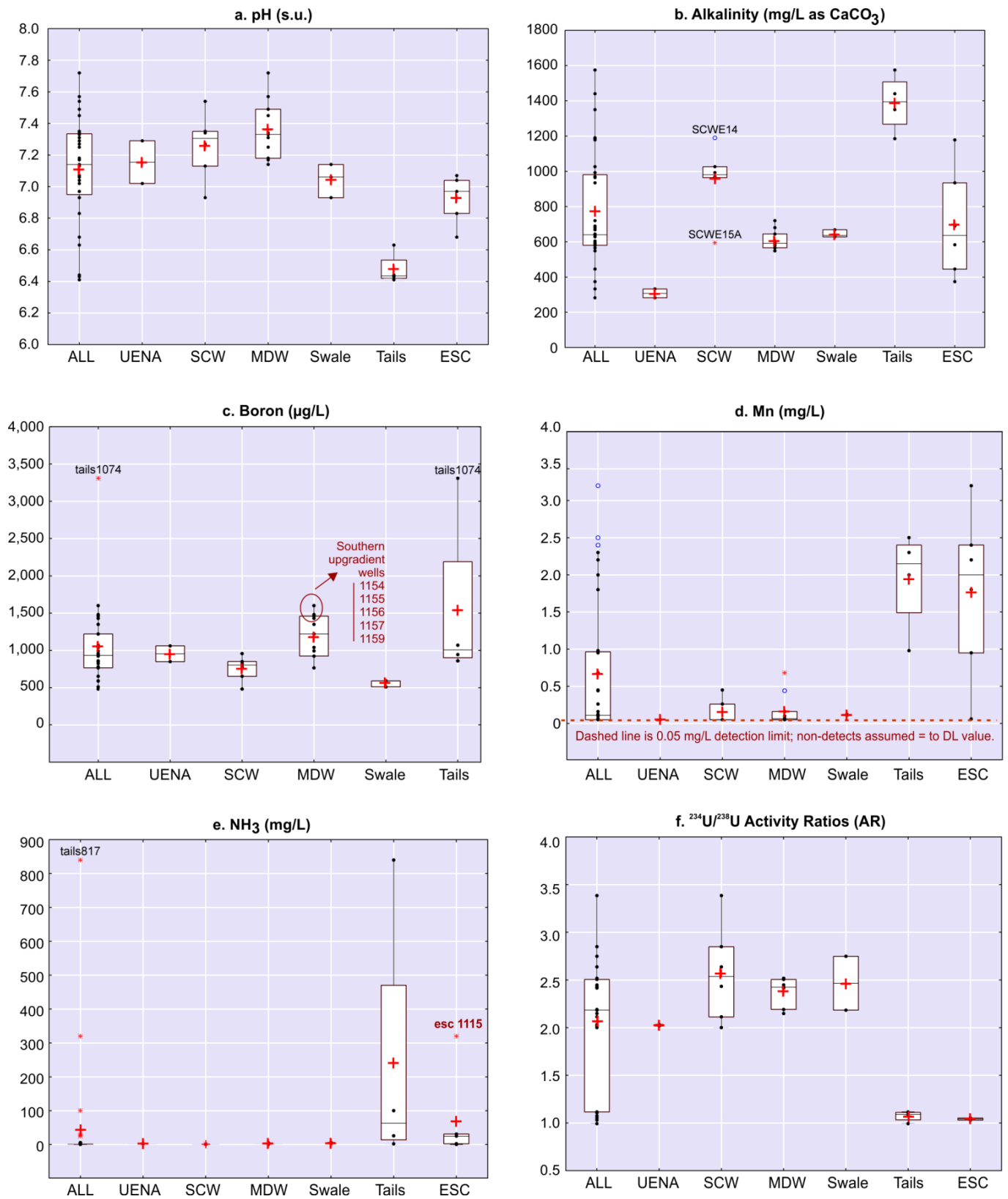| Variable	UENA (n = 2)		SCW (n = 6)		MDW (n = 11)		Swale (n = 3)		Tailings (n = 4)		Escarpment (n = 6)	
	Mean	**CV**	**Mean**	**CV**	**Mean**	**CV**	**Mean**	**CV**	**Mean**	**CV**	**Mean**	**CV**
Field Parameters												
Alkalinity	307	0.08	956	0.19	606.4	0.08	644	0.03	1,388	0.10	700.5	0.40
pH (s.u.)	7.16	0.02	7.26	0.03	7.36	0.02	7.04	0.01	6.48	0.01	6.9	0.02
Spec. Cond.	28,080	0.04	31,287	0.22	26,630	0.11	28,750	0.12	20,423	0.06	12,764	0.15
Primary Variables												
Ca (mg/L)	453	0.04	419.8	0.06	423.4	0.03	448.7	0.06	513.2	0.12	438.3	0.12
Cl (mg/L)	4,130	0.06	2,484	0.59	1,434	0.10	1,610	0.42	701	0.36	290	0.24
HCO_3 (mg/L)	374	0.08	1,164	0.19	738	0.08	784.8	0.03	1,693	0.10	853.9	0.40
K (mg/L)	47.65	0.07	82.4	0.25	51.7	0.29	76.6	0.08	134.7	0.49	135.5	0.24
Mg (mg/L)	1,295	0.07	1,067	0.34	1,388	0.10	1,720	0.38	2,312	0.11	1,122	0.15
Na (mg/L)	6,555	0.06	8,417	0.24	6,695	0.18	6,680	0.07	2,472	0.22	1,550	0.23
SO_4 (mg/L)	12,700	0.05	17,650	0.21	16,300	0.11	15,767	0.06	11,402	0.22	7,783	0.17
NO_3 (mg/L)	857.5	0.02	1,550	0.37	1,905	0.37	4,140	0.43	2,813	0.58	1,301	0.56
Se (µg/L)	292.5	0.15	1,868	0.30	944.8	0.47	3,707	0.37	202.5	0.94	373.3	0.91
U (µg/L)	44.9	0.14	148.3	0.22	152.1	0.13	118.6	0.22	4,382	0.66	1,202	0.24
Supplementary Variables												
B (µg/L)	955	0.11	757.5	0.2	1,184	0.24	563	0.07	1,546	0.66	—	—
Color (Pt-Co)	25	—	356	0.31	156.6	0.45	155.3	0.03	242	1.43	—	—
DOC (mg/L)	27.5	0.16	54.7	0.29	33.6	0.22	31.0	0.18	43.5	0.28	—	—
Mn (mg/L)	0.05	—	0.15	1.0	0.16	1.2	0.11	0.04	1.95	0.30	1.77	0.58
NH_3 (mg/L)	2.50	0.20	1.17	0.32	2.64	0.47	4.67	0.27	242	1.43	67.3	1.69
$^{234}U/^{238}U$ AR	2.03	0.004	2.57	0.18	2.38	0.06	2.47	0.11	1.07	0.05	1.04	0.01

Notes:
CV = standard deviation divided by the mean; CVs are shown in red to facilitate review.
Units for alkalinity and Spec. Cond. (specific conductance) are mg/L as $CaCO_3$ and µS/cm, respectively.
Means and CVs for Mn were calculated assuming nondetects were equal to the 0.05 mg/L detection limit (see Table 3).
UENA = Eagle Nest Arroyo; SCW = Salt Creek Wash; MDW = Many Devils Wash
s.u. = standard units; — = Not analyzed or not applicable

5.2 Graphical Portrayals of Major Ion Chemistry

The graphical representations in the previous section (VSS and box plots) are a suitable means to examine distributions of single constituents in a groundwater system. However, the ability to view multiple constituents simultaneously can often yield more information about the system. Many geochemical plotting methods have been developed to portray compositional variation in groups of constituents. Most plotting methods use groups of ions that compose the majority of dissolved constituents in natural waters. Two widely used methods, Piper diagrams and Stiff diagrams (Hem 1986), are used to evaluate the data from this study. Both Piper and Stiff diagrams use major ion concentrations, expressed as equivalents, to define groundwater signatures. Equivalents take into account the ionic charges associated with the major ion elements. Although the diagrams are expressed as equivalents, the term "concentration" is used for ease of discussion.

Although Piper diagrams are often used to classify groundwater types, they can also be used to determine if a groundwater composition is the result of mixing between two parent water sources. Each data point on a Piper diagram reflects only the relative concentrations of major ions, rather than absolute concentrations. In contrast to Piper diagrams, Stiff diagrams provide a

visual means of displaying absolute concentrations. Each apex on a Stiff diagram is an absolute concentration, and the overall size of the diagram reflects the total concentration of dissolved solids. Although the Piper and Stiff diagrams plot the same data, they portray it differently, and both help visualize compositional variation among samples.

All samples from this study are relatively high in sulfate, as indicated by their locations on a Piper diagram (Figure 8). On the cation triangle, all samples plot subparallel to the Na+K – Mg side, indicating variable concentrations of Na+K, and Mg, and a nearly constant proportion of Ca. Because of an increase in Mg/(Na+K), samples for the tailings and escarpment areas are separated from all other points. Eagle Nest Arroyo samples have the highest relative Cl concentrations. Many of the Salt Creek Wash samples have relatively higher concentrations of Na+K and Cl than most other samples.
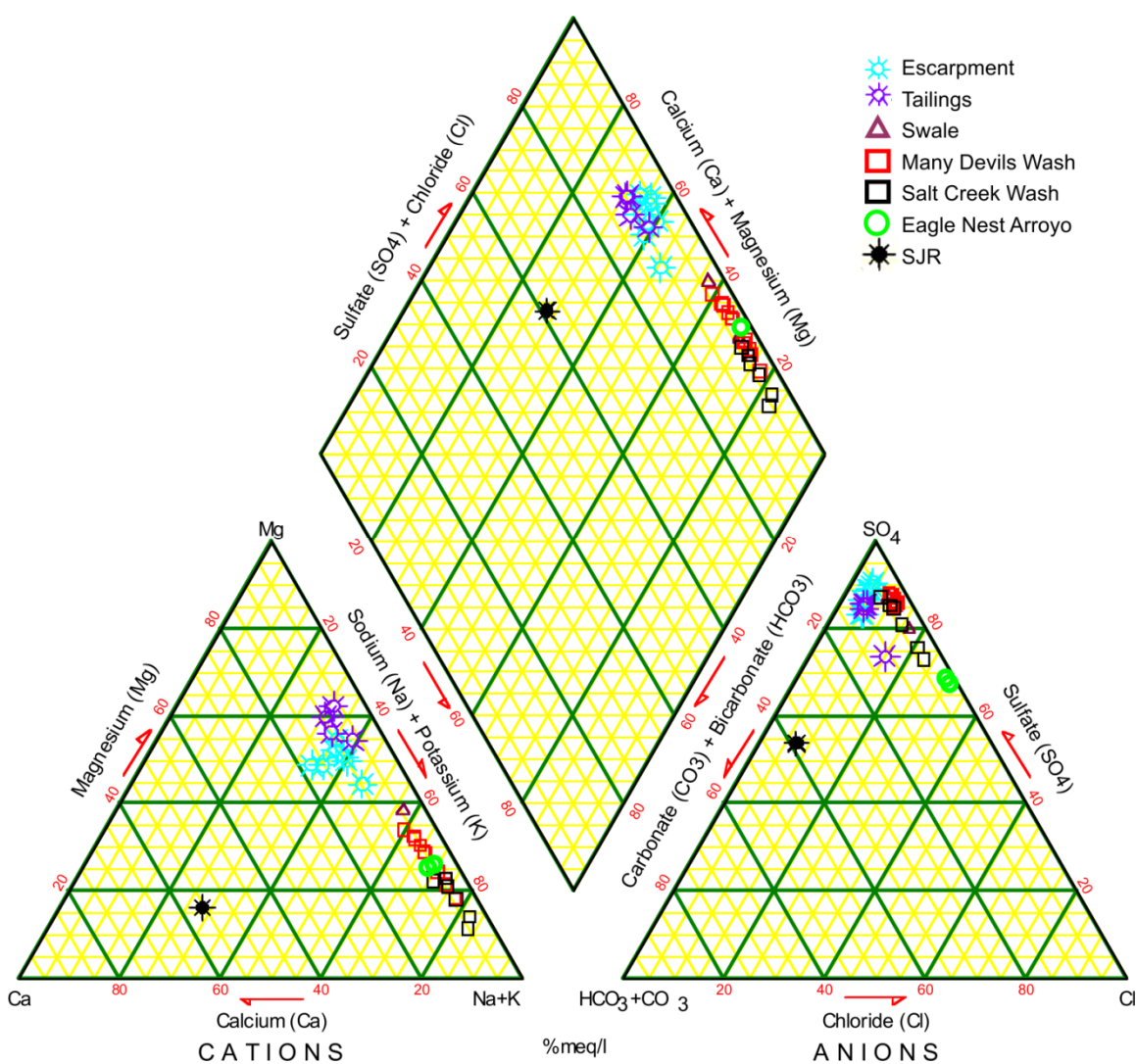

Figure 8. Piper Diagram
Escarpment data from September 2011; all other data from March 2012.

Stiff diagrams are evaluated qualitatively by comparing their shapes. Two general shapes, depicted by a tilted hourglass ( ) and an Erlenmeyer flask ( ), were revealed in the data collected for this study (Figure 9). Sample data from the tailings and escarpment areas have the flask appearance, whereas data from Many Devils Wash, Salt Creek Wash, and Eagle Nest Arroyo result in diagrams resembling the tilted hourglass. The flask shape is caused largely by a lower ratio of Na+K to Mg. Some of the hourglass-shaped diagrams, such as those for SCWS and SCWE14, have extensions of the upper left and lower right apexes, indicating enrichment in Na and SO_4. In most cases, the flask shapes from the tailings samples have wider bases than those from the escarpment samples, indicating higher concentrations of Mg and SO_4. The low concentrations of major ions in the sample from the San Juan River are apparent based on this sample's representation on the Stiff diagram as a thin vertical line (Figure 9).
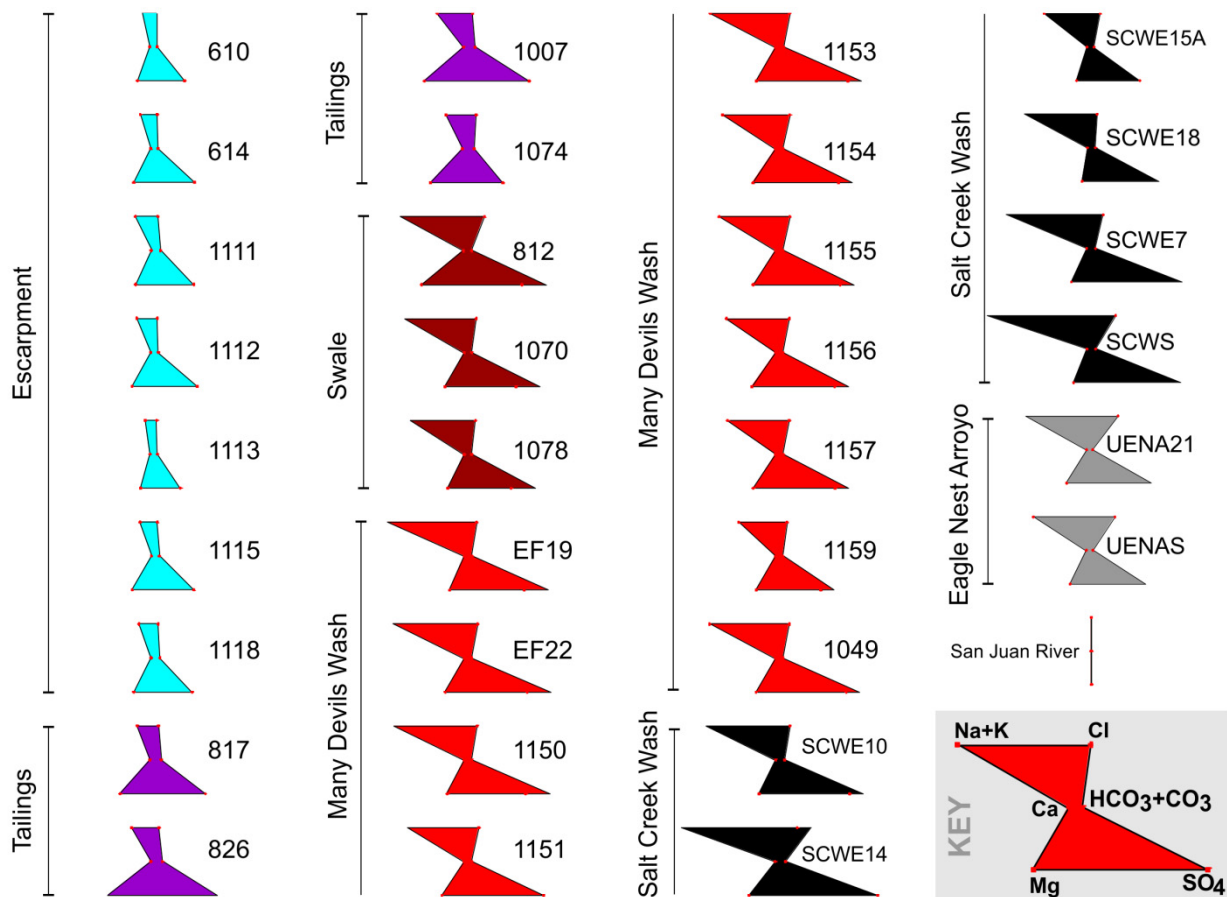

Figure 9. Stiff Diagrams

Escarpment data from September 2011; all other data from March 2012. All diagrams have the same scale. As shown above, the Stiff diagrams resemble either a tilted hourglass (, most samples), or a flask (, tailings and escarpment samples).

5.3 Multivariate Analysis of Major Ion Data Set

Similar to the approaches used by Güler et al (2002) and Cloutier et al. (2008), who used multivariate statistical techniques to supplement geochemical evaluations, multivariate statistical analyses were applied to the subset of constituents used to generate the Piper and Stiff diagrams (Figures 8 and 9): Na, Cl, SO_4, Ca, Mg, K, and HCO_3. The primary rationale for this approach was to verify the findings based on interpretation of the Piper and Stiff diagrams. As one of the goals of multivariate analysis is to identify patterns or fingerprints, the signature discriminations obtained using both hydrochemistry plotting and multivariate approaches should generally agree.

5.3.1 Principal Component Analysis

As discussed previously, PCA is a mathematical procedure used to transform a set of correlated variables into a new (smaller) set of uncorrelated variables, the principal components (PCs). The PCs are ordered such that the first few account for most of the variation present in the original variables.

PCA is used iteratively to yield a number of outputs, all of which require interpretation; with each step, there is an inherent tradeoff between simplicity and precision. The first output yielded by a PCA is a correlation matrix (Table 5). As discussed in Section 4.3.2, a Spearman correlation matrix was used because it is less sensitive to outliers than the more commonly used Pearson correlation matrix.

Table 5. Spearman Correlation Matrix: Major Ion Subset

Variables	Na	K	Ca	Mg	Cl	SO₄	HCO₃
Na		--	--	--	--	--	--
K	-0.291		--	--	--	--	--
Ca	-0.231	0.268		--	--	--	--
Mg	-0.044	-0.104	**0.453**		--	--	--
Cl	**0.780**	**-0.468**	-0.025	0.217		--	--
SO₄	**0.936**	-0.200	-0.216	0.105	**0.729**		--
HCO₃	0.133	**0.481**	-0.044	0.190	-0.107	0.197	

*Values in **bold** are different from 0 with a significance level α = 0.05; duplicate correlations are not shown.*

Table 5 demonstrates strong positive correlations between Na, SO_4, and Cl. These are somewhat apparent in the box plots of the major ions provided in Figure 6. Much weaker positive correlations are apparent between K and HCO_3 and between Ca and Mg. K and Cl are weakly negatively correlated. It is the combination (or collapse) of these variable correlations that PCA is designed to capture mathematically. To complement the correlation matrix in Table 5, a commonly used approach for assessing the relationship between multiple variables—a scatterplot matrix—is provided in Figure 10. In this figure, correlations for each variable combination listed above are plotted, and plot symbols are coded according to sample population.
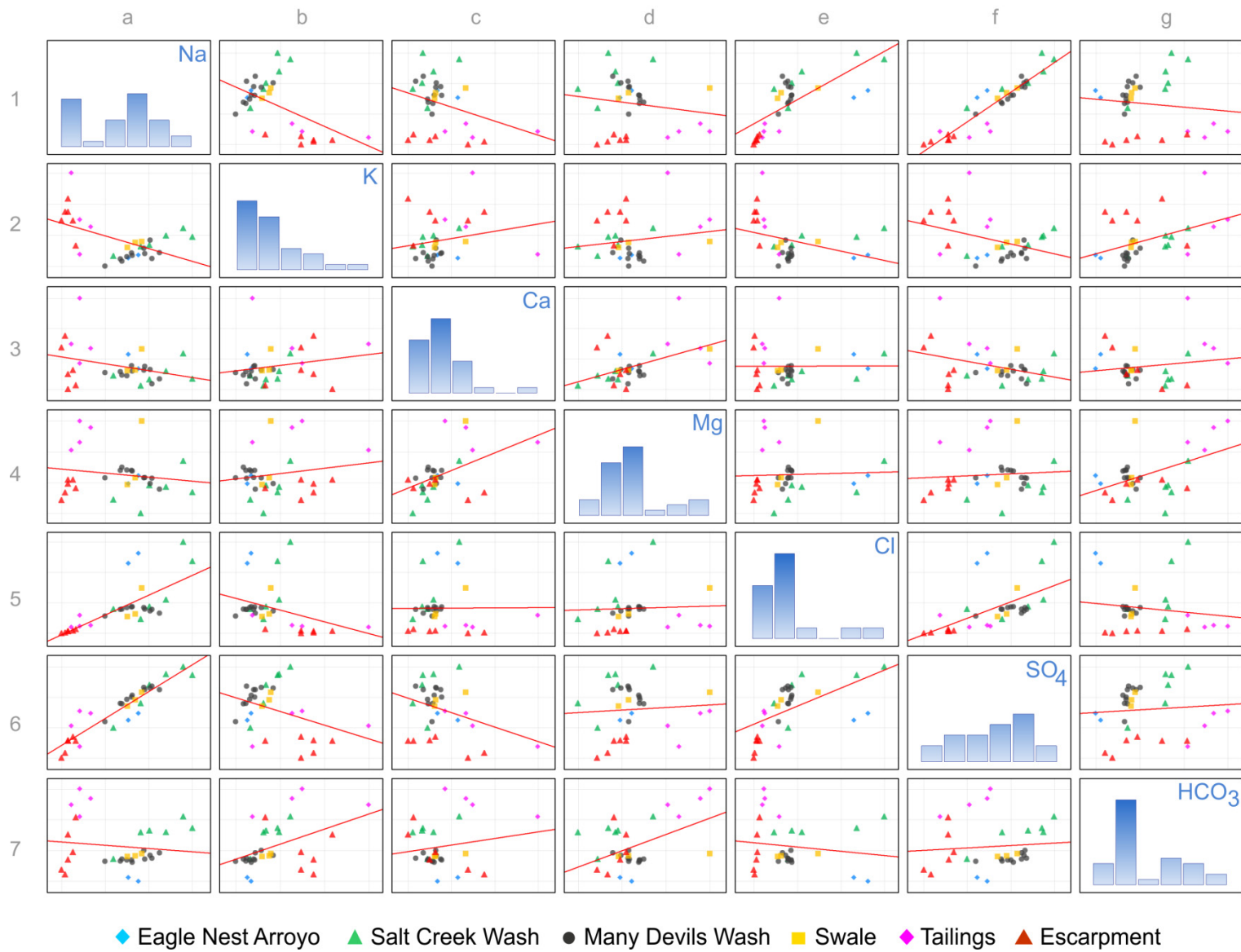
Figure 10. Scatterplot Matrix for Major Ion Subset

This plot shows correlations for each variable combination; alpha-numeric column and row headings are provided to facilitate discussion. In each row, the histogram of the entire distribution is shown, along with correlations with each other variable. For example, grids 1b and 2a plot the same data (Na vs. K), but in 1b Na is plotted on the y-axis, whereas in 2a, it is plotted on the x-axis.

Although depicting useful information, including obvious outliers, Figure 10 demonstrates the limitations of more traditional graphical approaches. Even with only seven variables, a small data set relative to many PCA applications, the scatterplot matrix in Figure 10 is rather difficult to interpret. The previously mentioned strong linear correlations between Na, SO_4, and Cl are apparent in Figure 10 as well (subplots 1e, 1f, 5f). And, although some clustering of sample populations is apparent, with tailings and escarpment area samples grouping separately from other populations, no consistent patterns or relationships between groups are evident.

To allow closer examination of the Na–Cl–SO_4 correlations, Figure 11 plots these three constituents in two dimensions. The correlations between Na and SO_4 are more apparent in this figure, as are the areas with elevated Cl concentrations (Eagle Nest Arroyo and Salt Creek Wash [SCWS and SCWE14]). This figure also highlights the dangers of assuming that a strong correlation applies to the entire data set. Although a linear correlation between Na and SO_4 is generally evident, this correlation does not apply to the tailings area samples. Similarly, the typically strong correlations between Cl and both Na and SO_4 are contradicted by the elevated Cl concentrations in Eagle Nest Arroyo samples (plotted in the center of Figure 11).
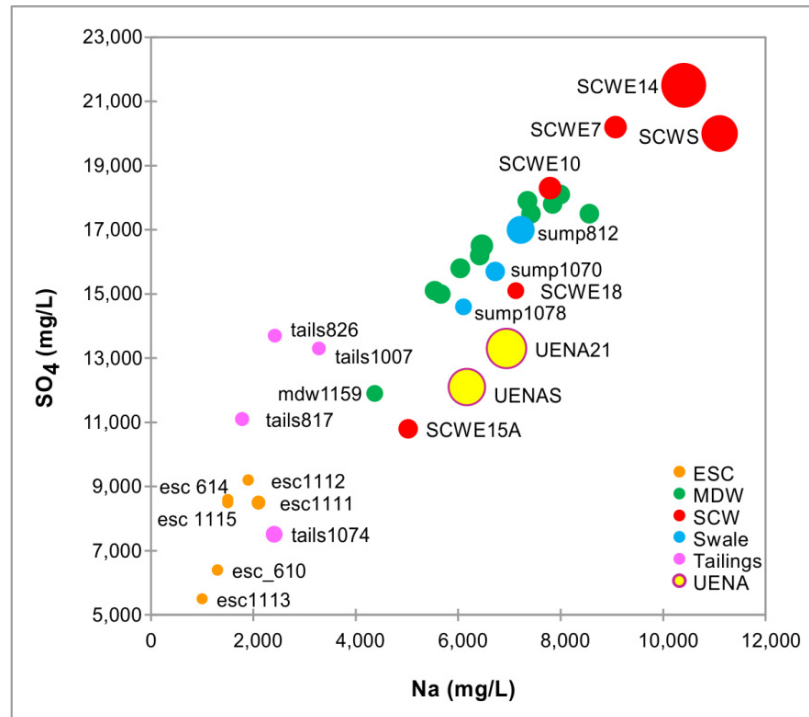
Figure 11. Bubble Plot of Na vs. SO_4 vs. Cl in Origins Project Samples
In this plot, the z-dimension, Cl, is reflected by the size of the plot symbol (or circle radius).
Cl concentrations range between 190 and 4,990 mg/L, with a mean of 1,510 mg/L.

Figures 10 and 11 highlight the need for alternative means of identifying chemical signatures on the basis of multiple correlations. Some clustering is evident in these exhibits, as indicated by the similarities in the chemistries of samples collected in the tailings and escarpment areas. Despite this clustering, patterns in the data are complex and difficult to interpret.

The correlations shown in Table 5 are translated into PCs by calculating eigenvalues; the greater the eigenvalue, the greater the proportion of variability explained by the component (Table 6).

Table 6. Eigenvalues, Explained Variability, and Principal Component Loadings: Major Ion Data Subset

Eigenvalues:

	PC1	PC2	PC3	PC4	PC5	PC6	PC7
Eigenvalue	2.87	1.58	1.42	0.68	0.24	0.18	0.03
Variability (%)	41.0	22.6	20.3	9.76	3.37	2.61	0.46
Cumulative %	41.0	63.6	83.8	93.6	96.9	99.5	100.0

Results for PCs with eigenvalues > 1 (the Kaiser criterion) are listed in red above.

Correlations between variables and factors (factor loadings):

	PC1	PC2	PC3	PC4	PC5	PC6	PC7
Na	**0.94**	0.10	-0.20	0.17	0.04	-0.12	0.13
K	-0.51	**0.53**	-0.49	0.37	-0.24	0.14	0.02
Ca	-0.28	0.57	**0.58**	0.46	0.18	-0.11	-0.02
Mg	0.09	**0.65**	0.59	-0.43	-0.20	0.00	0.04
Cl	**0.89**	0.08	0.25	0.12	0.08	0.33	-0.02
SO$_4$	**0.91**	0.23	-0.20	0.09	-0.17	-0.16	-0.11
HCO$_3$	-0.004	**0.70**	-0.59	-0.33	0.26	0.02	-0.02

For each variable, values in bold correspond to the factor for which the absolute value is the largest.

As shown in upper portion of Table 6, the first two components (PC1 and PC2) explain 41.0 percent and 22.6 percent of the total variability contained in the original variables, respectively. The third component (PC3) explains 20.3 percent of the variation, and the remaining components explain gradually decreasing contributions (with eigenvalues < 1).[4] The first two components together account for 63.6 percent of the information contained in the original data set, and addition of a third component increases the percentage of total explained variability to 83.8 percent. As shown in the lower portion of Table 6, the first PC (PC1) is most strongly correlated with Na, SO$_4$, and Cl, and the second component (PC2) is associated with HCO$_3$, Mg, and K. For Ca, Mg, and HCO$_3$, there is overlap in the representation of the PCs. For example, Ca and Mg are almost equally represented by PC2 and PC3. Given this overlap, the remaining analysis focuses on results for PC1 and PC2.

The correlations between the seven variables (Table 5) and between the variables and PCs (Table 6) are depicted graphically in the correlation circle provided in Figure 12. The correlation circle is a graphical tool for determining which variables contribute the most to the formation of the PCs.

---

[4] The total number of components is always less than or equal to the lesser between the number of variables and number of objects.
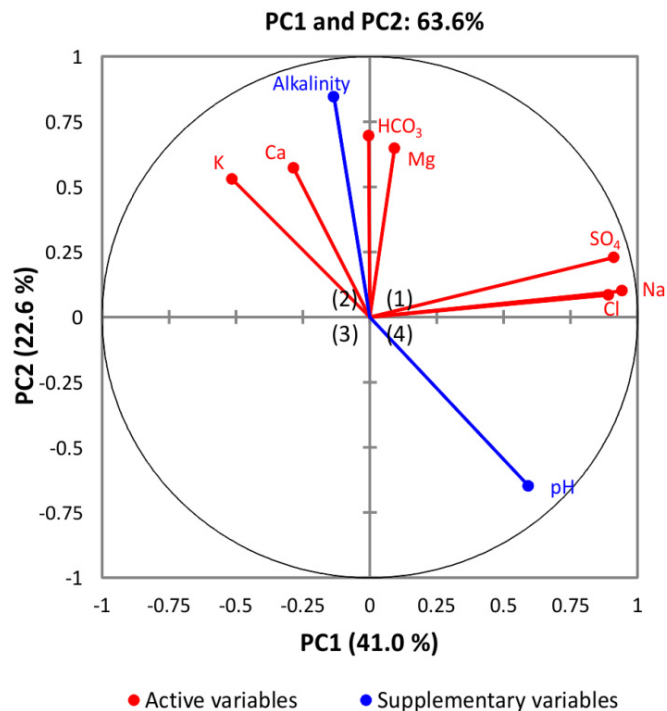
Figure 12. PCA Correlation Circle for Major Ions and Supplementary Variables Based on Spearman Correlation Matrix
This figure is a graphical representation of Tables 5 and 6 in that it depicts correlations between the variables, and the correlations between the variables and the factors. For the first PC (horizontal axis), accounting for most (41%) of the variation, Na, Cl, and SO_4 are well represented on PC1 based on the small angle between the vectors and the PC1 axis. For the 2nd PC, Mg and HCO_3 are most influential.

In Figure 12, each primary variable (each of the seven ions) is represented by a vector (red line). Although not used to derive the PCs, supplementary variables, pH and alkalinity (denoted by blue vectors) are also plotted to illustrate their associations with the other variables. The angle of the vectors relative to the two PC axes reflects the degree of association between the variables and the PCs. Similarly, the angle of each vector relative to other vectors reflects the degree of correlation between the variables. For example, vectors (chemical variables) separated by small angles are correlated, whereas those separated by 90° angles are independent (i.e., not correlated). Vectors oriented 180° from each other are negatively correlated. With this understanding, Figure 12 can be interpreted as follows:

- Na, Cl, and SO_4 are positively correlated with the first component, PC1 (the horizontal axis). In addition, the small angles between these vectors indicates that they are positively correlated with each other.

- HCO_3 and, to a lesser extent, Mg, are positively correlated with the second component, PC2 (the vertical axis).

- The position of the vectors for Ca and K, at about 45° angles to both PC1 and PC2 axes, indicates that these constituents are not as well represented in the PCA as are the other variables. This is also indicated by the smaller factor loadings shown for Ca and K in Table 6.

The foregoing PCA analysis based on the Spearman correlation matrix was initially performed using the more traditional Pearson correlation matrix. To illustrate the impacts of using one approach versus the other, Figure 13 compares the correlation circles yielded using these two methods.
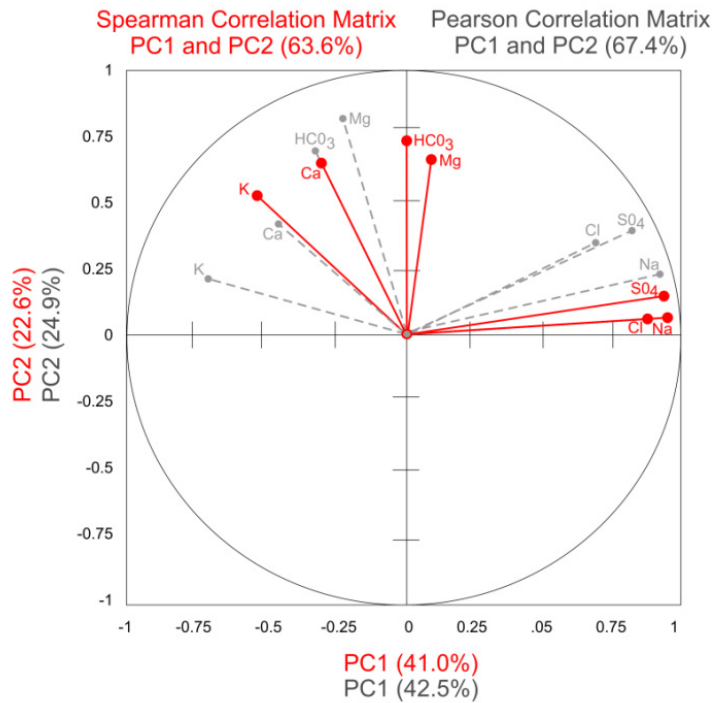

Figure 13. Correlation Circles Based on Spearman and Pearson Correlation Matrices

Although use of the Spearman correlation matrix accounts for less variation in the data set (roughly only 3 percent) than use of the Pearson correlation matrix, with the Spearman, most variables are better represented along the PC axes (Note: small angles for Na, Cl, and SO_4 [PC1] and HCO_3 and Mg [PC2]).

Figure 13 indicates that use of the Pearson correlation matrix explains more of the variation in the data set (67 percent vs. 64 percent for Spearman). However, the Spearman correlation matrix is easier to interpret because the variables are more aligned, and thus better represented, on the PC axes.

Correlations between variables, and between the variables and the PCs, were subsequently combined with the positioning of the data from the 32 sample locations in a biplot (Figure 14). In a biplot, the samples are points and the variables are the vectors. The vector placement is the same as that shown in the initial correlation circle. The positioning of the sample points is determined based on the factor scores for each retained PC. Whereas the factor loadings (listed in the bottom portion of Table 6) quantify the relationships between the *variables* and the PCs, factor scores quantify the relationships between the *samples* and the PCs based on their combined chemical signatures.
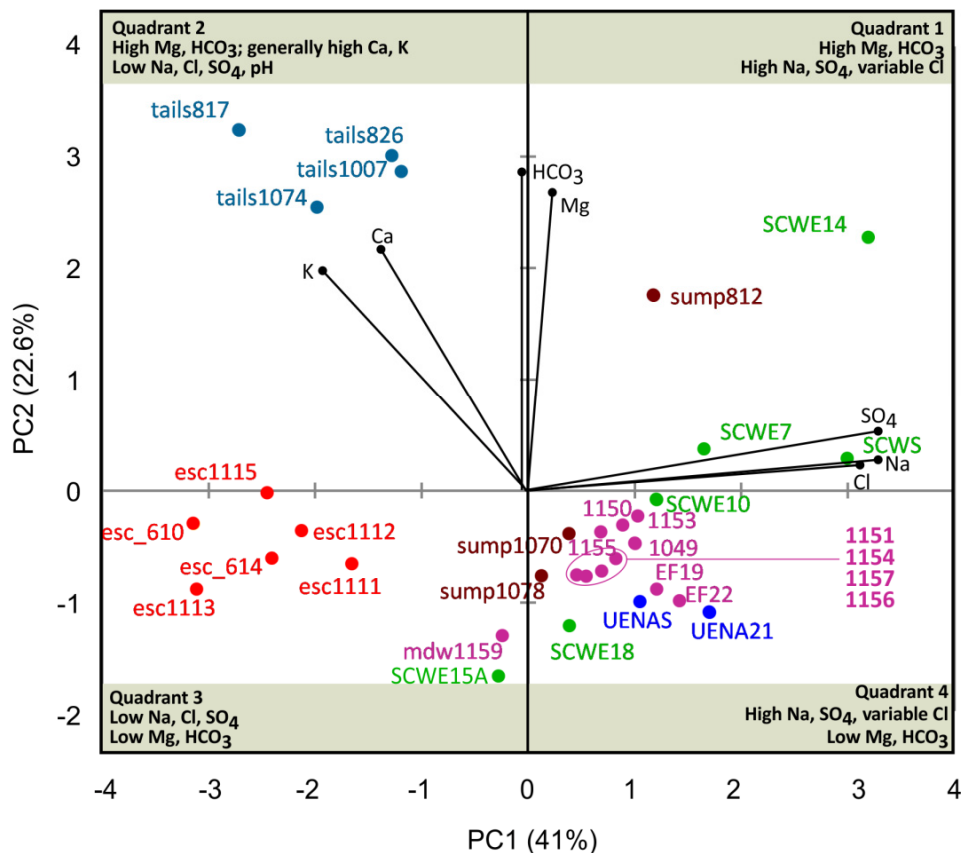
Figure 14. PCA Biplot for Major Ion Subset, PCs 1 and 2

PCA for major ions Na, K, Cl, SO₄, Ca, Mg, and HCO₃. Points (samples) are color-coded based on sample population. This biplot combines the information in the correlation circle (Figure 12) with the projection of the factor scores on the PCs. Objects clustered together (e.g., MDW samples) are similar in terms of chemical signature, while those farther apart (e.g., tails817 and UENA21) are dissimilar.

In the biplot (Figure 14), a number of clusters are evident. One of the most prominent is the clustering of the tailings samples in quadrant 2, due in large part to high concentrations of Mg, HCO_3, and K. This quadrant is also characterized by high alkalinity and low pH (see supplementary vector placement in Figure 12). Along with tailings area samples, escarpment area samples are also positioned in the left-hand side of the biplot, reflecting low concentrations of Na, Cl, and SO_4. However, due to lower Mg and HCO_3, the escarpment samples plot in quadrant 3 separately from the tailings. The separation of the tailings and escarpment area samples from those representing the other sample populations is consistent with the distinctions between the Stiff diagrams for these areas shown in Figure 9 (⬩ vs. ⬩).

Another prominent cluster is illustrated by the close grouping of most Many Devils Wash samples in quadrant 4, reflecting high Na and SO_4 and low Mg and HCO_3. The only exception to this grouping is mdw1159 (the southernmost Many Devils Wash location in Figure 2), which plots separately in quadrant 3. This reflects the fact that, relative to other Many Devils Wash locations, mdw1159 had the lowest concentrations of Na, Cl, and SO_4 (refer to Table 3 and Figure 6). The variability in chemical signatures for both the swale area and Salt Creek Wash is apparent in Figure 14, based on the lack of clustering of these samples in the biplot.

The most isolated points in the biplot (i.e., samples that don't cluster with others) include tails817, sump812, and SCWE14 (Figure 14). This reflects high concentrations of the influential variables. For example, the placement of tails817 in the uppermost portion of quadrant 2 reflects the high (outlier) K concentration shown in Figure 6. SCWE14's solitary placement in the upper-rightmost 1st quadrant of the biplot reflects the fact that concentrations of Na, Cl, and SO_4 were high in this sample (Cl and SO_4 were the maximum observed throughout the study areas), as were Mg, K, and HCO_3 (Figure 6). The sump812 sample plots separately from other swale area samples because it had the highest concentrations of all major ions within that sample population (Table 3).

Another representation of the chemical signatures revealed by the biplot is provided in Figure 15, which plots the normalized values of each variable for each sample location. Separation of the tailings area from other study areas on the basis of Mg and HCO_3 concentrations is prominent in this figure, as illustrated by the red bands in the rightmost portion of the plot. The high levels of Na and SO_4 characteristic of most Many Devils Wash, Salt Creek Wash, and swale area samples are also apparent. Exceptions to the latter are mdw1159 and SCWE15A, the only samples from areas other than the tailings and escarpment that plot on the negative PC1 axis in Figure 14. This placement is attributed to relatively low concentrations of Na and SO_4 in the two samples.
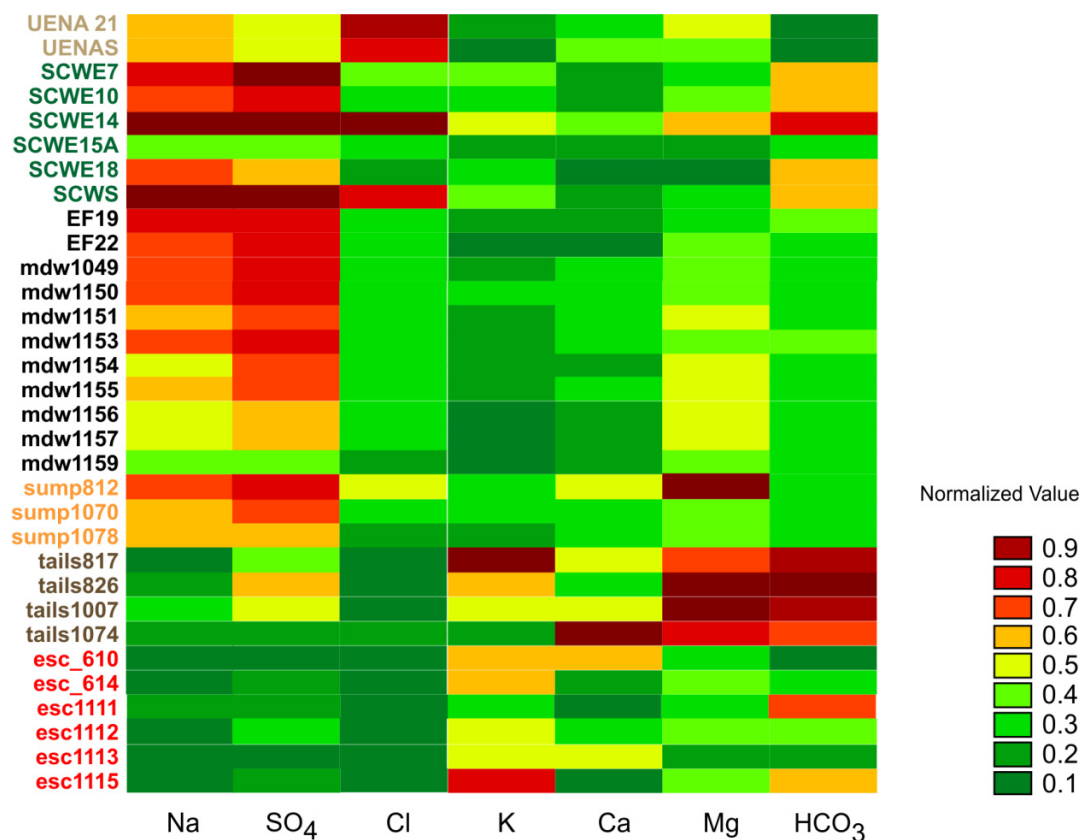
Figure 15. Two-Way Join Results for Major Ions Grouped by Study Area
This plot maps the normalized value for each variable and location rescaled to 0–1 based on the range.

To further assist interpretation of the biplot, Figure 16 plots the standardized mean values for each ion by study area. The most prominent discriminations in this figure are apparent for Na, where the mean values representing tailings and escarpment area samples are clearly lower than

those for other study areas (hence their placement in the left quadrants of the biplot in Figure 14). Standardized mean values for K in tailings and escarpment area samples are also distinguished from the means in remaining sample populations, again illustrating that tailings and escarpment area samples have different chemical signatures than those in other locations. The obvious separation between tailings and escarpment area samples in Figure 14 is also apparent here, as evidenced by the difference in means between Ca, Mg, and HCO_3. Standardized mean ion concentrations for Many Devils Wash samples are notably different from the tailings area samples for all variables except Cl.
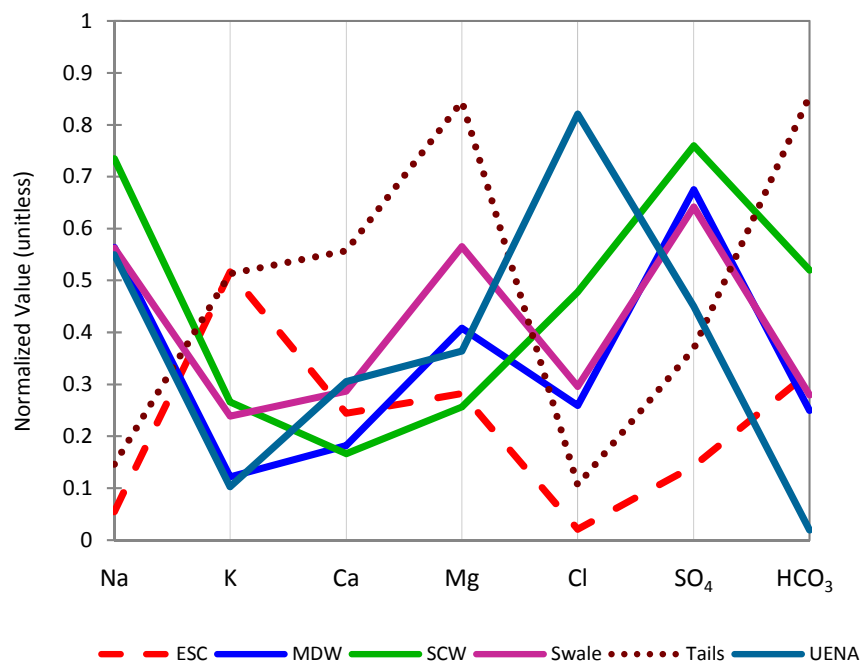

Figure 16. Parallel Coordinates Plot for Major Ions
Mean values are standardized to facilitate comparisons between different variables; group means for each variable are listed in Table 4.

Statistical techniques employed up to this point in the analysis have been limited to exploratory and descriptive methods. For example, the positioning of the tailings and escarpment area samples in the leftmost quadrants of the biplot in Figure 14 is readily apparent, suggesting that there is discrimination on the first PC, the Na-SO_4-Cl signature. But is this separation significant, or is it due to unexplained variation? To test for the significance of the discrimination of the objects (samples) on the PCs, a one-way ANOVA was run on the PCA factor scores, the coordinates used to generate the biplot.[5] Differences between groups were significant at the $p < 0.05$ level for both PC1 and PC2 (meaning that there is less than a 5 percent chance of obtaining the observed results if the null hypothesis—no difference exists between groups—is true). Corresponding F statistics, degrees of freedom and *p*-values are shown below.

PC1, Na-SO_4-Cl signature: $F_{5,26} = 25.167$, $p < 0.0001$[6]
PC2, HCO_3-Mg-K signature: $F_{5,26} = 14.687$, $p < 0.0001$

---

[5] For example, in Figure 14, the factor scores for the outlier Salt Creek Wash sample SCWE14 are 3.191 and 2.277 for PC1 and PC2, respectively, whereas those for esc1115 are −2.452 (PC1) and −0.017 (PC2).

[6] The F statistic -ratio (25.167 for PC1) is the ratio of the variance between groups to the variance within groups. The subscripts 5 and 26 are the corresponding degrees of freedom (between and within groups, respectively).

A limitation of ANOVA is that it only tests the hypothesis that all group means are equal; it does not identify which groups differ from each other. Therefore, a post-hoc test, Tukey's Honestly Significant Difference (HSD) test was performed to determine which between group-comparison(s) accounted for the significant differences (Tables 7a and 7b).

Table 7a. Post-Hoc Tukey (HSD) Results for PC1 Factor Scores: Major Ion Subset

Group	UENA	SCW	MDW	Swale	Tailings	ESC
UENA		--	--	--	--	--
SCW	1.000		--	--	--	--
MDW	0.909	0.413		--	--	--
Swale	0.854	0.504	0.998		--	--
Tailings	0.001	0.0001	0.0002	0.006		--
ESC	0.0002	0.0001	0.0001	0.0002	0.736	

Probabilites for each between-group comparison are shown in the matrix above.
p-values listed in red font are significant (<0.05).

Table 7b. Post-Hoc Tukey (HSD) Results for PC2 Factor Scores: Major Ion Subset

Group	UENA	SCW	MDW	Swale	Tailings	ESC
UENA		--	--	--	--	--
SCW	0.561		--	--	--	--
MDW	0.988	0.521		--	--	--
Swale	0.488	0.999	0.502		--	--
Tailings	0.0002	0.0002	0.0001	0.001		--
ESC	0.938	0.891	0.995	0.808	0.0001	

See notes following Table 7a (above).

For PC1, the principal component accounting for most of the variation in the data and reflecting relative concentrations of Na, SO_4, and Cl, the chemical signatures for Many Devils Wash, the swale, and the analog sites are similar to each other ($p \geq 0.413$). These chemical signatures are also significantly different from those for the tailings and escarpment areas ($p \leq 0.006$, with most < 0.0001) (Table 7a). For PC2 (reflecting HCO_3, Mg, and K), tailings area samples differ significantly from all other groups ($p \leq 0.001$). The tailings area samples are also significantly different from the escarpment area samples (Table 7b). This is because Mg and HCO_3 distributions in escarpment samples do not noticeably differ from other non-tailings groups (Figure 6d, 6e). The overall ANOVA and Tukey HSD results can be simplified as follows:

- Based on PC1 (Na-SO_4-Cl signature), tailings and escarpment area samples differ significantly from all other areas but are similar to each other. Many Devils Wash, the swale area, and the two analog sites are similar to each other.

- Based on PC2 (HCO_3-Mg-K signature), only the tailings area samples differ significantly from other populations. All other between-group comparisons are not significant.

5.3.2 Cluster Analysis

To further explore the water-chemistry relationships between the study areas, two cluster analyses were performed on the major ion subset. The first used Ward's hierarchical method and the other employed PAM, a more robust partitioning technique. The Euclidean distance measure was used for both approaches.

Cluster Analysis Using Ward's Method

As introduced in Section 4.3.3, the results of hierarchical clustering procedures are expressed graphically in the form of a dendrogram, or tree diagram. Figure 17 presents the dendrogram using Ward's method for the seven major ion variables. In this figure, the nodes of the dendrogram represent the grouped classes or clusters, while the length of the branches indicates the distance between the groups. Cases (samples) are arranged according to similarity.
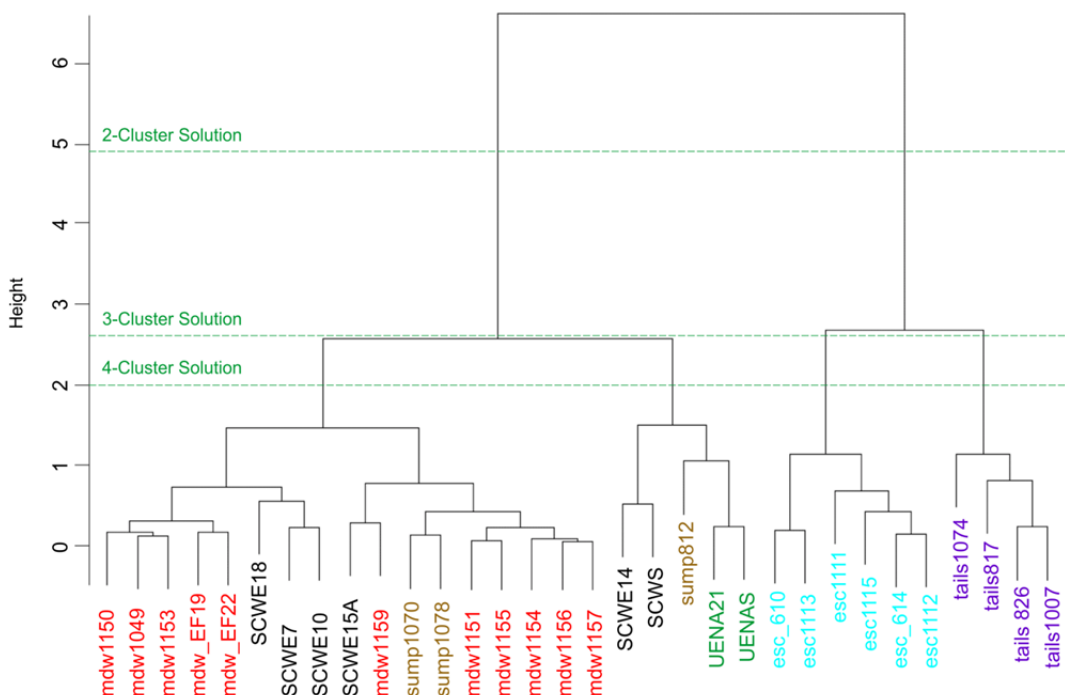

Figure 17. Dendrogram Produced Using Ward's Method (Euclidean Distance Metric) for Major Ions

n=32 cases; cluster variables = Na, K, Ca, Mg, Cl, SO_4, HCO_3. Where to cut or prune the "tree" (see dashed arrows) is a critical factor in interpreting results. Study areas are color-coded to facilitate review.

Based on the length of the branches in the dendrogram above, the 2-cluster solution is most prominent (Figure 17). The first (left-hand) cluster consists of Many Devils Wash, Salt Creek Wash, Eagle Nest Arroyo, and swale area (sump) samples. The second (right-hand) cluster consists of escarpment and tailings area locations. In the 3-cluster solution, escarpment area samples are distinguished from those from the tailings area, and in the 4-cluster solution, some of the outliers identified previously (SCWE14 and SCWS) fall out into a separate group. This is more apparent in Figure 18, which better illustrates the groupings for various cluster solutions. In both figures, it is not immediately apparent which cluster solution is most meaningful.
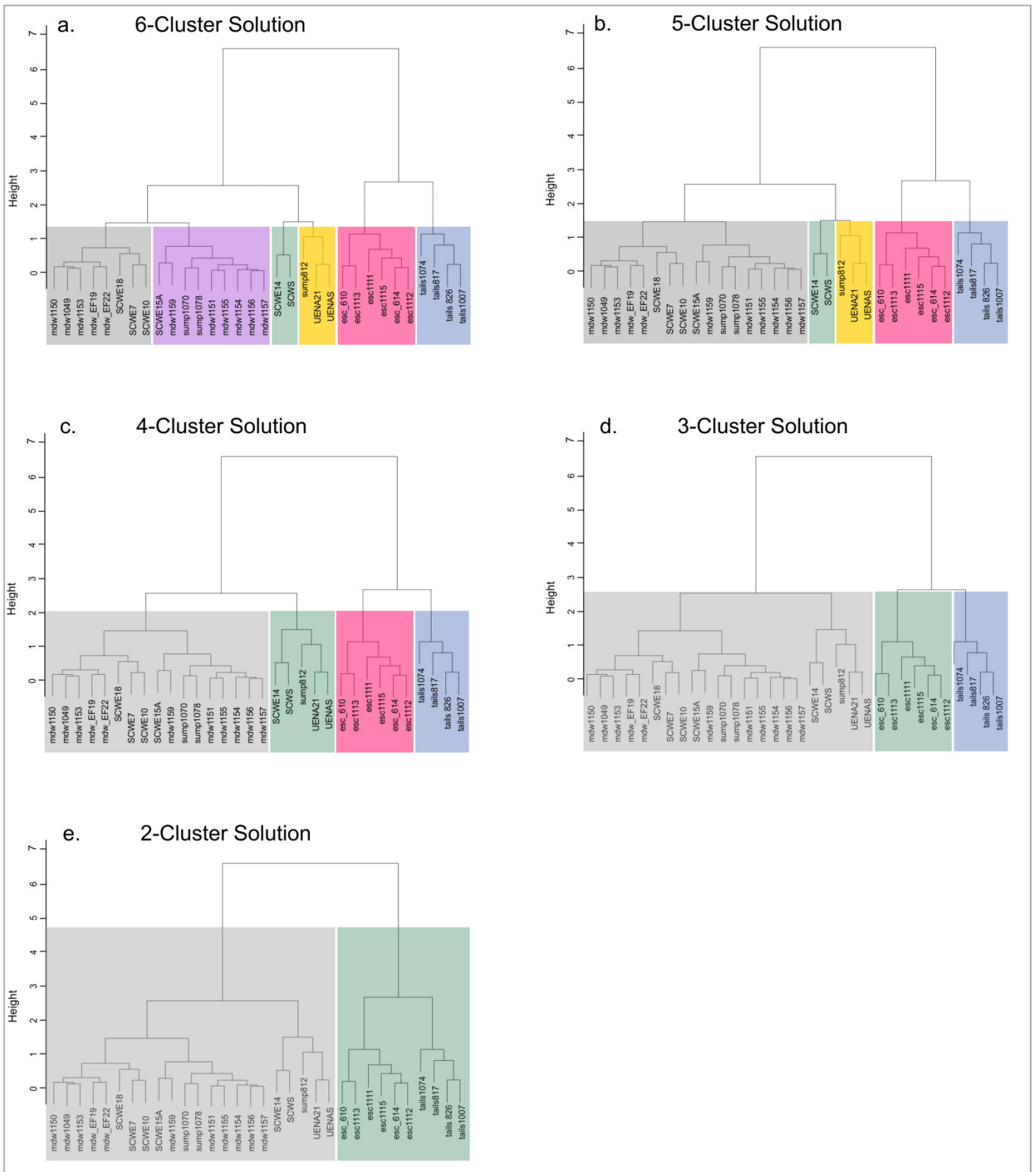
Figure 18. Dendrograms Produced Using Ward's Method Showing Various Cluster Solutions

The maximum number of clusters solutions shown above (six) corresponds to the number of sample populations evaluated in this study. For all solutions, tailings and escarpment area samples separate from samples in all of the remaining four study areas.

To facilitate interpretation of the cluster groupings, Figure 19 combines the dendrogram in Figure 17 with the Stiff diagrams from Figure 9. For purposes of this presentation, and given the number of sample populations evaluated in this study, the dendrogram is divided into six partitions. As shown below, the agreement of the cluster partitions with the chemical signatures defined using the Stiff diagrams is striking. This is particularly true for the 2-cluster solution, which separates the tailings and escarpment area samples, characterized by flask (⚑) Stiff diagrams, from all remaining samples, characterized by the hourglass (⚑) diagrams.

The dendrogram in Figure 19 is also helpful in revealing more subtle distinctions. For example, the separation of tailings area samples from those representing the escarpment in the 3-cluster solution is reasonable given apparent differences in the corresponding Stiff diagrams. The more slender flasks characterizing the escarpment samples reflect lower Mg, HCO_3, and SO_4 concentrations. The Stiff diagrams for esc_610 and esc1113, located at the base of the escarpment just below the disposal cell (Figure 2), are more slender than the other escarpment samples and separate in the dendrogram. This is attributed to lower concentrations of Mg, Na, Cl, SO_4, and HCO_3 at these locations (Table 3).
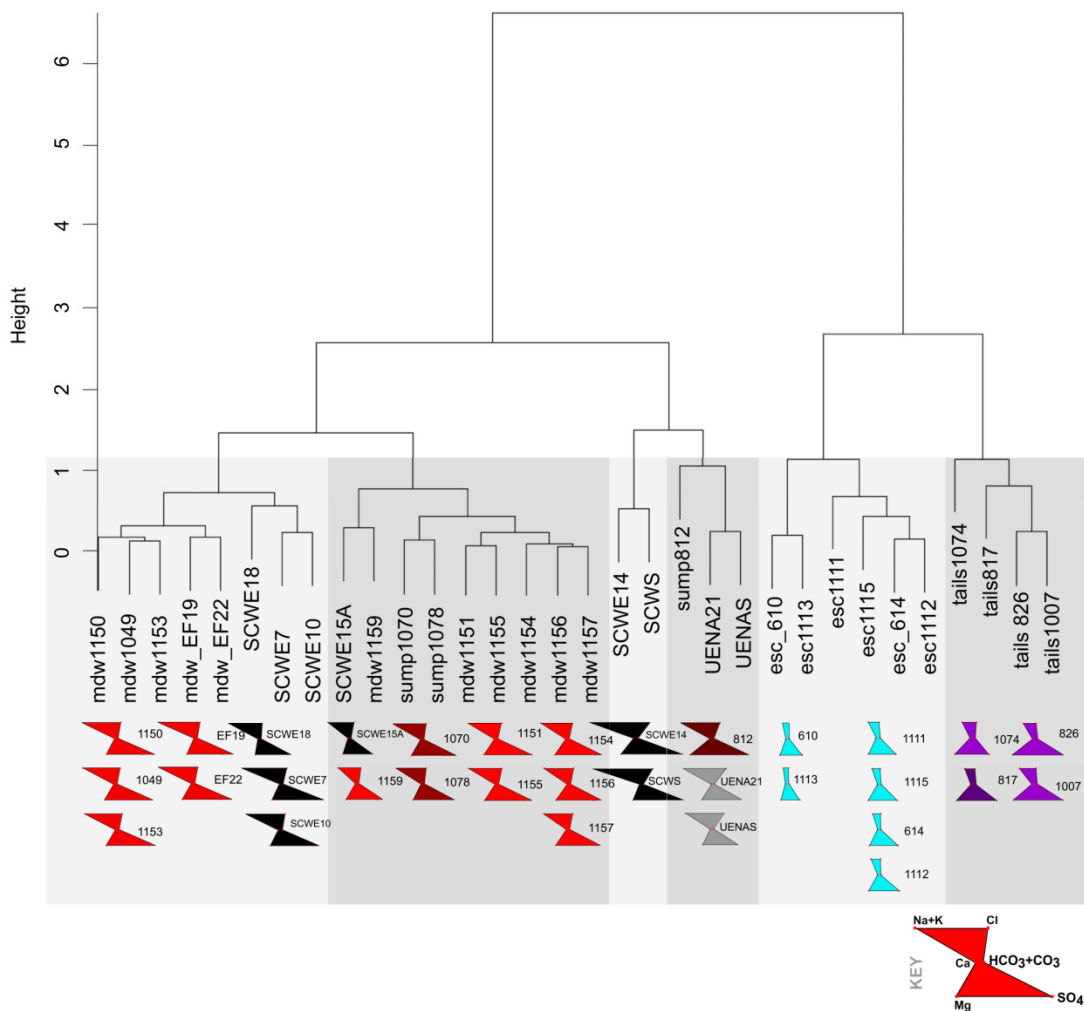

Figure 19. Dendrogram for the Major Ions and Corresponding Stiff Diagrams
Whereas Figure 9 distinguished between two chemical signatures (hourglass vs. flask-shaped diagrams), the cluster groupings shown in this figure facilitate identification of more subtle differences.

Separation of the tailings and the escarpment area samples from other groups, apparent in Figures 17–19 and previous figures, is logical from a water chemistry perspective. Separation in the 5- and 6-cluster solutions of Salt Creek Wash outliers SCWS and SCWE14, where Na and SO$_4$ concentrations were high (Table 3), is also understandable. But it is not clear which cluster solution in Figure 18 is optimal—that is, *which solution provides a reliable basis for discussion and further interpretation?*

Determining the number of clusters to use as the basis for forming conclusions or a hypothesis is one of the key decisions that must be made when performing cluster analysis. For this study, the optimal number of clusters was determined from the maximal average silhouette width using the silhouette plot diagnostic developed by Kaufman and Rousseeuw (1990). Figure 20 shows an initial example of a silhouette plot, based on the 6-cluster solution shown in Figure 18a.
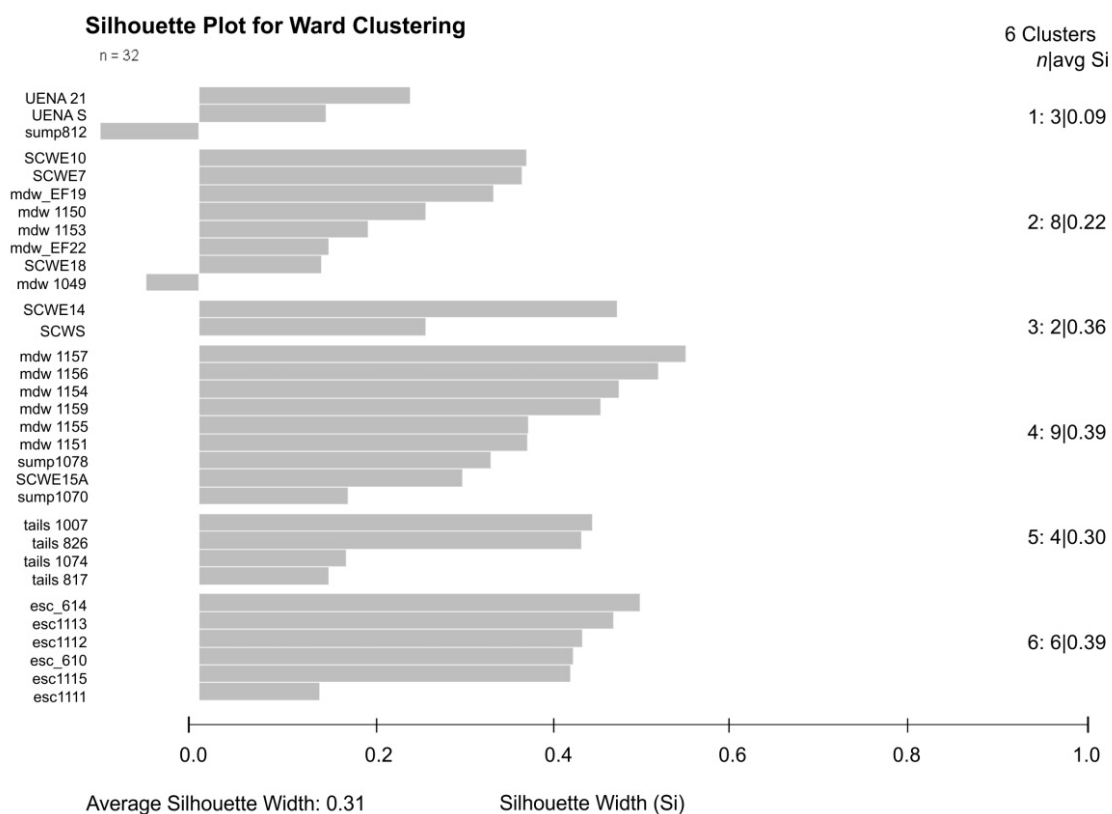
Figure 20. Silhouette Plot for 6-Cluster Solution Using Ward's Method, Major Ion Subset
The width of the bars indicates the strength of clustering for each object. Negative bars indicate unsatisfactory classification. The right margin of the plot lists the cluster number, the number of cases in each cluster, and the average silhouette width.

With possible silhouette widths ranging from −1 to +1, the average silhouette width in this case is 0.31. According to Kauffman and Rousseauw (1990), this is indicative of a rather weak structure; however, in practice, silhouette widths greater than 0.5 may be difficult to achieve. Silhouette widths for sump812 (swale area) and mdw1049 are negative, indicating that these cases are misclassified. Based on individual silhouette widths, many well-classified cases occur in southern Many Devils Wash (cluster 4) and for most escarpment area samples (cluster 6).

Figure 21 shows the silhouette plots corresponding to the five Ward's method cluster solutions (from Figure 18). Average silhouette widths for each of these cluster solutions are listed below, followed by the number of misclassified cases (in parentheses):

- 6-cluster solution: 0.31 (2)
- 5-cluster solution: 0.42 (1)
- 4-cluster solution: 0.41 (3)
- 3-cluster solution: 0.44 (0)
- 2-cluster solution: 0.43 (0)

As shown above, the 3- and 2-cluster solutions have the highest average silhouette widths (0.44 and 0.43, respectively) and no misclassified cases. Therefore, these are considered the "best" solutions. The 3-cluster solution represents the tailings, the escarpment, and remaining samples. The 2-cluster solution distinguishes between the tailings and escarpment areas and all remaining samples. The average silhouette width for the 3-cluster solution (0.44) is just slightly greater than that obtained for the 2-cluster solution (0.43). However, they are basically equivalent, and both solutions are easily interpreted based on the chemical signatures discussed previously and illustrated in Figures 9 and 19.

The cluster analysis using Ward's method confirms the results obtained with PCA, that the chemistries of tailings and escarpment area samples are different from those in other areas. To verify these findings, an alternative cluster analysis method, PAM, was also employed. This verification approach is recommended by Everitt et al. (2011), who state that: "simply applying a particular method of cluster analysis to a data set and accepting the solution at face value is in general not adequate."

Cluster Analysis Using PAM (Partitioning Around Medoids)

As discussed in Section 4.3, because Ward's method may be sensitive to outliers (which are present in this data set as shown in Figures 5 through 7), the PAM (partitioning) method was also applied because it is robust to outliers. Whereas the hierarchical Ward's method produces a dendrogram (clusters form as branches), in the output from PAM (a clusplot), clusters are displayed as spheres (Pison et al. 1999). Within each sphere or cluster, the representative object is the cluster medoid, the object of the cluster for which the average dissimilarity (in this case based on Euclidean distance) between all the objects of the cluster is minimal (Kaufman and Rousseeuw 1990).

PAM was run iteratively using the R script to yield partitions into 2 to 6 groups as shown in Figure 22. In general, cluster groupings are very similar to those produced using Ward's method, as are the silhouette widths. Average silhouette widths for each cluster solution are listed below, again followed by the number of misclassified cases (in parentheses):

- 6-cluster solution: 0.32 (1)
- 5-cluster solution: 0.38 (2)
- 4-cluster solution: 0.35 (2)
- 3-cluster solution: 0.44 (0)
- 2-cluster solution: 0.43 (0)

Silhouette Plot for Ward Clustering with k=6
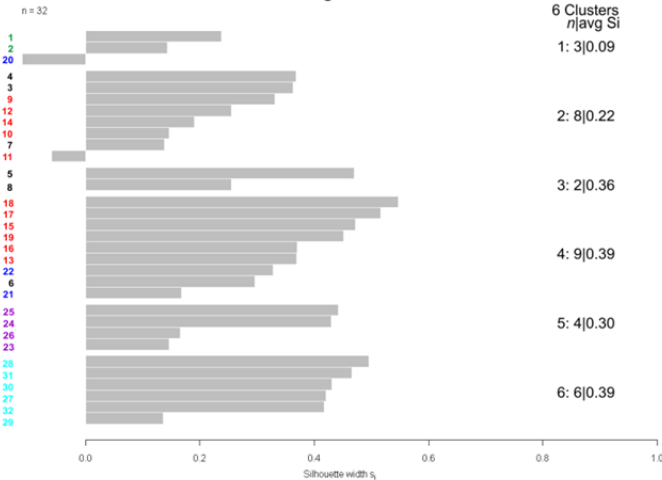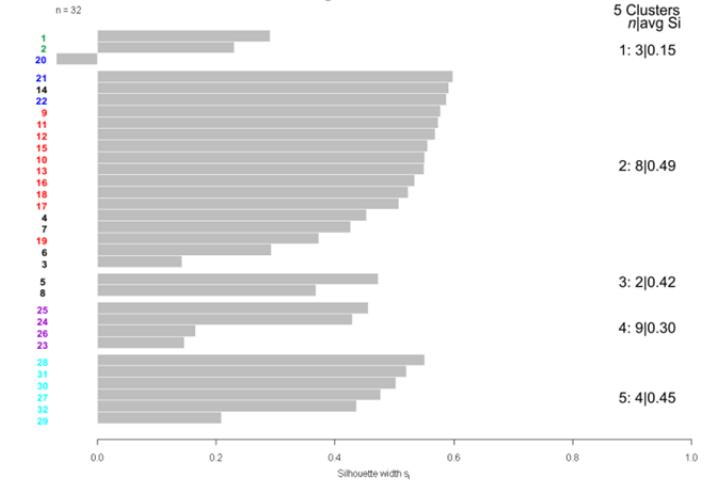
n = 32

6 Clusters
n|avg Si

1: 3|0.09

2: 8|0.22

3: 2|0.36

4: 9|0.39

5: 4|0.30

6: 6|0.39

Silhouette width s_i

Average Silhouette Width: 0.31

Silhouette Plot for Ward Clustering with k=5

n = 32

5 Clusters
n|avg Si

1: 3|0.15

2: 8|0.49

3: 2|0.42

4: 9|0.30

5: 4|0.45

Silhouette width s_i

Average Silhouette Width: 0.42

Silhouette Plot for Ward Clustering with k=4

n = 32

4 Clusters
n|avg Si

1: 5|-0.002

2: 17|0.52

3: 4|0.30

4: 6|0.45

Silhouette width s_i

Average Silhouette Width: 0.41

Silhouette Plot for Ward Clustering with k=3

n = 32

3 Clusters
n|avg Si

1: 22|0.45

2: 4|0.30

3: 6|0.49

Silhouette width s_i

Average Silhouette Width: 0.44

Silhouette Plot for Ward Clustering with k=2

n = 32

2 Clusters
n|avg Si

1: 22|0.51

2: 10|0.26

Silhouette width s_i

Average Silhouette Width: 0.43

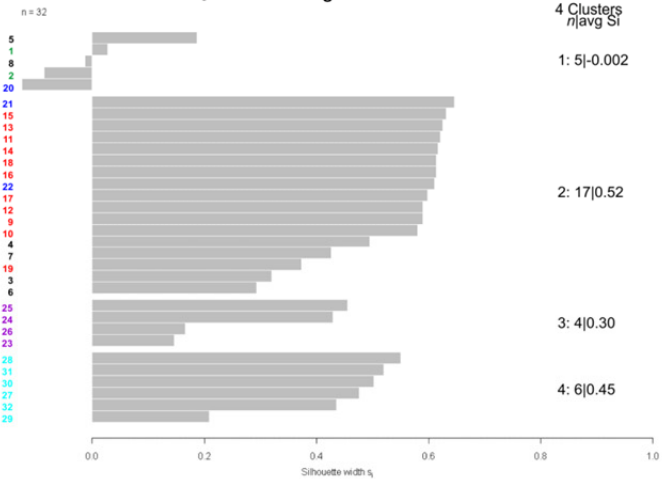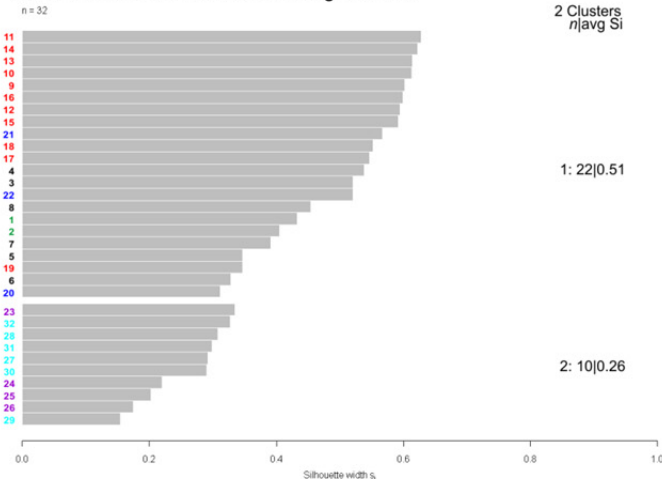| 1	UENA21	17	mdw1156
2	UENAS	18	mdw1157
3	SCWE7	19	mdw1159
4	SCWE10	20	sump812
5	SCWE14	21	sump1070
6	SCWE15A	22	sump1078
7	SCWE18	23	tails817
8	SCWS	24	tails826
9	mdw_EF19	25	tails1007
10	mdw_EF22	26	tails1074
11	mdw1049	27	esc_610
12	mdw1150	28	esc_614
13	mdw1151	29	esc1111
14	mdw1153	30	esc1112
15	mdw1154	31	esc1113
16	mdw1155	32	esc1115

Figure 21. Silhouette Plots for Cluster Analysis Using Ward's Method: Major Ion Data Set

Results for 2- through 6-cluster solutions are shown above; k= the number of clusters. Based on average silhouette widths and the number of misclassified cases (indicated by negative silhouette widths), the 2-and 3-cluster solutions are optimal.

Figure 22. Clusplots of Major Ion Data Using the Partitioning Around Medoids (PAM) Method
As shown in previous figures, tailings and escarpment samples separate from all others for all cluster solutions. Misclassified cases were case 21 (clusplot a) and cases 4 and 7 in clusplots b and c.
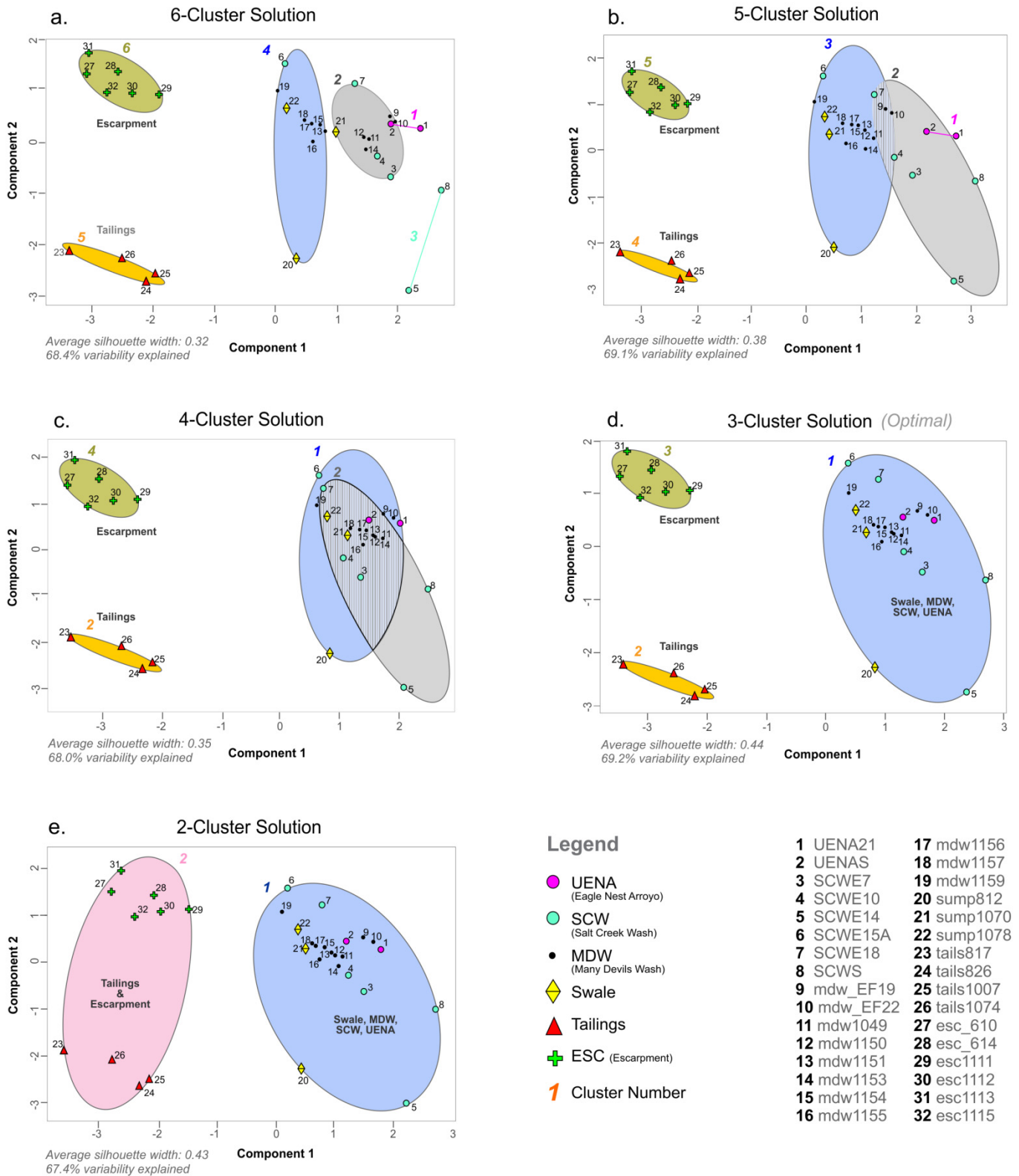
The results shown in Figure 22 agree closely with those shown for Ward's method above. Tailings and escarpment samples separate for all permutations; Many Devils Wash samples group with the analog sites and swale area samples. The clusplots differ from the dendrograms, however, because degrees of separation are more apparent. For example, the outliers in the biplot (SCWE14, SCWS, and sump812; cases 5, 8, and 20 in Figure 22) plot on the outer edges of the spherical clusters. Clusplots plots are also somewhat reminiscent of the PCA biplots in that clusters are illustrated in two dimensions, and the percent variability explained by the solution (listed below each plot in Figure 22) is identified.

For the PCA, ANOVA was applied to test whether the separation in groups based on the factor scores was statistically significant. Although some investigators have applied tests such as t-tests to cluster groups (Güler et al. 2002), Everitt et al. (2011) advise that tests such as ANOVA are inappropriate for comparing clusters groups (based on the variables used in the analysis). This is because the clustering technique has the effect of maximizing between-cluster differences on the variables (i.e., it forces formation of groups, so they would be more likely to be discriminated using ANOVA).

To identify those variables discriminating between groups for the 3-cluster solution, Figure 23 plots the standardized mean of each variable. This figure is similar to Figure 16, which plotted mean variable concentrations by study area, except that those groups characterized by interaction with the Mancos Shale—Many Devils Wash, Salt Creek Wash, Eagle Nest Arroyo, and the swale area—formed the first cluster (C1). Similar to the distinctions identified in Section 5.3.1, the Mancos Shale group (C1) differs from the tailings and the escarpment due to lower K and higher Na, Cl, and SO_4. The reason the 3-cluster solution was deemed optimal is apparent given the separation between the tailings and the escarpment samples due to different Ca, Mg, HCO_3, and (less marked) SO_4 signatures.
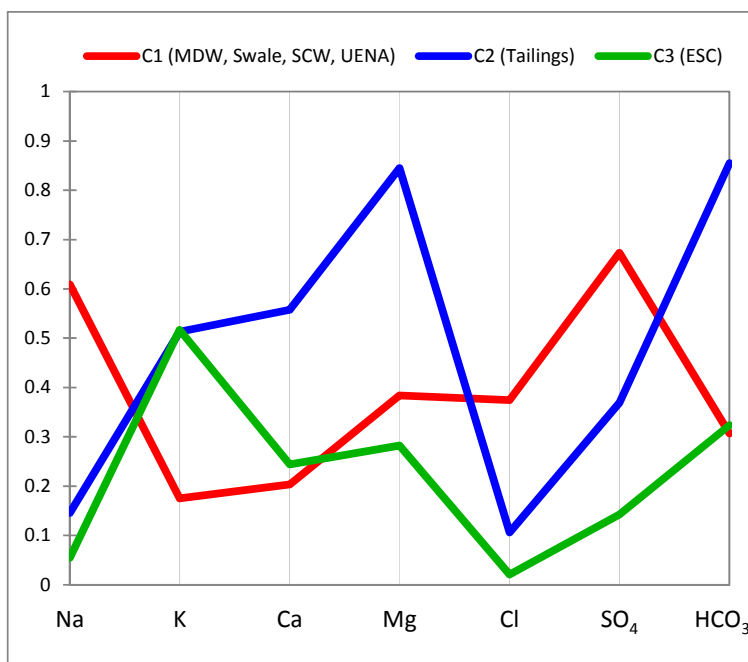

Figure 23. Parallel Coordinates Plot of Mean Ion Concentrations for the 3-Cluster PAM Solution

As a final verification step in the cluster analysis, it was important to examine whether including the correlated variables Na, Cl, and SO_4 was biasing the results in any way. Therefore, the Mahalanobis distance measure was used in lieu of Euclidean distance to account for the redundancy in these variables. Using both Ward's method and PAM, use of Mahalanobis distance yielded the same results as those produced using the Euclidean distance measure, in terms of both cluster membership and silhouette widths.

5.4   Multivariate Analysis of Extended Data Set

The preceding analysis for the major ions supported the distinctions identified using standard geochemical plotting techniques. That is, chemical signatures in Many Devils Wash samples are similar to those in other areas having a Mancos Shale influence (Salt Creek Wash, Eagle Nest Arroyo, and the swale area) and different from those of the tailings and escarpment areas. But some of the key constituents driving previous speculation that contamination in Many Devils Wash derived from the Shiprock site—nitrate, selenium, and uranium—have not yet been addressed. These constituents, along with sulfate, are common to both milling waste and Mancos-derived seepage, and (as shown in Figures 3–5) magnitudes vary widely between some study areas. In this section, the same statistical approaches used to evaluate the major ions, PCA and cluster analysis, are applied to an expanded data set that includes these additional contaminants.

5.4.1   Principal Component Analysis

Table 8 shows the correlation matrix derived for the expanded data set. This table is partially redundant with the initial correlation matrix (Table 5), so this discussion will focus on correlations not previously identified. (The positive correlations between Na, SO_4, and Cl have been well established.)

Table 8. Spearman Correlation Matrix: Extended Data Set: Major Ions + NO_3, Se, and U

Variables	Na	K	Ca	Mg	Cl	SO₄	HCO₃	NO₃	Se	U
Na		–	–	–	–	–	–	–	–	–
K	-0.291		–	–	–	–	–	–	–	–
Ca	-0.231	0.268		–	–	–	–	–	–	–
Mg	-0.044	-0.104	**0.453**		–	–	–	–	–	–
Cl	**0.780**	**-0.468**	-0.025	0.217		–	–	–	–	–
SO₄	**0.936**	-0.200	-0.216	0.105	**0.729**		–	–	–	–
HCO₃	0.133	**0.481**	-0.044	0.190	-0.107	0.197		–	–	–
NO₃	0.268	0.163	0.266	0.231	0.073	0.272	0.263		–	–
Se	**0.749**	-0.170	-0.280	-0.146	**0.492**	**0.706**	0.142	**0.450**		–
U	**-0.456**	**0.610**	0.281	0.228	**-0.566**	-0.307	**0.498**	0.164	**-0.417**	

*Values in **bold** are different from 0 with a significance level α = 0.05; duplicate correlations are not shown.*

Table 8 shows that Se is positively correlated with Na and SO_4, and to a lesser extent with Cl and NO_3; it is negatively correlated with U, albeit weakly. U is positively correlated with K and HCO_3, and weakly negatively correlated with Cl, Na, and Se. NO_3 is weakly correlated with Se. Table 9 presents the eigenvalues, the explained variability, and the PC loadings for the expanded data set based on these correlations.

Table 9. Eigenvalues, Explained Variability, and Principal Component Loadings: Extended Data Set

Eigenvalues:

	PC1	PC2	PC3	PC4	PC5	PC6	PC7	PC8	PC9	PC10
Eigenvalue	3.85	2.24	1.52	0.88	0.63	0.31	0.23	0.19	0.13	0.03
Variability (%)	38.5	22.4	15.2	8.80	6.26	3.14	2.30	1.87	1.29	0.28
Cumulative %	38.5	60.9	76.1	84.9	91.1	94.3	96.6	98.4	99.7	100.0

Results for PCs with eigenvalues > 1 (the Kaiser criterion) are shown in red above.

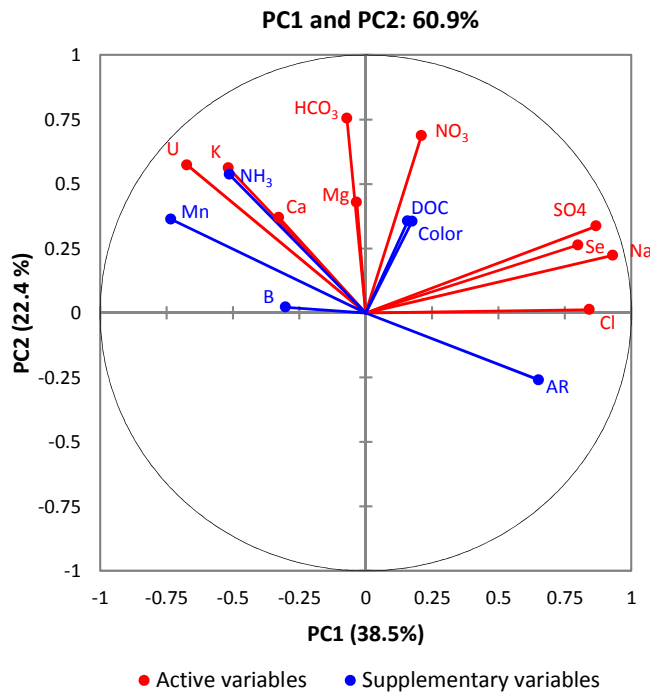**Correlations between variables and factors (factor loadings):**

	PC1	PC2	PC3	PC4	PC5	PC6	PC7	PC8	PC9	PC10
Na	**0.931**	0.223	-0.087	-0.059	0.158	0.112	-0.095	-0.005	-0.105	0.122
K	-0.517	**0.562**	-0.370	0.110	0.429	-0.062	0.250	-0.132	0.017	0.019
Ca	-0.327	0.370	**0.682**	0.301	0.382	-0.075	-0.144	0.157	-0.051	-0.015
Mg	-0.034	0.429	**0.752**	-0.348	-0.255	-0.072	0.235	-0.002	-0.032	0.033
Cl	**0.843**	0.012	0.345	-0.175	0.230	-0.025	-0.065	-0.147	0.246	-0.017
SO_4	**0.868**	0.337	-0.056	-0.170	0.131	0.217	0.090	0.028	-0.135	-0.100
HCO_3	-0.071	**0.754**	-0.360	-0.409	-0.078	-0.286	-0.203	0.001	-0.028	-0.021
NO_3	0.210	**0.688**	0.096	0.561	-0.338	0.060	-0.068	-0.191	-0.004	-0.011
Se	**0.799**	0.263	-0.270	0.283	-0.113	-0.148	0.144	0.266	0.117	0.006
U	**-0.673**	0.574	-0.099	-0.180	-0.060	0.364	-0.059	0.124	0.143	0.016

*For each variable, values in **bold** correspond to the factor for which the absolute value is the largest.*

As shown in Table 9, the first two components (PC1 and PC2) explain 38.5 percent and 22.4 percent, respectively, of the total variability contained in the original variables. The third component explains 15.2 percent of the variation, and the remaining components explain gradually decreasing contributions (with eigenvalues < 1). The first two components together account for 60.9 percent of the variation in the original data set. This value is slightly lower than the 63.5 percent accounted for in the PCA of the major ion data set. Addition of a third component increases the percentage of total explained variability to 76.1 percent. The correlation matrix in the lower portion of Table 9 can be interpreted as follows:

- Consistent with the PCA of the major ions (Table 6), PC1 is again strongly associated with Na, SO_4, and Cl.

- Reflecting the contribution of the new contaminant variables, PC1 is strongly correlated with Se and negatively correlated with U.

- Listed in decreasing order of correlation, PC2 is most associated with HCO_3, NO_3, and K. The correlations with HCO_3 and K are consistent with those revealed in the initial PCA (Table 6).

- PC3, accounting for only 15 percent of the variability in the data, is correlated with Ca and Mg.

These associations are shown graphically in the correlation circle provided in Figure 24. Similar to the initial correlation circle plot (Figure 12), each primary variable is represented by a vector (denoted by the red lines). A new set of supplementary variables, including B, Mn, NH_3, DOC, color, and $^{234}U/^{238}U$ activity ratios, is represented by the blue vectors. Although the supplementary variables are not used to derive the PCs, they provide qualitative information that is useful in interpreting the PCA results.

Figure 24. Correlation Circle on Extended Data Set: Major Ions plus Se, NO₃, and U

Similar to the correlation circle in Figure 12, this figure graphically represents the correlations between variables and factors shown in Tables 8 and 9.

Figure 24 is interpreted as follows:

- Na, Cl, and SO_4 are positively correlated with PC1 and with each other, as is Se. Selenium is not as well represented as the other PC1 variables given its slightly shorter vector length.

- Uranium's negative correlation with PC1 is apparent based on its positioning in the upper-left negative PC1 quadrant. Although at about a 45° angle, so not as well represented as the variables noted above, based on vector length, U is still a prominent variable.

- HCO_3 and NO_3 are well represented on PC2 based on the length of the vectors. Of these two variables, HCO_3 is most influential given its close alignment with the PC2 axis.

- K is correlated with U (based on the acute angle). Positioned at about a 45° angle to both PC1 and PC2 axes, K is about equally represented on the two PCs (also see Table 9).

- Ca and Mg are not well represented by the first two PCs due to their short vector lengths. As shown in Table 9, these variables are most strongly associated with PC3.

- Supplementary variables Mn and NH_3 are correlated with U, whereas $^{234}U/^{238}U$ activity ratios (AR vector) are inversely correlated with U. Boron, DOC and color are not well represented; that is, they don't account for much variation in the data. However, DOC and color are strongly correlated, as their vectors overlap.

Based on these correlations and variable influences, the biplot in Figure 25 quantifies the relationship between the samples and the PCs and illustrates the unique chemical signatures.
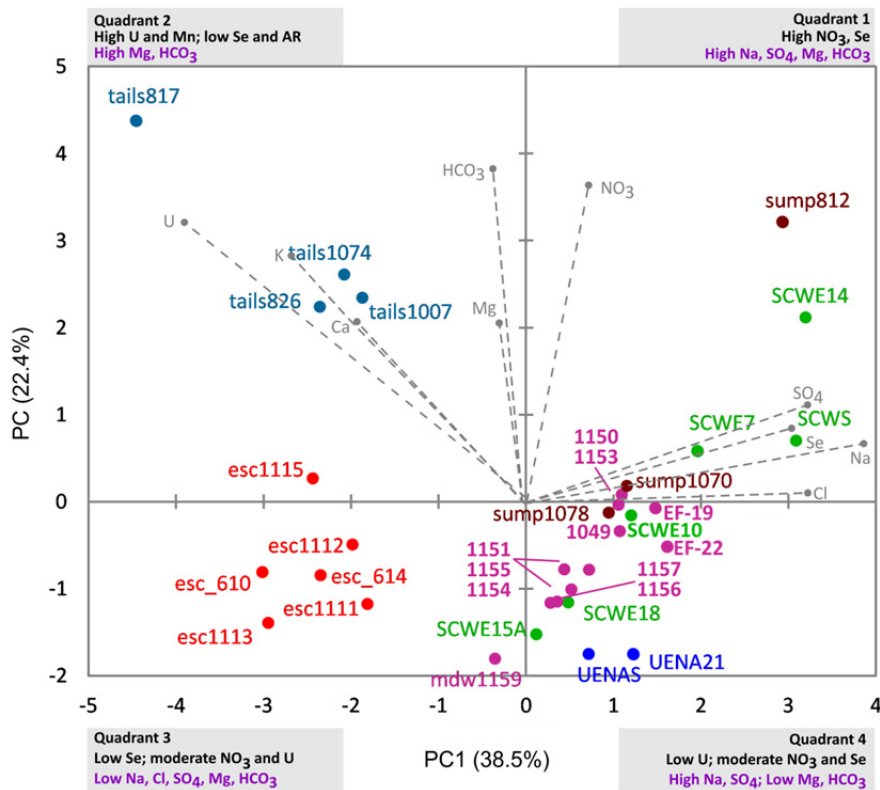
Figure 25. PCA Biplot for Extended Data Set: Major Ions plus NO$_3$, Se, and U

Even with the addition of the three primary contaminant variables, this biplot is very similar to that shown in Figure 14 for the major ions. Differences in positioning of some objects stem from extreme values (U in tails817, and NO$_3$ and Se in sump812, shown in Figure 5.

The biplot for the extended data set (shown above in Figure 25) is similar to the initial biplot (Figure 12) developed for the major ions. The tailings again group separately in the 2nd quadrant for reasons discussed previously (high HCO$_3$ and K), as well as high U, NO$_3$, and low Se. Based on the supplementary vector placement shown in Figure 24, quadrant 2 is also characterized by high Mn and low ^{234}U/^{238}U activity ratios. The isolated positioning of tailings sample 817 in this quadrant reflects the high (study-wide maximum) concentrations of U (9,380 µg/L) and K (238 mg/L) measured in this sample (Table 3, Figures 5d and 6f).

Escarpment area samples are again positioned largely in the 3rd quadrant, reflecting low concentrations of most ions—Na, Cl, SO$_4$, Mg, and HCO$_3$—and, like the tailings, low Se. The positioning of the samples is nearly identical to that shown in Figure 14, except for esc1115, which plots in the 2nd quadrant due to the high NO$_3$ concentration in this sample (see Table 3 and Figure 5a).

When the biplot in Figure 25 is compared with that for the major ions (Figure 14), several differences are apparent. First, although Many Devils Wash samples still cluster together for the large part (in quadrant 4), more separation is apparent due to the influence of NO$_3$, Se, and U. In fact, the separation is similar to that identified earlier for boron in Section 5.1 (Figure 7c), except that an inverse trend is reflected. Whereas boron was more elevated in southern

Many Devils Wash upgradient wells (1154–1159) relative to most in the northern area of the wash, the opposite trend occurs for NO_3, Se, and U (refer to Figure 4 VSS plots).

The southernmost well, mdw1159, is again isolated in the biplot (falling barely into quadrant 3), because this sample had the lowest concentrations of most constituents within Many Devils Wash (including NO_3, SO_4, Se, and U; refer to Figures 5–6 and Table 3). Swale area samples also plot differently relative to their positioning in the initial (major ion) PCA biplot. In Figure 25, sump1078 and sump1070 cluster with northern Many Devils Wash samples, whereas sump812 plots as an extreme in quadrant 1 due to study-wide maximum (outlier) concentrations of Se and NO_3 (Figure 5) and high Mg (Figure 6e). Eagle Nest Arroyo samples are more isolated in the biplot (Figure 25) due to low concentrations of NO_3, Se, and U relative to other study areas (refer to Figures 4–5 and Table 4). In terms of water chemistry, Salt Creek Wash samples are more variable as indicated by their scatter in the biplot.

Characterization of the chemical signatures for each of the quadrants (for example, the extent to which NO_3 influenced sample placement)—was more difficult for this PCA. This may be due to the fact that none of the new variables aligned with the PC axes, which in turn likely reflects the greater degree of scatter in NO_3, Se, and U concentrations relative to the distributions of the major ions (Figures 5 and 6). Figure 26 plots the standardized mean values of these constituents, along with supplementary variables Mn and B.
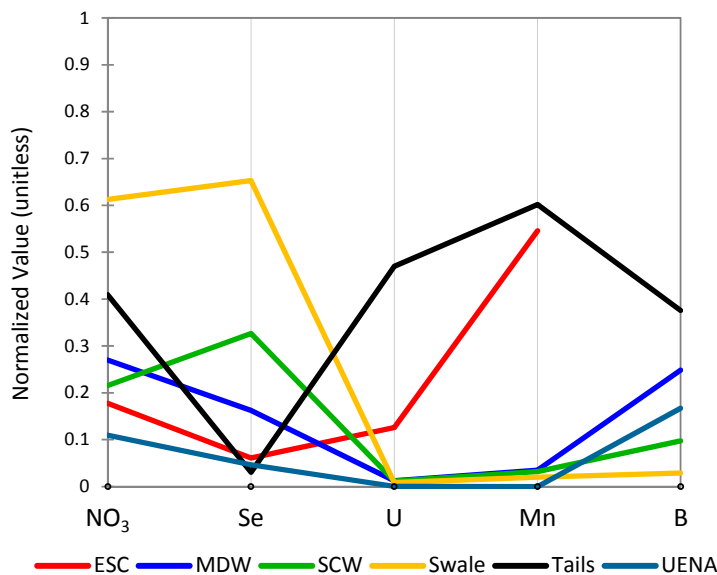

Figure 26. Parallel Coordinates Plot for NO₃, Se, U, and Supplementary Variables B and Mn

In Figure 26, the discriminations between tailings and escarpment area samples and other areas, shown previously for the major ions (Figure 16) are not as apparent. For example, mean NO_3 concentrations do not differ notably between groups except for the swale area (this mean was skewed by the high sump812 result). Like NO_3, Se is also high in swale area samples. However, concentrations are moderate in Salt Creek Wash and Many Devils Wash, and low in Eagle Nest Arroyo as well as in the tailings and escarpment areas. As illustrated previously in Figures 3–5,

U concentrations are highest in the escarpment areas and, most notably, tailings area samples. Mn, a supplementary variable in this analysis, is generally limited to the tailings and escarpment areas. Although the mean B is highest in the tailings area samples due to the tails1074 extreme, overall, B concentrations did not vary widely between groups (refer to box plots in Figure 7).

As done for the major ions, ANOVA was run on the PC factor scores for the expanded data set. Consistent with the previous findings for the major ion subset, differences between groups were significant for both PC1 ($F_{5,26} = 25.631$, $p < 0.0001$) and PC2 ($F_{5,26} = 11.25$, $p < 0.0001$). Tables 10a and 10b document corresponding results for the Tukey HSD post-hoc test pairwise comparisons.

Table 10a. Post-Hoc Tukey (HSD) Results for PC1 Factor Scores: Extended Data Set

Group	UENA	SCW	MDW	Swale	Tailings	ESC
UENA		--	--	--	--	--
SCW	0.918		--	--	--	--
MDW	0.999	0.327		--	--	--
Swale	0.946	1.000	0.589		--	--
Tailings	0.001	0.0001	0.0001	0.0001		--
ESC	0.001	0.0001	0.0001	0.0001	0.997	

Probabilities for each between-group comparison are shown in the matrix above.
p-values listed in red font are significant (<0.05).

Table 10b. Post-Hoc Tukey (HSD) Results for PC2 Factor Scores: Extended Data Set

Group	UENA	SCW	MDW	Swale	Tailings	ESC
UENA		--	--	--	--	--
SCW	0.207		--	--	--	--
MDW	0.693	0.612		--	--	--
Swale	0.034	0.686	0.083		--	--
Tailings	0.0002	0.002	0.0001	0.171		--
ESC	0.787	0.660	1.00	0.109	0.0002	

See notes following Table 10a (above).

Based on PC1—the PC accounting for most of the variation in the data (reflecting the contributions of Na, SO_4, Cl, Se, and U)—the chemical signatures for Many Devils Wash, the swale area, and the analog sites are again similar to each other ($p \geq 0.327$) but significantly different from the tailings and escarpment areas ($p \leq 0.001$; Table 10a). Expressed more simply, the ANOVA and post-hoc results for PC1 indicate that:

- MDW = UENA = SCW = swale (groups are not significantly different from one another)
- MDW ≠ tailings; MDW ≠ escarpment area ($p = 0.0001$)
- tailings = escarpment ($p = 0.997$)

The post-hoc Tukey HSD results for PC2 (reflecting HCO_3, NO_3, and K) differ from those presented in Table 7b for the major ions. In the first ANOVA and post-hoc test runs, chemistries of the tailings area samples differed significantly from those of all other areas for both PC1 and PC2. In this PCA, by including NO_3 as a variable, the tailings area samples still differed significantly from Many Devils Wash and the analog sites ($p \leq 0.002$), but not from the swale area. This is likely because NO_3 concentrations are highest in these two areas.

5.4.2 Cluster Analysis

The same methods (Ward and PAM) applied in Section 5.3.2 for major ions were used to extend the cluster analysis to include NO_3, Se, and U. Ca and Mg were not maintained because they were not well represented in the second PCA (Figure 24), potentially serving as "masking variables" according to Everitt et al (2011). Except for more elevated concentrations in the tailings (Figures 7e, 7g), Ca and Mg did not vary significantly between groups. (These variables were included initially to be consistent with the ions represented in the Piper and Stiff diagrams.) Also, given the size of this data set ($n = 32$ cases), it was considered prudent to limit the number of variables addressed. Thus, the following eight variables were used: Na, Cl, SO_4, Mg, HCO_3, NO_3, Se, and U.

Cluster Analysis Using Ward's Method

Figure 27 presents the dendrogram using Ward's for the expanded data set.

Euclidean Distance: 8 Variables
(Na, Cl, SO_4, K, HCO_3, NO_3, Se, U)
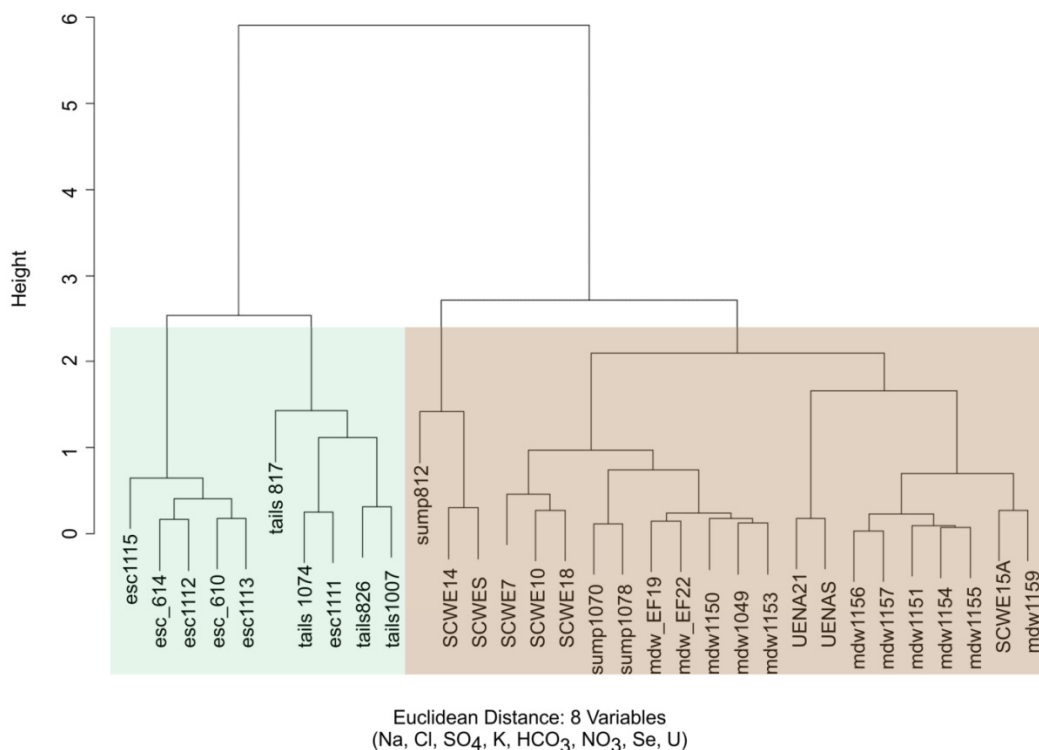
Figure 27. Dendrogram for Extended Data Set Using Ward's Method
Alternate shading assuming a 2-cluster solution is shown to facilitate review.

The 2-cluster solution in Figure 27 is similar to that resulting from both the Ward and PAM methods in the previous section (Figures 17–19), in that there is clear separation between the tailings and escarpment groups and the remaining sample populations. Other cluster partitions, for example, the separation of Salt Creek Wash outliers SCWE14 and SCWS and Eagle Nest Arroyo samples, are also similar. In this iteration, the sump812 and tails817 samples separate more prominently. This separation likely reflects the extreme outlier concentrations of selenium and uranium detected in these samples, respectively (refer to box plots in Figure 5).

To identify which (if any) partitioning is meaningful, silhouette plots were examined for each of the (2- through 6-) cluster solutions. Silhouette widths for all solutions were close to zero (0.01–0.02), and many cases were misclassified. As an example, Figure 28 shows the silhouette plots for the 6-cluster solution (resembling most others) and the "optimal" 2-cluster solution.
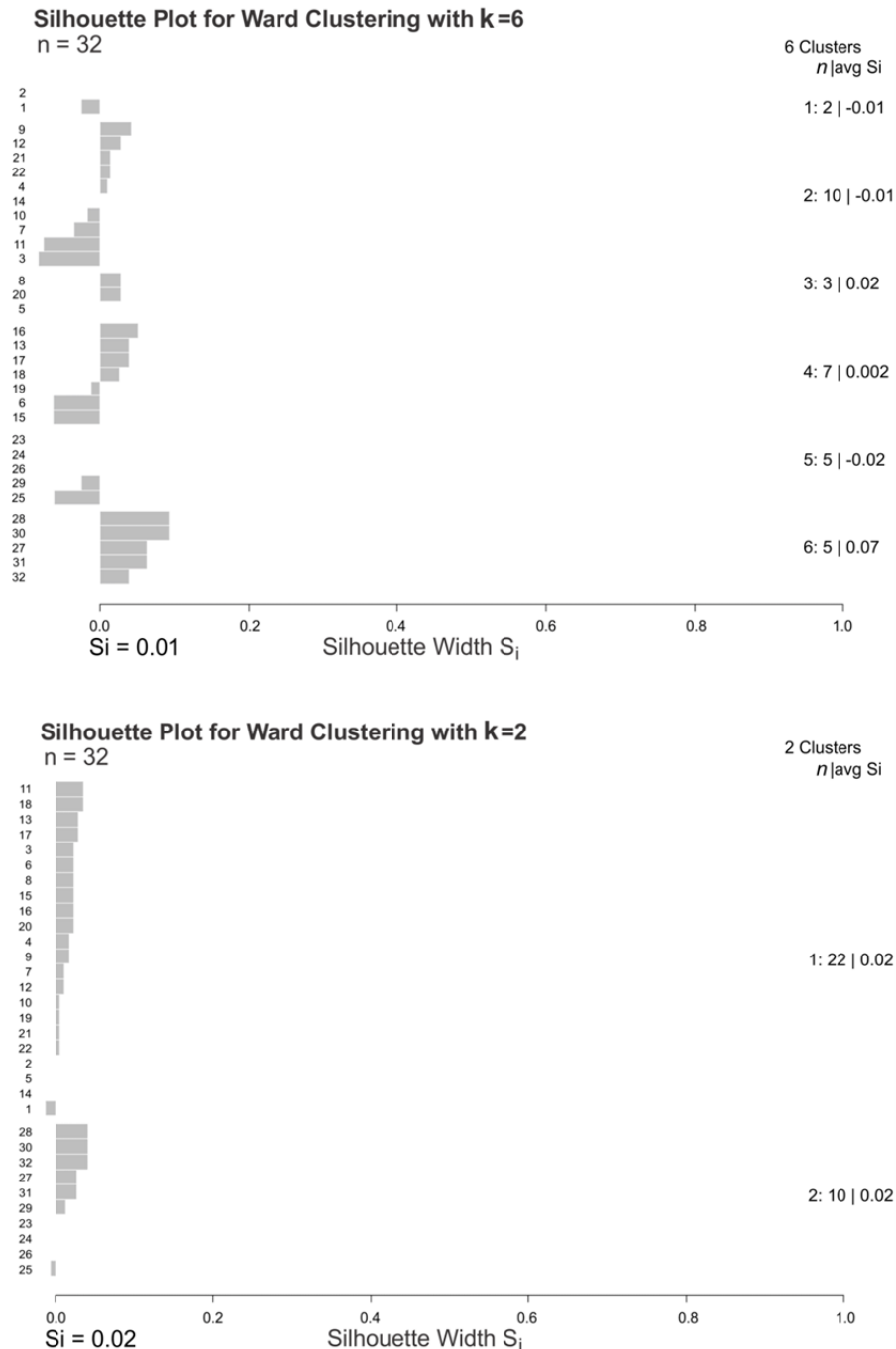

Figure 28. Silhouette Plots for 6- and 2-Cluster Solutions Using Ward's Method on Extended Data Set
k = number of groups. In both examples above, silhouette widths are small, indicating poor cluster structure. (Possible silhouette widths range from −1 to +1 based on Kauffman and Rousseauw [1990].) Many cases, those with $s_i < 1$, are misclassified in the 6-cluster solution. A cross-reference of case numbers with corresponding sample locations is provided in Figure 29.

A reasonable explanation for the poor overall structure is that NO$_3$, Se, and in particular U are highly skewed and are characterized by much scatter, as shown in Figures 4 and 5. Although Ward's method is a commonly applied in cluster analysis, Everitt et al. (2011) caution that the method is sensitive to outliers. The validity of their cautionary guidance is verified here. Therefore, PAM, a technique considered robust to outliers, was applied.

Cluster Analysis Using PAM—Major Ions + NO$_3$, Se, and U

For the extended data set, consistent with the approach used for the major ions, PAM was run iteratively to yield partitions into 2 to 6 groups (Figure 29). In general, cluster groupings are very similar to those yielded initially (Section 5.3.2; Figure 22): tailings and escarpment samples separate for all permutations, and Many Devils Wash samples group with the analog sites and swale area samples. Average silhouette widths for each cluster solution (indicated below each plot in Figure 29) are listed below. For comparison, silhouette widths for the corresponding major ion solutions (Figure 22) are listed in parentheses:

- 6-cluster solution: 0.31   (s_i for major ions = 0.32)

- 5-cluster solution: 0.34   (s_i for major ions = 0.38)

- 4-cluster solution: 0.37   (s_i for major ions = 0.35)

- 3-cluster solution: 0.38   (s_i for major ions = 0.44)

- 2-cluster solution: 0.38   (s_i for major ions = 0.43)

For all solutions, silhouette widths are notably greater than those obtained using Ward's method, and no cases were misclassified. While average silhouette widths for the larger (4- to 6-) cluster solutions are similar to those reported previously for the major ion subset, those for the 2- and 3- cluster solutions are smaller, probably reflecting the skewed distributions of NO$_3$, Se, and U. Based on average silhouette width, the 4-, 3- and 2-cluster solutions are very similar. The 4-cluster solution is characterized as follows:

- Many Devils Wash (MDW) samples partition into two groups: mdw1151 and all southern (upgradient) wells (cluster 1) and northern MDW samples that group with the swale area (cluster 3). Again, the reason northern vs. southern area MDW samples separate (an exception being northern well mdw1151) is due to lower constituent concentrations in the southern part of the wash.

- Salt Creek Wash samples cluster together (cluster 2) except for samples with lower ion concentrations (SCWE15A and SCWE18), which group with southern MDW samples.

- UENA samples also group with southern MDW samples (cluster 1) due to lower concentrations of NO$_3$, Se, and U and most ions. UENA21 and UENAS plot separately from other cluster 1 members (samples) due to elevated Cl.

- Tailings and escarpment area samples again separate from all other populations (cluster 4).

With progressively smaller cluster solutions, the above groups collapse, but the separation between tailings and escarpment samples is maintained. Based on average silhouette width and the percentage of explained variability (shown below each plot in Figure 29), the 2-cluster solution (tailings and escarpment areas and others) is considered "optimal" (Figure 29e).
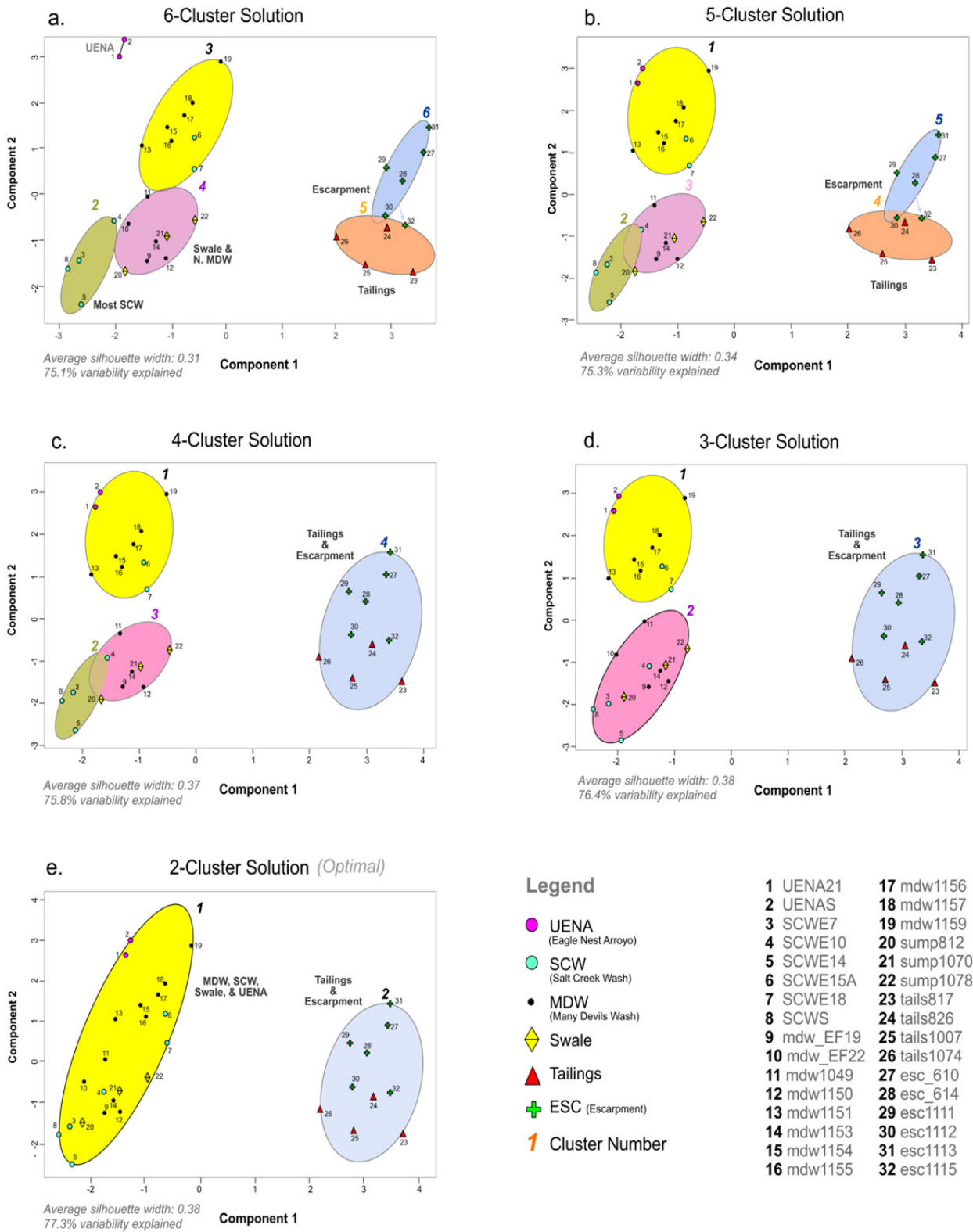
Figure 29. PAM Results for Extended Data Set (8 Variables)

Variables used were Na, K, Cl, SO$_4$, HCO$_3$, NO$_3$, Se, and U. Consistent with previous exhibits and analyses, tailings and escarpment samples separate from all others for all cluster solutions.

To identify those variables discriminating between groups for the 2- and 3-cluster solutions, Figure 30 plots the standardized means for each variable. In Figure 30a (the 2-cluster solution), Many Devils Wash, swale, and analog sites (reflecting interaction with Mancos Shale) are characterized by high Na, Cl, SO_4, and Se and low (relative to tailings and escarpment samples) K, HCO_3, and U. NO_3 is not discriminating for this solution. For the 3-cluster solution (Figure 30b), the same general trends are apparent, except that there is more stagger for most constituents, reflecting the differences in magnitude between Eagle Nest Arroyo and southern Many Devils Wash relative to the remaining analog and swale area samples.
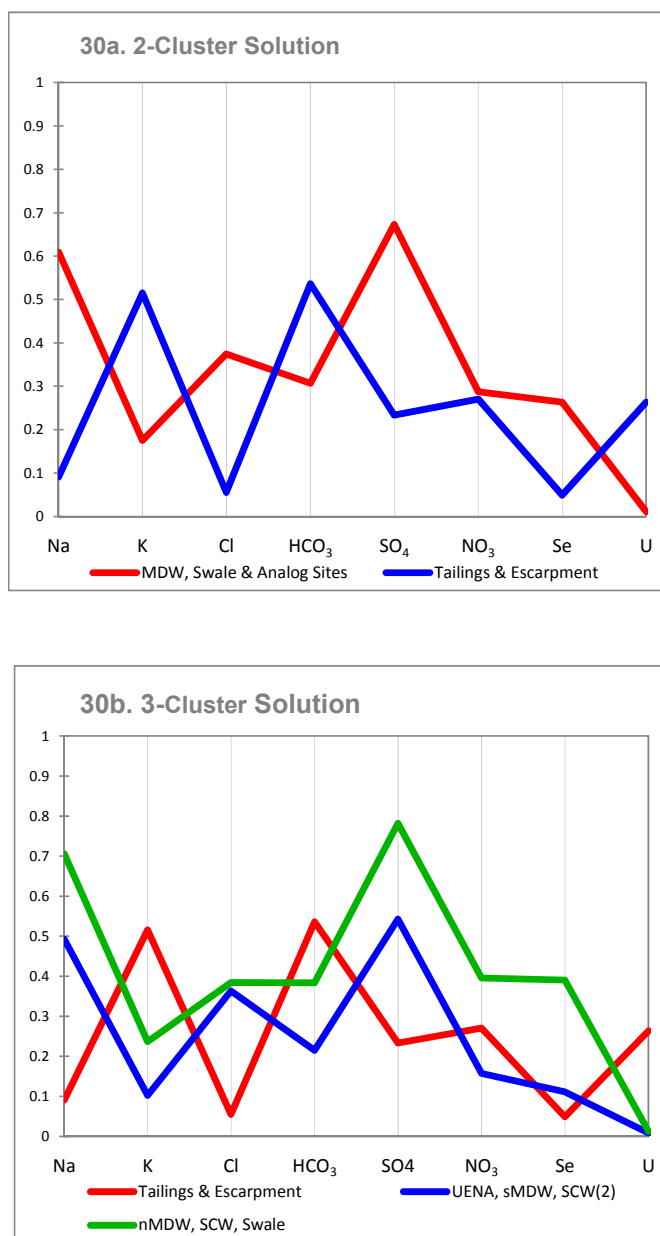

Figure 30. Parallel Coordinates Plot of Variable Means for 2- and 3-Cluster Solutions Based on PAM for Extended Data Set

In Figure 30b, nMDW refers to northern Many Devils Wash samples (except for mdw1151), sMDW includes samples mdw1154–1159 and (exception) mdw1151; SCW(2) refers to SCWE15A and SCWE18 (the Salt Creek Wash samples with the lowest variable concentrations).

6.0   Discussion

For all analysis permutations—for the major ion subset, and when the data set was expanded to include NO_3, Se, and U, there was clear (in a number of cases, statistically significant) separation between samples collected from Many Devils Wash, the analog sites, and the swale area, and samples collected from the tailings and escarpment areas. A reasonable explanation for this finding is that the contaminants in Many Devils Wash, the swale, and the analog sites are derived from interaction with the Mancos Shale, and contaminants from the tailings disposal cell feed the shallow alluvium near the mill site and were transported by groundwater to the floodplain escarpment. This interpretation is supported by recent findings documented in the companion isotope study (DOE 2012a).

The tailings discriminated from other areas (in most cases, along with the escarpment) based on Na, SO_4, HCO_3, and U signatures. Similar discrimination is apparent for supplementary variables not carried through the analysis—Mn, NH_3, and, in particular, $^{234}U/^{238}U$ activity ratios. Selenium, commonly associated with Mancos Shale, was less discriminating given variable and elevated concentrations in the swale area. Based on the degree to which variables were represented on the PC axes and the cluster structure (based on silhouette widths), the major ions best explained the differences between groups. Addition of NO_3, Se, and U revealed similar similarities and differences, but the results were not as compelling, probably because of the large scatter in these variables.

6.1   Limitations and Assumptions

In this analysis, multivariate statistical methods were used to compare chemical signatures between several separate groundwater systems. There are uncertainties and potential pitfalls inherent in using such an approach. For example, it is well known that groundwater interacts with aquifer minerals along flow paths, causing changes in the chemical composition (Plummer et al. 1983). Therefore, it is not expected that samples collected from an individual groundwater system (e.g., Salt Creek Wash) will have the same chemical compositions. Since the evaluation makes comparisons between aquifers, there is an implicit assumption that the variability in the chemical signatures along flow paths is small relative to the variability between individual sample populations. This assumption is supported by relatively consistent groupings of samples from an individual aquifer. Variations exist, however, as demonstrated by the lower concentrations of many constituents in several wells in the southern portion of Many Devils Wash compared to those in the northern area, and this variation may be due to groundwater-aquifer interactions. Even with these intra-aquifer variations, most of the samples from an individual area group near each other when compared to the other sample populations. Thus, it seems that comparing separated groundwater systems is a valid approach.

Most of the data used in the statistical analysis were derived from samples collected at the same time. However, because samples are collected at various positions along groundwater flow paths, they represent different times of recharge and variable lengths of residence in the aquifer. These variations should be reflected by chemical changes over time at a single sampling location. Some of the locations—such as the tailings, escarpment, and swale—have been sampled repeatedly for over a decade as part of the Shiprock site semiannual sampling (DOE 2012c). Other, more recently established locations (in Many Devils Wash, Salt Creek Wash, and UENA) have been sampled at least four times in the last several years. Examination

of the historical data indicates that, overall, groundwater chemistry at individual locations has been fairly constant through time.

The set used in this analysis includes only 32 cases (small for cluster analysis), group sizes are unequal, data are not normally distributed for most variables, and outliers are present. These conditions sometimes pose mathematical problems in that they can impact cluster structure. To offset these limitations, robust statistical techniques were employed to the extent possible. But, even when employment of robust techniques yields significant or even statistically irrefutable results, the results are not meaningful *unless* they can be reasonably explained by the geochemistry and a conceptual model of the groundwater system. For both PCA and cluster analysis, a number of "solutions" are possible, and there is inherent subjectivity—in the selection of specific methods to employ, and in identifying the "best" solution.

6.2   Other Related Investigations

Naftz et al. (2012) applied PCA to differentiate natural weathering of sediments from uranium ore material in their assessment of potential migration of radionuclides and trace elements from the White Mesa uranium mill in southeastern Utah. Güler et al. (2002) showed the utility of coupling traditional geochemical plotting techniques (Stiff and Piper diagrams) with multivariate statistical methods in general classifications of groundwater chemistry data. In their investigations of a Paleozoic bedrock aquifer near Montreal, Canada, Cloutier et al. (2008) used an approach combining Stiff diagrams with the cluster analysis dendrogram to classify groundwater and to determine the evolution of groundwater chemistry.

The only other multivariate statistical analysis at the Shiprock site was undertaken by Schryver et al. (2006). Their study encompassed the tailings, swale, escarpment, and floodplain areas (*n*=23 samples). These investigators used nonlinear PCA to predict classes of microbial biomarkers (phospholipid fatty acids [PLFA]) based on the groundwater geochemistry (inorganic carbon, ionic strength, nitrate, uranium, and tritium). They found that gram-negative bacteria and PLFA were highest in wells with the lowest contaminant levels; tritium and uranium were the most important geochemical factors in predicting biomarker abundance.

Although this report addressed chemical, rather than isotopic, signatures, the results are similar to those reported in the companion study (DOE 2012a). In that study, isotopes of hydrogen (^{2}H/^{1}H, ^{3}H), nitrogen (^{15}N/^{14}N), oxygen (^{18}O/^{16}O), sulfur (^{34}S/^{32}S), and uranium (^{234}U/^{238}U) were used to fingerprint groundwater in Many Devils Wash and make comparisons with the same study areas evaluated herein (the Shiprock mill site and the two analog sites). That study revealed that δ^{34}S and uranium activity ratio values were the most diagnostic isotopic parameters for distinguishing between Mancos-related contamination and mill-related contamination. The δ^{34}S values of Mancos-derived sulfate were depleted, with most values less than −20 ‰ (parts per thousand), whereas milling-derived sulfate had δ^{34}S values near 0 ‰. Milling-derived uranium has an activity ratio near the secular equilibrium value of 1, whereas Mancos-derived uranium had higher activity ratios that were typically more than 2.

Contaminated seeps were identified in early Shiprock site investigations (DOE 2000). A 2010 investigation of geology and groundwater in Many Devils Wash found chemical signatures (based on NO_3, Se, SO_4, and U) indicating that the groundwater and the seeps have a common source (DOE 2011b). In this multivariate analysis, in most cases, Many Devils Wash samples

grouped with the Shiprock swale samples. Continuity of the groundwater system has not been established, but the groundwater elevation in the swale is higher than that in Many Devils Wash north of mdw1154 (Figure 2). Thus, if a pathway were available through the Mancos Shale, groundwater could flow from the sump area to the Many Devils Wash area.

An investigation of the Colorado Plateau (DOE 2011c; Morrison et al. 2012) indicated that high concentrations of boron, major ions, nitrate, selenium, and uranium are likely to occur as a natural process of interaction between groundwater and Mancos Shale.

7.0   Conclusions

Chemical signatures of the groundwater in Many Devils Wash, analog sites, and the Shiprock site tailings, floodplain escarpment, and swale samples were compared using traditional geochemical plotting tools (Piper and Stiff diagrams) and multivariate statistical methods. These analyses indicate a commonality in chemical signatures between groundwater samples from Many Devils Wash, the swale, and the analog sites that are distinct from the tailings and escarpment samples. The most discriminating variables were Na, SO_4, HCO_3, and U. Selenium, commonly associated with Mancos Shale, was less discriminating given variable and elevated concentrations in the swale area. Consistent with the findings in a recent isotope study (DOE 2012a), the variations in the chemical signatures are interpreted as being derived from two independent sources: (1) interaction with the Mancos Shale and (2) tailings fluids.

Dubes and Jain (1995) clarify the purpose of cluster analysis, in stating that "clustering techniques are tools for discovery rather than ends in themselves"; this philosophy can be extended to PCA as well. Although the initial geochemical characterization (Piper and, in particular, the stiff diagrams) was fundamental in distinguishing between groups, some subtleties were not as apparent, such as differences in chemistry between tailings and escarpment samples. The data visualization tools provided by both PCA and cluster analysis were helpful in this regard.

Variability in the sample populations influenced by Mancos Shale exists, as exemplified by the observation of high Cl, but low concentrations of HCO_3, NO_3, Se, and U in Eagle Nest Arroyo samples. Nonetheless, for all permutations and variable subsets, geochemical signatures of water chemistry in Many Devils Wash are similar to those of the analog sites and the swale area, and different from those of the tailings and, in most cases, the escarpment. Ultimately, the separation evidenced by both the PCA and cluster analysis, is well explained by known geochemical and hydrogeological processes within the study areas.

An unexpected result of this study was that the constituents receiving the greatest focus in previous site investigations (NO_3, Se, and U, the primary contaminants at the Shiprock site) were less useful than the major ions in discriminating between the sample populations investigated in this study. The combination of the Stiff diagrams with the dendrogram for the major ions best illustrated the differences in chemical signatures between the Mancos Shale and tailings-related sources. These distinctions were also evident in the PCA biplots, where tailings and escarpment are samples grouped separately from those from all other study areas.

8.0   Acknowledgments

9.0   References

Ali, G., A.G. Roy, M. Turmel, and F. Courchesne, 2010. "Multivariate analysis as a tool to infer hydrologic response types and controlling variables in a humid temperate catchment," *Hydrol. Process*, 24: 2912–2923.

ASTM D 4448-01 (Reapproved 2007). *Standard Guide for Sampling Ground-Water Monitoring Wells*, American Society for Testing and Materials, West Conshohocken, Pennsylvania, October.

Cloutier, V., R. Lefebvre, R. Therrien, and M.M. Savard, 2008. "Multivariate statistical analysis of geochemical data as indicative of the hydrogeochemical evolution of groundwater in a sedimentary rock aquifer system," *Journal of Hydrology*, 353: 294–313.

DOE (U.S. Department of Energy), 2000. *Final Site Observational Work Plan for the Shiprock, New Mexico, UMTRA Project Site*, GJO-2000-169-TAR, Rev. 2, Grand Junction Office, Grand Junction, Colorado, September.

DOE (U.S. Department of Energy), 2002. *Final Groundwater Compliance Action Plan for Remediation at the Shiprock, New Mexico, UMTRA Project Site*, GJO-2001-297-TAR, Grand Junction Office, Grand Junction, Colorado, July.

DOE (U.S. Department of Energy), 2003. *Baseline Performance Report for the Shiprock, New Mexico, UMTRA Project Site*, GJO-2003-431-TAC, Grand Junction Office, Grand Junction, Colorado, September.

DOE (U.S. Department of Energy), 2005. *Refinement of Conceptual Model and Recommendation for Improving Remediation Efficiency at the Shiprock, New Mexico, Site*, GJO 2004-579-TAC, Office of Legacy Management, Grand Junction, Colorado, July.

DOE (U.S. Department of Energy), 2011a. *2010 Review and Evaluation of the Shiprock Remediation Strategy*, LMS/SHP/S05030, Office of Legacy Management, Grand Junction, Colorado, January.

DOE (U.S. Department of Energy), 2011b. *Geology and Groundwater Investigation Many Devils Wash, Shiprock Site, New Mexico*, LMS/SHP/S06662, ESL-RPT-2011-02, Office of Legacy Management, Grand Junction, Colorado, April.

DOE (U.S. Department of Energy), 2011c. *Natural Contamination from the Mancos Shale*, LMS/S07480, ESL-RPT-2011-01, Office of Legacy Management, Grand Junction, Colorado, April.

DOE (U.S. Department of Energy), 2012a. *Application of Environmental Isotopes to the Evaluation of the Origin of Contamination in a Desert Arroyo: Many Devils Wash, Shiprock, New Mexico*, LMS/SHP/S09197, ESL-RPT-2012-01, Office of Legacy Management, Grand Junction, Colorado, September.

DOE (U.S. Department of Energy), 2012b. *Characterization and Isolation of Constituents Causing Red Coloration in Desert Arroyo Seepage Water*, LMS/S09339, ESL-RPT-2012-02, Office of Legacy Management, Grand Junction, Colorado, September (Draft).

DOE (U.S. Department of Energy), 2012c. *March and April 2012 Groundwater and Surface Water Sampling at the Shiprock, New Mexico, Disposal Site*, LMS/SHP/S00312, Office of Legacy Management, Grand Junction, Colorado, June.

DOE (U.S. Department of Energy), 2012d. *Shiprock, New Mexico, Disposal Cell Internal Water Balance and Cell Conditions*, LMS/SHP/S08254, Office of Legacy Management, Grand Junction, Colorado, February.

Dubes, R., and A.K. Jain, 1995. "Clustering techniques: the user's dilemma," *Pattern Recognition,* 8: 247–260.

Everitt, B.S., S. Landau, M. Leese, and D. Stahl, 2011. *Cluster Analysis*, 5th ed., John Wiley & Sons, Ltd., 330 pp.

Fritz, S.J. 1994. "A survey of charge-balance errors on published analyses of potable ground and surface waters," *Ground Water*, 32(4): 539−546.

Güler, C., G. Thyne, J. McCray, and K. Turner, 2002. "Evaluation of graphical and multivariate statistical methods for classification of water chemistry data," *Hydrogeology Journal*, 10: 455−474.

Helsel, D., 2010. "Much ado about next to nothing: incorporating nondetects in science," *Annals of Occupational Hygiene*, 54(3): 257−262.

Hem, J.D., 1986. *Study and Interpretation of the Chemical Characteristics of Natural Water, 3rd Edition*, U.S. Geological Survey Water-Supply Paper 2254, 263 pp.

Jolliffe, I.T., 1986. *Principal Component Analysis*, Springer-Verlag, New York, New York.

Kaufman, L. and P.J. Rousseeuw, 1990. *Finding Groups in Data: An Introduction to Cluster Analysis*, Wiley Series in Probability and Mathematical Statistics, New York.

Kaiser, H.F., 1960. "The application of electronic computers to factor analysis," *Educational and Psychological Measurement,* 20: 141–151.

Khattree, R. and D. Naik, 2000. *Multivariate Data Reduction and Discrimination with SAS Software*, Cary, SAS Institute Inc.

Morrison, S.J., C.S. Goodknight, A.D. Tigar, R.P. Bush and A. Gil, 2012. "Naturally occurring contamination in the Mancos Shale," *Environ. Sci. Technol*, 46: 1379–1387.

Naftz, D.L., A.J. Ranalli, R.C. Rowland, and T.M. Marston, 2012. *Assessment of Potential Migration of Radionuclides and Trace Elements from the White Mesa Uranium Mill to the Ute Mountain Ute Reservation and Surrounding Areas, Southeastern Utah*, U.S. Geological Survey Scientific Investigations Report 2011-5231, prepared in cooperation with the Ute Mountain Ute Tribe and U.S. Environmental Protection Agency Region 8.

Osmond, J.K., and J.B. Cowart, 1976. "The theory and uses of natural uranium isotopic variations in hydrology," International Atomic Energy Agency, *Atomic Energy Review*, 14: 621–679.

Pison, G., A. Struyf, and P.J. Rousseeuw, 1999. "Displaying a clustering with CLUSPLOT," *Computational Statistics & Data Analysis*, 30: 381–392.

Plummer, L.N., D.L. Parkhurst, and D.C. Thorstenson, 1983. "Development of reaction models for ground-water systems," *Geochim. et Cosmochim. Acta*, 47: 665–686.

Schryver, J.C., C.C. Brandt, S.M. Pfiffner, A.V. Palumbo, A.D. Peacock, D.C. White, J.P. McKinley, and P.E. Long, 2006. "Application of nonlinear analysis methods for identifying relationships between microbial community structure and groundwater geochemistry," *Microbial Ecology*, 51: 177−188.

Schuenemeyer, J.H. and L.J. Drew, 2011. *Statistics for Earth and Environmental Scientists*, John Wiley & Sons, Inc.

This page intentionally left blank